The University Of Sheffield.

Development of the chick hypothalamus

Travis (Sheung Ching) Fu

A thesis submitted in partial fulfilment
of the requirements for the degree of
Doctor of Philosophy

The University of Sheffield
Faculty of Science
Department of Biomedical Science

October 2016

Acknowledgements

I would like to express my special appreciation and thanks to my supervisors Marysia Placzek and Matt Towers; together, you have been a great mentor to me. I thank you for encouraging my research studies and challenging my way of thinking to help me grow as a scientist. Your support and advice of the past four years on my PhD journey have been invaluable. I would also like to thank past and present members of the Placzek and Towers lab for their friendship and support over the years. A special thanks to Pam for helping me stand on my own in the lab.

Table of Contents

ACKNOWLEDGEMENTS II

ABBREVIATIONS XI

ABSTRACT 1

CHAPTER 1: INTRODUCTION 3

1.1. The hypothalamus 3

1.2. Architecture of the adult hypothalamus 4

1.3. Models of forebrain organisation 7

1.3.1. The columnar model of forebrain organisation 8

1.3.2. The prosomeric model of forebrain organisation 8

1.3.3. Evidence for and against the prosomeric model 10

1.3.4. Evidence through gene expression patterns 11

1.3.5. Evidence through transcription factor function 12

1.3.6. Evidence through lineage tracing analysis 13

1.4. Development of the hypothalamus 14

1.4.1. Origins of hypothalamic cells during neural plate stage and their topology at early neural tube stages 14

1.4.2. The prechordal mesoderm is required for DVM and hypothalamic induction 17

1.4.3. *Shh* and Nodal act cooperatively to induce the hypothalamus 18

1.4.4. Activation of *Shh* expression in the hypothalamus 20

1.4.5. Further hypothalamic development requires downregulation of Shh 21

1.4.6. Role of neuroepithelial-derived *Shh* in the hypothalamus 23

1.5. Development of the Pituitary 26

1.5.1. FGFs govern outgrowth of the infundibulum 27

1.5.2. Development of Rathke's pouch is dependent on signals from the ventral diencephalon 28

1.6. Thesis Aims 30

CHAPTER 2

MATERIALS AND METHODS 33

2.1. Chick husbandry and embryo techniques 33

2.1.1. Fate mapping of the ventral prosencephalon 33

2.1.2. Summary of fate maps 35

2.1.3. EdU labelling 35

2.1.4. Cyclopamine treatment of embryos 36

2.1.5. Dissections and flat-mounting 36

2.2. Histological techniques 37

2.2.1. Toluidine blue staining 37

2.2.2. Preparation of embryos for analyses in whole mount and sections 37

2.2.3. Riboprobe synthesis 38

2.2.4. In situ hybridisation analyses on whole mount embryos and embryonic sections 40

2.2.5. Double chromogenic *in situ* hybridisation for $p57^{Kip2}$ and Shh 41

2.2.6. Single and double fluorescent *in situ* hybridisation 41

2.2.7. Double immunohistochemistry of Lim3 and *in situ* hybridisation of *Fgf10* 42

2.2.8. Whole mount immunohistochemistry of Tuj1 42

2.3. Image capture and manipulation 43

2.3.1. Imaging whole mount embryos 43

2.3.2. Imaging flat-mounted embryos and embryonic sections 43

2.3.3. Confocal imaging 43

2.3.4. Image manipulation 43

2.3.5. Measurements of mRNA expression and morphological features 44

2.3.6. Statistics 44

CHAPTER 3

MORPHOLOGY OF THE CHICK HYPOTHALAMUS 45

3.1. Introduction 45

3.2. Results 46

3.2.1. Identification and subdivision of the hypothalamus on the basis of morphology at E5 46

3.2.2. Identification and subdivision of the hypothalamus on the basis of morphology at E3 47

3.2.3. Topology and Morphology of the Forebrain Neuroepithelium at HH10 49

3.3. Discussion 51

CHAPTER 4

FATE MAPPING THE VENTRAL MIDLINE OF THE HH10 CHICK PROSENCEPHALON 52

4.1. Introduction 52

4.2. Results 53

4.2.1. The ventral midline of the posterior prosencephalon gives rise to the hypothalamus 53

4.2.2. The ventral midline of the posterior prosencephalon extends anteriorly relative to adjacent basal cells 54

4.2.3. Fate mapping hypothalamic progenitors relative to the prosencephalic neck provides inconsistent results 56

4.2.4. Neuroepithelial cells overlying different sub-regions of the prechordal mesoderm can be accurately targeted 62

4.2.5. Ventral midline cells above the anterior prechordal mesoderm gives rise to the caudal anterior and rostral tuberal hypothalamus 63

4.2.6. Ventral midline cells above the medial prechordal mesoderm gives rise to the tuberal hypothalamus 65

4.2.7. Ventral midline cells above the posterior prechordal mesoderm gives rise to the caudal tuberal and mammillary

hypothalamus 65

4.2.8. Ventral midline cells anterior to *region A* and underlying prechordal mesoderm gives rise to the rostral anterior hypothalamus 68

4.2.9. Ventral midline cells anterior to *region A* and underlying prechordal mesoderm does not extend anteriorly relative to adjacent basal cells 70

4.3. Discussion 71

4.3.1. Predictive morphological landmarks for the hypothalamus at HH10 72

4.3.2. Anisotropic growth of the mammillary hypothalamus between E3 and E5 73

4.3.3. The ventral midline of medial and posterior prosencephalon is hypothalamic and not diencephalic 74

Chapter 5

Gene expression analysis of the anterior and tuberal hypothalamus 76

5.1. Introduction 76

5.2. Results 77

5.2.1. Subdivision of the anterior and tuberal hypothalamus on the basis of *Six3* and *Fgf10* expression 77

5.2.2. *Region A* cells give rise to the caudal anterior and rostral tuberal hypothalamus 79

5.2.3. Analysis of expression patterns in the chick hypothalamus at E1.5 (HH10) 79

5.3. Discussion 81

Chapter 6

Model of anterior hypothalamic development 89

6.1. Introduction 89

6.2. Results 90

6.2.1. Proposed models of development of the anterior hypothalamus 90

6.2.2. Growth of the Anterior, Tuberal, and Mammillary Hypothalamus is Anisotropic 90

6.2.3. The anterior hypothalamus is less proliferative than the tuberal hypothalamus ... 92

6.2.4. *p57^{Kip2}* is expressed in the anterior hypothalamus at E1.5 ... 95

6.2.5. *p57^{Kip2}* expression in the anterior hypothalamus requires Shh signalling ... 100

6.2.6. Shh is required for normal morphology of the anterior and tuberal hypothalamus ... 104

6.2.7. Shh is required for normal anterior pituitary development ... 105

6.2.8. Downregulation of Shh signalling disrupts distribution of cells that populate the anterior hypothalamus ... 107

6.3. Discussion ... 110

6.3.1. Growth of the anterior hypothalamus is anisotropic ... 110

6.3.2. Role of *p57^{Kip2}* in generation of neurons in the anterior hypothalamus ... 111

6.3.3. Role of Shh signalling in development of the infundibulum and Rathke's pouch ... 112

CHAPTER 7

DISCUSSION ... 114

7.1. Discussion ... 115

7.1.1. Novel systematic fate mapping of the hypothalamic ventral midline and its implications ... 115

7.1.2. The ventral midline of the posterior prosencephalon at HH10 gives rise to hypothalamic cells ... 117

7.1.3. Insights into morphogenesis of the hypothalamus between HH10 and HH20 ... 119

7.1.4. Shh affects differentiation and growth of the chick anterior hypothalamus ... 120

7.1.5. Implications for hypothalamic disorders ... 122

7.2. Future directions ... 123

7.2.1. Fate mapping of the basal hypothalamus ... 123

7.2.2. Using pluripotent stem cells to model hypothalamic development ... 123

7.2.3. Model for development of the anterior hypothalamus *124*

SUPPLEMENTARY DATA *125*

REFERENCES *127*

Figure List

Figure 1.1 | Architecture of the human adult hypothalamus 5

Figure 1.2 | Models of forebrain organization: columnar versus prosomeric 9

Figure 1.3 | Fate maps of the prosencephalon over HH4 to HH10 15

Figure 1.4 | Expression of Shh in the hypothalamus is dynamic 21

Figure 1.5 | Morphogenesis of Rathke's pouch and the infundibulum 29

Figure 2.4 | Cyclopamine concentration curve analysis 36

Figure 3.1 | Morphology and subdivisions of the E5 chick hypothalamus 46

Figure 3.2 | Morphology and subdivisions of the E3 chick hypothalamus 48

Figure 3.3 | Morphology of the prosencephalon at HH10 and neighbouring structures 50

Figure 4.1 | Fate map of ventral midline of the posterior prosencephalon 55

Figure 4.2 | Fate map of the ventral midline and adjacent basal plate of the posterior prosencephalon 57

Figure 4.3 | Fate maps based on measurements from the prosencephalic neck are not replicative 60

Figure 4.4 | Triple fate map of the ventral midline of the prosencephalon along the anteroposterior axis 61

Figure 4.5 | Focal injections into different subregions of the prechordal mesoderm 64

Figure 4.6 | Representative fate maps of *regions A*, *B*, and *C* 66

Figure 4.7 | Fate map of ventral midline and adjacent basal plate anterior to *region A* and the prechordal mesoderm 69

Figure 4.8 | Fate map of ventral midline of *region A* and adjacent basal plate cells 70

Figure 4.9 | Summary of fate map experiments 71

Figure 5.1 | Expression profile of *Tbx2* in E5 and E3 chick hypothalamus 82

Figure 5.2 | Expression profile of *Six3* and *Foxg1* in the E5 chick hypothalamus 83

Figure 5.3 | *Fgf10* expression in the E5 chick tuberal hypothalamus 84

Figure 5.4 | Expression profile of *Six3*, *Foxg1*, and *Fgf10* in the E3 chick hypothalamus 85

Figure 5.5 | Region A cells give rise to *Fgf10*$^{+}$ rostral tuberal hypothalamus 86

Figure 5.6 | Region B cells are restricted to *Fgf10*$^{+}$ tuberal hypothalamus 87

Figure 5.7 | Expression profile of *Six3*, *Foxg1*, and *Fgf10* in the HH10 chick prosencephalon 88

Figure 6.1 | Models of development of anterior hypothalamic development 91

Figure 6.2 | Growth of the hypothalamus over E1.5 and E5 is anisotropic 93

Figure 6.3 | EdU analysis of HH15 anterior and tuberal hypothalamus 94

Figure 6.4 | Expression of *p57*^{Kip2} and p27^{Kip1} in the ventral anterior hypothalamus 96

Figure 6.5 | Expression of *p57*^{Kip2} in the hypothalamus between HH10 and HH18 97

Figure 6.6 | Immunostaining for Tuj1 in the anterior hypothalamus at HH20 98

Figure 6.7 | Updated model of anterior hypothalamic development 99

Figure 6.8 | Expression of *Shh* relative to *Fgf10*, Foxg1, and *p57*^{Kip2} 102

Figure 6.9 | Shh signalling is blocked between HH10 and HH15 in response to cyclopamine treatment 103

Figure 6.10 | *p57*^{Kip2} is downstream of Shh signalling 103

Figure 6.11 | Shh is required for proper growth of the anterior hypothalamus 106

Figure 6.12 | Shh is required for proper morphology of the

infundibulum and Rathke's pouch 108

Figure 6.13 | Shh is required for proper distribution of region A cells 109

Figure 7.1 | Schematic of proposed hypothalamic morphogenesis 121

Figure S1 | Area a extends anteriorly to give rise to cells in the ventral midline of the prosencephalon 125

Figure S2 | Region C injection relative to prechordal mesoderm on sagittal sections 126

Figure S3 | Relative expression pattern of *Six3* and *Fgf10* unaffected in cyclopamine-treated embryos 126

Tables

Table 1.1 | Overview of hypothalamic nuclei functions 6

Table 2.1 | plasmids used in this study for *in situ* hybridisations 39

Table 2.2 | Primary antibodies used in this study 43

Table 2.3 | Secondary antibodies used in this study 43

Table 4.1 | Summary of measurement-based fate maps 60

Abbreviations

AH	anterior hypothalamus
ANR	anterior neural ridge
c.f	cephaic flexure
DVM	diencephalic ventral midline
hp	hypopyseal placode
hyp	hypothalamus
inf	infundibulum
MAM	mammillary hypothalamus
mes	mesencephalon (midbrain)
met	metencephalon (hindbrain)
os	optic stalk
p1-p3	prosomere 1 to prosomere 3
PM	prechordal mesoderm
RDVM	rostral diencephalic ventral midline
RP	Rathke's pouch
SCH	suprachiasmatic area/nucleus
tel	telencephalon
TUB	tuberal hypothalamus
c.f	cephaic flexure
hyp	hypothalamus
inf	infundibulum
mes	mesencephalon (midbrain)
met	metencephalon (hindbrain)
os	optic stalk
p1-p3	prosomere 1 to prosomere 3
RP	Rathke's pouch
tel	telencephalon
hp	hypopyseal placode
RDVM	rostral diencephalic ventral midline
PM	prechordal mesoderm
AH	anterior hypothalamus
MAM	mammillary hypothalamus
TUB	tuberal hypothalamus
SCH	suprachiasmatic area/nucleus
DVM	diencephalic ventral midline
ANR	anterior neural ridge

Abstract

The hypothalamus in the ventral forebrain is critical to homeostasis. In comparison to other regions of the CNS, its development is poorly understood. In particular there is ongoing debate regarding the relationship of the hypothalamus with the telencephalon versus the diencephalon, regarding the influence of the prechordal mesoderm on the hypothalamus, and regarding development of particular hypothalamic subdomains. Many of the issues arise because we do not, currently, have a basic understanding of the origins of the hypothalamus, i.e. the position of hypothalamic progenitors in the early neural tube.

As yet, not study has systematically fate-mapped hypothalamic progenitors in the early chick neural tube. However, previous fate mapping studies in our lab have shown that a region that is widely accepted to harbour thalamic progenitors will actually give rise to hypothalamic cells.. Having a better, and accurate, understanding of where hypothalamic precursors are situated at early neural tube stages and their relative position to neighbouring tissues is a critical first step in understanding the development of the hypothalamus.

In this study, I identify the position of ventral midline hypothalamic precursors in the Hamburger and Hamilton stage (HH)10 chick embryo using fluorescent lipophilic dyes to systematically fate map the ventral midline of the prosencephalon. I demonstrate that the prevalent model of hypothalamic origins at HH10 is incorrect. My studies begin to identify

differential migration/movement of adjacent cell populations that help us better understand morphogenesis of the hypothalamus. Further, my studies allow me to address the molecular signature of hypothalamic progenitors. Analysis of markers that define distinct subdomains in the developed (E3-E5) hypothalamus reveals that the anterior and tuberal hypothalamus cannot be distinguished at HH10. This has prompted me to propose a novel model of hypothalamic development, in which the hypothalamus is initially tuberal in character, the anterior and mammillary hypothalamus developing subsequently from tuberal progenitors. Finally, preliminary studies suggest a role for Shh in development of anterior hypothalamic cells from tuberal progenitors: pharmacological blockade of Shh signalling over a narrow time window leads to disrupted differentiation and growth of the anterior hypothalamus. Tuberal progenitors accumulate abnormally, and the infundibulum and Rathke's pouch fail to develop normally. Together my study builds on earlier work showing that Shh is required for hypothalamic induction. It shows a critical later role for Shh signalling in growth and differentiation of the neurogenic anterior hypothalamus and in the formation of the tuberal infundibulum, a domain that will orchestrate development of the pituitary gland, a critical brain-body interface.

Chapter 1: Introduction

1.1. The hypothalamus

The hypothalamus is located in the ventral part of the vertebrate forebrain. It is an evolutionarily ancient part of the brain that acts as a master homeostatic regulator. It controls physiological and behavioural processes that are crucial to life, governing an organism's survival and reproduction, and so propagation of the species. The functions of the hypothalamus include the control of energy and fluid balance, growth and reproductive behaviours, stress responses and sleep-wake states (Saper and Lowell 2014). Many of the key roles of the hypothalamus are mediated through its control of hormones located in the adjacent anterior pituitary gland (Fig.1.1C).

Unlike the cortex, hindbrain, and spinal cord, where neurons are organised in a columnar, or striated manner, the organisation of the hypothalamus is less obvious, and the many neurons that are so important in regulating homeostasis are arranged in a patchwork of nuclei (Fig.1.1B). The complex architecture of the hypothalamus is one reason why our understanding of hypothalamic development has lagged behind other parts of the central nervous system,

Yet, understanding hypothalamic development is important. Mutations in genes that control hypothalamic development lead to congenital abnormalities (Zhao *et al.* 2012; Sobrier *et al.* 2006; McCabe *et al.* 2011; Woods *et al.* 2005; Machinis and Amselem 2005; Pfaeffle *et al.* 2008; di Iorgi

et al. 2009). These include abnormalities in the hypothalamus and eyes, leading to phenotypes such as cyclopia, holoprosencephaly and septo-optic dysplasia. In addition, they include abnormalities of the anterior pituitary, including growth and reproductive problems, Cushing's disease, acromegaly and thyroid-deficiencies. Emerging studies suggest that dysregulation of hypothalamic development and function can similarly occur due to complex environmental factors: maternal nutrition during gestation leads to metabolic, neurological and behavioural consequences that may underlie complex human conditions such as eating disorders and chronic stress (Michaud 2001; Swaab 2004; McCabe *et al.* 2011; Schindler *et al.* 2012; MacKay and Abizaid 2014). Finally, obtaining a better understanding of hypothalamic development provides valuable insights into the directed differentiation of human embryonic stem cells (ES) and induced pluripotent stem cells (iPS) to hypothalamic neuronal fates - studies with potential for future novel therapies for conditions such as obesity (Merkle *et al.* 2015; Wang *et al.* 2015).

1.2. Architecture of the adult hypothalamus

The adult hypothalamus is traditionally divided into four regions. From rostral to caudal, they are the preoptic, anterior, tuberal, and mammillary areas (Fig.1.1B). Each region contains functionally distinct nuclei, which are composed of a cluster of neuronal cell bodies. The preoptic area is the rostral-most region of the hypothalamus. It lies above the optic chiasm and harbours nuclei that are important to the control of fertility and reproduction, thermoregulation, and electrolyte balance. The anterior hypothalamus lies posterior to the preoptic area. Within the ventral portion of the anterior hypothalamus is the suprachiasmatic nucleus (SCH), which governs the circadian cycle and sleep-wake systems (Moore 2007). The anterior hypothalamus also harbours nuclei with neurosecretory functions critical for endocrine functions, such as the paraventricular nucleus (PVN). Posterior to the anterior hypothalamus lies the tuberal hypothalamus. Its neurons function in energy homeostasis and stress homeostasis. Finally, posterior to the tuberal hypothalamus, and at the caudal-most region of

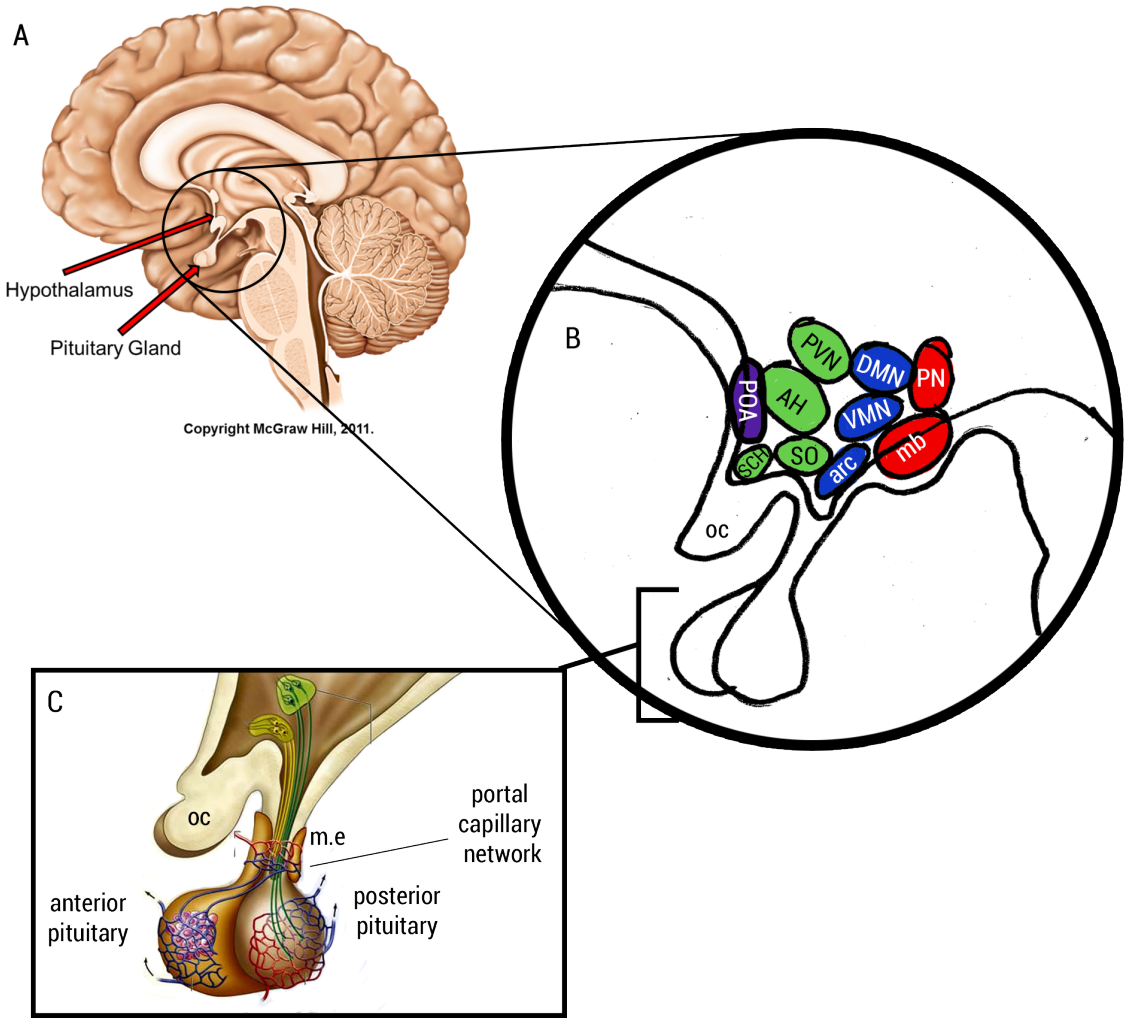

Figure 1.1 | Architecture of the human adult hypothalamus

(A) Schematic of brain from a sagittal view. The hypothalamus is located at the base of the brain and is attached to the pituitary gland, from which it effects control over the endocrine system. (B) The hypothalamus is traditionally subdivided into four regions: preoptic (purple), anterior (green), tuberal (blue) and mammillary (red). Within the preoptic is the preoptic nucleus (POA). The anterior hypothalamus harbours the suprachiasmatic nucleus (SCH), supraoptic nucleus (SO), anterior hypothalamic nucleus (AH), and paraventricular nucleus (PVN). The tuberal hypothalamus contains the arcuate nucleus (arc), ventromedial nucleus (VMN), and dorsomedial nucleus (DMN). The mammillary hypothalamus contains the mammillary bodies (mb) and posterior hypothalamic nucleus (PN). (C) Side view schematic of the pituitary gland, consisting of the posterior pituitary (neurohypophysis) and the anterior pituitary (adenohypophysis). Parvocellular neurosecretory neurons (green) extend to the posterior pituitary and directly release hormones into the bloodstream. Magnocellular neurosecretory neurons (yellow) extend to the portal capillary network in the median eminence (m.e) to release hormone-releasing and hormone-inhibiting hormones to indirectly regulate hormone release by the anterior pituitary. oc,optic chiasm.

Table 1.1 | Overview of hypothalamic nuclei functions

Region	Nucleus	Functions	Reference
Preoptic	Preoptic nucleus (POA)	reproduction thermoregulation fluid balance	Moore 2007
Anterior	Suprachiasmatic nucleus (SCH)	circadian cycle sleep-wake systems	Saper 2006
	Supraoptic nucleus (SO)	reproduction fluid balance	Augustine *et al.* 2016
	Anterior hypothalamic nucleus (AH)	thermoregulation	Boulant 2000
	Paraventricular nucleus	fluid balance reproduction appetite	Swaab *et al* 1995
Tuberal	Arcuate nucleus (arc)	energy balance	Minor *et al* 2009
	Ventromedial nucleus (VMN)	energy balance stress reproduction	Kim *et al* 2011
	Dorsomedial nucleus (DMN)	energy balance	Bellinger and Bernardis 2002
Posterior	Mammillary bodies (mb)	memory stress reproduction	Dillingham *et al* 2015
	Posterior hypothalamic nucleus (PN)	cardiac regulation thermoregulation	Martin 1992

the hypothalamus, is the mammillary hypothalamus, which contains the mammillary bodies whose neurons play important roles in stress and arousal.

In addition to harbouring defined neurons, the tuberal hypothalamus contains two specialised glial-cell rich areas, the median eminence and the posterior pituitary. Glial-like cells in the median eminence, termed tanycytes, and glial cells of the posterior pituitary, form regulatory interfaces between the brain and the peripheral body. Neurosecretory axons that project from regions such as the PVN (Fig.1.1C) project to the median eminence and posterior pituitary. These neurosecretory neurons, are categorised as magnocellular or parvocellular. Parvocellular terminals release hormones that directly enter the bloodstream through the posterior pituitary; magnocellular neurons release hormones into the portal capillary network in the median eminence to indirectly regulate hormone release by cells of the anterior pituitary. This provides the basis for hypothalamic control of the endocrine system. Thus, like the PVN, the median eminence and posterior pituitary are critical to the neuroendocrine function of the hypothalamus (Pearson and Placzek 2013). At the same time, glial-like tanycytes provide a conduit for the transport of circulating metabolites and hormones from the body to the brain. Additionally, they act as stem cells (Rizzoti and Lovell-Badge 2016). Tanycytes and pituicytes are therefore thought to be master regulators of hypothalamic function: importantly, both derive from the infundibulum, an embryonic structure that grows out of the floor of the tuberal hypothalamus (Pearson and Placzek 2013).

1.3. Models of forebrain organisation

Over the last century, a number of models of forebrain organisation have been proposed. The aim of these models has been to provide a framework to understand how the forebrain, including the hypothalamus, may develop and function.

1.3.1. The columnar model of forebrain organisation

At the start of the 20th century, development of the forebrain was largely influenced by the columnar model (Herrick 1910; Kuhlenbeck 1973). This model postulates that the forebrain neuraxis is organised into longitudinal columns that extend along the anteroposterior/rostro-caudal axis (note I use these terms interchangeably). In the columnar model, the telencephalon is the most rostral end of the neural plate/neural tube and is the most ventral part of the diencephalon, lying underneath the epithalamus, dorsal thalamus, and ventral thalamus (Fig.1.2A). Analysis of gene expression patterns, such as *Nkx2.2* and *Shh* provide support for the idea that there may be some longitudinal organisation or pattern along the entire anterior-posterior axis (Bedont *et al.* 2015).

However, as far back as 1890, His suggested a different organisation of the forebrain, into transverse units along the anteroposterior neuraxis (His 1893). This model gained a lot of favour in the early 1990s, when gene expression analysis provided some support for a new, and now- prevalent prosomeric model (Rubenstein *et al.* 1994).

1.3.2. The prosomeric model of forebrain organisation

The prosomeric model postulates that the vertebrate central nervous system is organised into a series of transverse segments along the neural tube, called prosomeres (Rubenstein *et al.* 1994). These are proposed to be lineage-restricted developmental units, which ultimately differentiate into defined parts of the CNS. In this way, they are proposed to be similar to the lineage-restricted compartments found in the Drosophila embryo and the vertebrate rhombomeres of the hindbrain (see below).

The prosomeric model has undergone several modifications since it was first proposed (Rubenstein *et al.* 1994; Puelles and Rubenstein 2003; Puelles *et al.* 2012; Ferran *et al.* 2015). In the original model, the forebrain (prosencephalon) is segmented into 6 prosomeres. From caudal to rostral, these are: the diencephalon, composed of prosomeres p1 to p3 and the secondary prosencephalon, composed of prosomeres p4-p6 (Rubenstein *et*

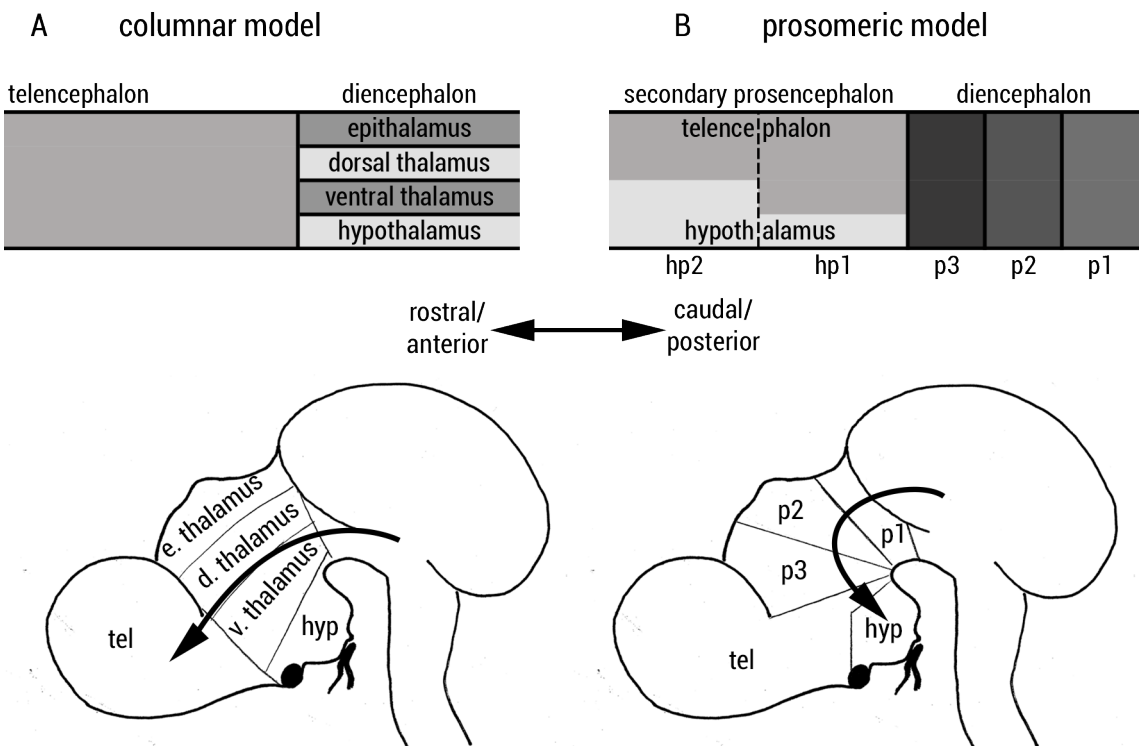

Figure 1.2 | Models of forebrain organization: columnar versus prosomeric

(A) In the columnar model, the hypothalamus is the ventral part of a longitudinally diencephalic domain and lies posterior to the telencephalon. The consequence of this organisation is that the rostral/anterior end of the neural tube is the telencephalon (direction of arrow). (B) The prosomeric model subdivides the forebrain into transverse segments and thus, the hypothalamus is the ventral part of the secondary prosencephalon, together with the dorsal telencephalon. The secondary prosencephalon is further split into two prosomeres - hp1 and hp2. As a result, the rostral/anterior end of the neural tube is in the hypothalamus (direction of arrow).

al. 1994). In the original model, the hypothalamus was believed to arise from p4 and p5, ie to lie posterior to the telencephalon. In the latest iteration of the model, the secondary prosencephalon is reorganised into two hypothalamo-telencephalic prosomeres (hp1 and hp2). Anterior, tuberal, and mammillary hypothalamus are placed in hp2, while the retromammillary hypothalamus and the telencephalon are placed in the hp1 domain (Puelles and Rubenstein 2015). Consequently, this places the hypothalamus, instead of the telencephalon, as the rostral-most structure of the neural tube (Fig.1.2B). Importantly, however, and most controversially, all of the iterations of the prosomeric models suggest a distinctive and novel feature: the placing of the hypothalamus into a novel segmental unit, the secondary prosencephalon, a developmental unit that will give rise to the hypothalamus and telencephalon. The secondary prosencephalon is a developmental unit, such as the diencephalon, within the prosencephalon that is defined as giving rise to the telencephalon and the hypothalamus. This is in contrast with previous models, in which the hypothalamus, together with the thalamus (or p1-p3), formed the diencephalon. Crucially, this model suggests that there is early no lineage-restriction between the telencephalon and hypothalamus and that they share a similar genetic programme. At the same time it suggests a lineage-restriction between p3 and the secondary prosencephalon, ie suggests that the hypothalamus should not be considered a diencephalic structure and that the development of the hypothalamus and diencephalon occur under fundamentally distinct genetic programmes.

1.3.3. Evidence for and against the prosomeric model

The idea behind the prosomeric model is that spatially-restricted transcription factors underpin genetic programs for the development of each prosomeric segments as a unit. This concept is best showcased by the Drosophila Bauplan (body plan), in which a hierarchy of *Hox* gene expression identifies transverse sections along the anteroposterior axis of the body; each section is lineage-restricted and under control of a different *Hox* gene (Reichert and Bello 2010). Similarly in the vertebrate CNS, studies

found that *Hox* expression domains exhibit sharp boundaries that correlate with the lineage-restricted hindbrain rhombomere units (r1-r8), which are visually identifiable by constrictions in the wall of the neural tube (Fraser *et al.* 1990; Krumlauf 1993; Kiecker and Lumsden 2005). Studies have shown that regional expression of *Hox* genes confer rhombomere identity (Keynes and Krumlauf 1994). For example, *Hox*b1 is important in specifying rhombomere 4 (r4) identity. In *Hox*b1$^{-/-}$ mice, r4 markers are absent in r4 and instead ectopic expression of genes characteristic of r2 are upregulated (Studer *et al.* 1996). In contrast, gain-of-function studies in chick, in which *Hox*b1 is ectopically expressed in r2 result in induced expression of genes characteristic of r4 motor neurons in r2 and thus suggests a respecification of r2 to r4 fate (Bell *et al.* 1999).

In contrast to the vertebrate hindbrain, *Hox* genes are not expressed in the forebrain and a similar hierarchical organisation of gene expression has not been identified. However, these types of studies have been extrapolated in the prosomeric model to argue that other key transcription factors identify lineage-restricted compartments, ultimately governing all aspects of development of that compartment. What, is the evidence for this? In particular, what is the evidence for a distinct border between the secondary prosencephalon, containing the telencephalon/hypothalamus, and p3? And what is the evidence for a common programme for development of the hypothalamus and telencephalon?

1.3.4. Evidence through gene expression patterns

Expression patterns in the forebrain are spatially complex and no single gene has been identified to define an entire prosomere. However, the main evidence for the prosomeric model came initially through analyses showing that particular homeodomain (HD)-containing transcription factors, including *Foxg1*, *Six3*, *Otx*, and *Irx3* show transverse patterns of expression. For example, the prosomeric p3 and caudal hypothalamic (i.e. diencephalic and secondary prosencephalic) boundary in mice was suggested through the caudal expression limit of *Sim-1*, *Otp*, and *Brn-2* genes in the caudal prosencephalon and rostral expression limit of *Arx*, *Dlx*, and *Pax6* expression

in the rostral p3 prosomere (Puelles and Rubenstein 2003). In chicken, however, studies have failed to identify this diencephalic-secondary prosencephalic boundary (Puelles and Rubenstein 2003). Nonetheless, the identification of genes that are expressed in a complementary manner in the diencephalon and secondary prosencephalon was put forward to support the idea that the hypothalamus is developmentally distinct from the diencephalon. However, most of these studies analysed mice at E15.5, long after the events that initially pattern the neural plate and neural tube. Further analyses at earlier time points, showed in fact, that the relevant gene expression patterns are highly dynamic both spatially and temporally. For example, as outlined above, expression of *Arx* in the E15.5 mouse was initially proposed to demarcate the p3 and secondary prosencephalic boundary (Puelles and Rubenstein 2003). However, subsequent studies showed that *Arx* is expressed in the hypothalamus (i.e. secondary prosencephalon) at E11.5 (Shimogori *et al.* 2010) and thus does not demarcate this border at earlier stages. Many other transcription factors also traverse this proposed p3-secondary prosencephalic boundary at E11.5 including *Emx2*, Lhx5, and Foxd1 (Shimogori *et al.* 2010).

1.3.5. Evidence through transcription factor function

Further support for the idea that the secondary prosencephalon is a compartmental unit that consists of the telencephalon and hypothalamus, and is distinct from the diencephalon, came through analysis of *Six homeobox 3* (*Six3*) expression and function.

Expression analyses in chick and mouse showed that *Six3* is confined to the telencephalon and hypothalamus (i.e. the secondary prosencephalon in the prosomeric model Kobayashi *et al.* 2002; Oliver *et al.* 1995)) and abuts expression of iroquois-related homeobox 3 (*Irx3*) in the diencephalon. Further studies then showed that *Six3* and *Irx3* are responsible for defining the competence of cells to respond to Fgf8 and Shh signalling, and hence their ability to differentiate to particular fates (Kobayashi *et al.* 2002). Thus, *Six3* is required in cells for their competence to respond to Shh signalling and upregulate the telencephalic marker, *Foxg1*, and the hypothalamic

marker, *Nkx2.1*. Similarly, *Irx3* is required for cells to upregulate *En1* and *Nkx6.1* in response to Fgf8. Furthermore, *Six3* and *Irx3* can mutually repress each other's expression. On this basis it was proposed that these genes contribute to the demarcation and establishment of two distinct regions in the forebrain governed by different genetic programs - the secondary prosencephalon and the diencephalon.

The prosomeric model argues that gene expression patterns reveal different genetic programs and thus predictions can be made about the developmental consequences of disrupting genes expressed in a single prosomere. Early reports suggested that in *Six3*-null mice, the entire secondary prosencephalon was lost, supporting the idea that *Six3* is required for providing identity to a single compartment, which will form the hypothalamus and telencephalon (Lagutin *et al.* 2003; Puelles and Rubenstein 2003). However, *Six3* was shown to exert its effects by repressing Wnt signalling, which caudalises the neural tube (Lagutin *et al.* 2003; Yamaguchi 2001). A later study went on to show that in *Six3*-null mice, many hypothalamic markers are still present at the 15 somite stage, including *Nkx2.1*, *fezf2* and Six6. Thus the posterior and tuberal hypothalamus form, but not the anterior hypothalamus. Moreover, in *Six3*$^{-/-}$ Wnt$^{-/-}$ mice, the prethalamus and caudal hypothalamus are rescued but the telencephalon and anterior hypothalamus are not (Lavado *et al.* 2008). This suggests that *Six3* may only be responsible for development of the telencephalon and anterior hypothalamus and not for the tuberal and mammillary hypothalamus, i.e. not the entire postulated secondary prosencephalon. Instead, it suggests that *Six3* promotes tuberal and posterior hypothalamus by protecting cells from posteriorising signals that would otherwise confer a 'diencephalic' fate.

1.3.6. Evidence through lineage tracing analysis

Do lineage tracing experiments provide evidence for compartmentalisation of prosomeres? Fate mapping studies in the neural plate of several species have been performed, and used to support the idea that the neural plate can be partitioned into transverse units that will predict later prosomeres (Fernández-Garre *et al.* 2002; Jacobson 1959; Staudt and Houart 2007; Woo and

Fraser 1995; Inoue *et al.* 2000; Eagleson and Harris 1990). However, for the most part, these fate mapping studies have been performed only crudely. Few genetic lineage tracing studies have been performed, as relevant promoters/enhancers have not yet been found. To date, only one genetic lineage tracing study provides evidence for a p2-p3 alar boundary: *Gbx2*$^{+}$ cells and their descendants populate the epithalamus (alar p2) and form a sharp boundary that delineates the epithalamus from the thalamus (Chen *et al.* 2009). Less refined fate mapping analyses, using quail-chick chimeras have been used to argue that the p1-p3 prosomeres are organised into transverse compartments in the early chick neural tube (Garcia-Lopez *et al.* 2004). However, retroviral lineage-tracing and dextran-labelling studies in chick identified dispersal of daughter cells that crossed interprosomeric boundaries; cells labelled in the ventral thalamus at HH18 (E3) were found to disperse into the telencephalon after 48h (Golden and Cepko 1996; Larsen *et al.* 2001).

Together, then, the question of whether the early neural tube is organised into longitudinal or transverse domains remains a highly controversial subject (Puelles *et al.* 2012; Bedont *et al.* 2015; Puelles and Rubenstein 2015). It remains possible that neither model is correct.

1.4. Development of the hypothalamus

Regardless of whether they are closer in lineage and development to a telencephalic cell or a diencephalic cells, what do we know about the development of hypothalamic cells? Where do they originate, and what signals and transcription factors are involved in their induction and development?

1.4.1. Origins of hypothalamic cells during neural plate stage and their topology at early neural tube stages

The central nervous system originates from the neural plate, which undergoes neurulation to form the neural tube. Identifying the hypothalamic progenitor territories at these stages is important for our understanding

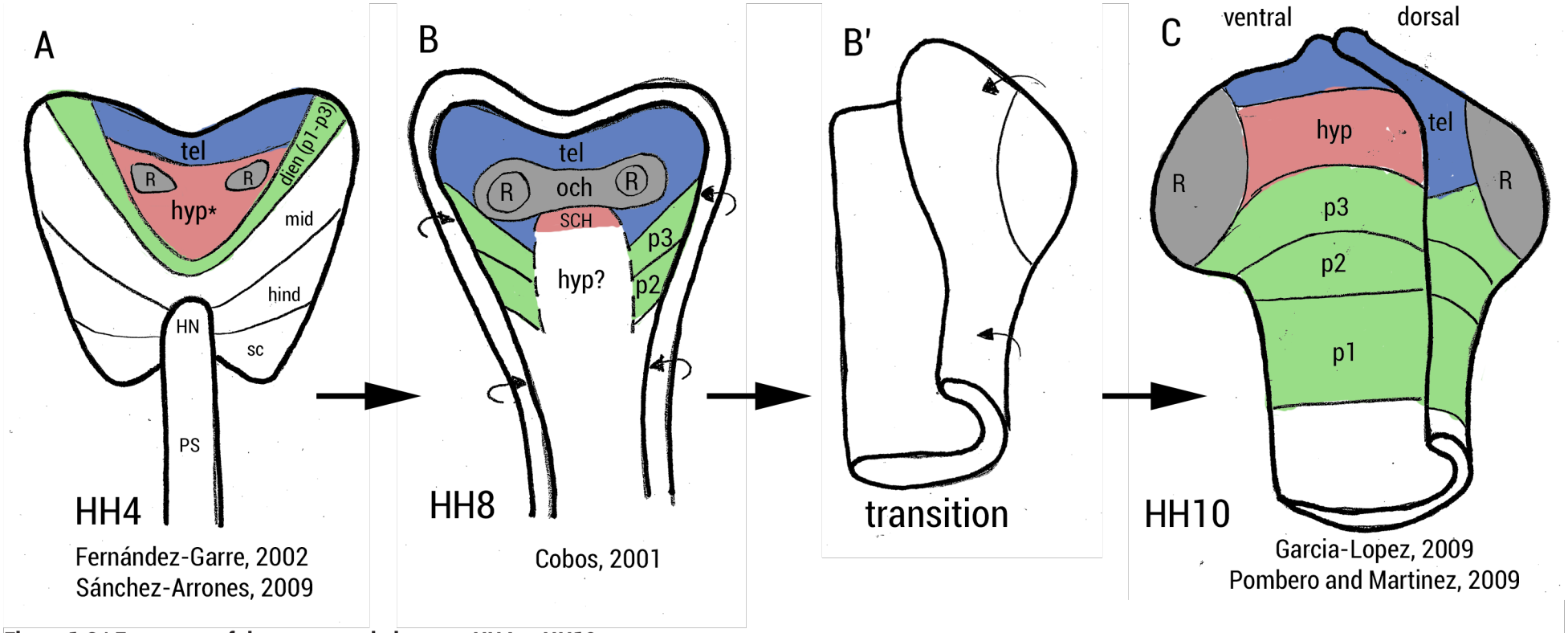

Figure 1.3 | Fate maps of the prosencephalon over HH4 to HH10

(A-C) Schematic summary of published fate maps of the telencephalon, hypothalamus, and diencephalon during the neural plate stage at HH4 (A), neurulation at HH8 (B), and early neural tube stage at HH10 (C). (B') represents neural tube folding on the right side of the embryo. In (C), the neural tube has been dissected such that the left side shows the ventral half and the right side shows the dorsal half. Colours correspond to the telencephalon (blue), hypothalamus (red), and diencephalon (green). At HH8 the anterior-most region of the hypothalamus, the suprachiasmatic area (SCH), has been fate mapped, however, the rest of the hypothalamus has not been fate mapped. (D) Schematic overview of contradicting fate maps of similar regions in the embryo at HH10; in the left panel, the region highlighted in green gave rise to the diencephalon but in the right panel, the regions highlighted in red gave rise to the hypothalamus. dien, diencephalon; hind, hindbrain; HN; Hensen's node; hyp, hypothalamus; mid, midbrain; och, optic chiasm; p1-p3, prosomeres 1-3; R, retina; sc, spinal cord; tel, telencephalon;

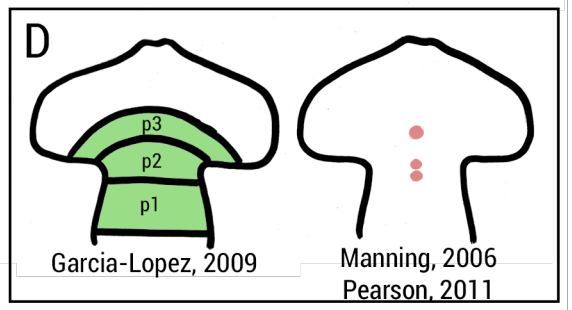

of hypothalamic development as it provides a positional reference for insightful comparison with adjacent tissues, and with the expression pattern of relevant transcription factors and signals; additionally, it provides insight into migrational behaviours and patterns of growth that contribute to morphogenesis. However, our current understanding of where the hypothalamus is during neurulation and early neural tube stages remain obscure due to a lack of extensive fate maps targeted at hypothalamic progenitors.

Fate mapping studies of the chick neural plate (HH4-5) have suggested the origins of the major subdivisions of the vertebrate central nervous system (Fig.1.3A; Fernández-Garre *et al.* 2002; Sánchez-Arrones *et al.* 2009). However, it is important to note that these studies were by no means systematic, ie provide an incomplete fate map, especially with respect to the hypothalamus and diencephalon. Fate mapping studies of the chick, at slightly later stages (HH7-8, i.e during neurulation and prior to neural tube closure) have provided a more extensive map of the position of the telencephalon, optic fields, and the rostral hypothalamus, especially the preoptic and suprachiasmatic regions (Fig.1.3B, Couly and Le Douarin 1987; Balaban *et al.* 1988; Cobos *et al.* 2001). However, the precise position of the remaining regions of the hypothalamus - the anterior, tuberal, and mammillary - remain obscure (Cobos *et al.* 2001).

Recent studies have begun to elucidate the major subdivisions of the chick neural tube at HH10 including the telencephalon and diencephalon (Pombero and Martinez 2009; Garcia-Lopez *et al.* 2004; Garcia-Lopez *et al.* 2009). Fate maps conducted in quail-chick chimeras by *Garcia-Lopez et al. (2004)* suggest that the hypothalamus lies in the anterior prosencephalon (Figs.1.3C,D). By contrast, studies in our lab conducted on chick embryos at a similar time (HH9-10) suggest that the future ventral midline of the hypothalamus lies in a territory proposed to be diencephalic by the *Garcia-Lopez et al. (2004)* fate mapping study (Fig.1.3D; Manning *et al.* 2006; Pearson *et al.* 2011).

In summary, as yet, no study has taken a systematic or targeted approach to fate-map cells in the early chick embryo that will give rise to the

hypothalamus.

1.4.2. The prechordal mesoderm is required for DVM and hypothalamic induction

In early embryogenesis, several tissues produce diffusible signals that induce and pattern the neural plate. Key amongst these is the Node/organiser, which secretes BMP antagonists that induce the neural plate. Cells in the Node/organiser then differentiate into axial mesoderm. Axial mesoderm ventralises the neural tube and induces the floor plate, a specialised cell group that occupies the ventral-most region of the neural tube. The floor plate extends from the spinal cord, hindbrain and midbrain to the caudal diencephalon. More anteriorly, the ventral midline is occupied by a floor plate-like structure - the so-called 'diencephalic ventral midline' (DVM). The DVM exhibits floor plate-like characteristics, namely, the expression of *Shh* and transient expression of *Foxa2* and chordin (Placzek and Briscoe 2005). It can be distinguished from the floor plate by the expression of Bmp7 and lack of netrin-1 (Dale *et al.* 1999). The DVM comprises at least 2 cell populations: rostral diencephalic ventral midline (RDVM) cells and caudal diencephalic ventral midline cells. These can be distinguished through expression of *Nkx2.1* in the RDVM and prolonged expression of *Foxa2* in the caudal DVM. The floor of the hypothalamus is thought to originate from RDVM cells (Dale *et al.* 1999; Manning *et al.* 2006). However, no study has performed a systematic fate map analysis of RDVM cells, to determine their precise relationship with the hypothalamus.

All DVM cells, including RDVM cells, originate in a common area of the newly-induced neural plate, a region of the epiblast called '*area a*' – originally described by Schoenwolf as anterior to Hensen's node in a HH4 chick neural plate (Schoenwolf *et al.* 1989; Patten *et al.* 2003). Here they are specified at HH4-5 by prechordal mesoderm (PM), to form *Shh*-expressing DVM cells. The PM is a fan-shaped structure (Adelmann 1922) that forms the anterior-most portion of axial mesoderm, and is the first portion of axial mesoderm to extend from the node/organiser, ahead of the rod-shaped notochord (Kingsbury 1920). Surgical (Patten *et al.* 2003; Shimamura and

Rubenstein 1997; García-Calero *et al.* 2008) or genetic ablation (Chiang *et al.* 1996; Pera and Kessel 1997; Aoto *et al.* 2009; Warr *et al.* 2008) of the PM at HH4 to HH5 results in disruption of forebrain development, in particular, a failure of hypothalamic development (Patten *et al.* 2003; García-Calero *et al.* 2008). The hypothalamic markers *Nkx2.1* and *Shh* are not induced, and embryos develop with holoprosencephaly, a failure of the prosencephalon to split into two hemispheres, and cyclopia. Further studies revealed that the PM induces hypothalamic character, including expression of *Shh* and *Nkx2.1*, in the DVM over a short but critical time window (Shimamura and Rubenstein 1997; Cordero *et al.* 2004). Further hypothalamic development then appears to occur progressively: ablation of the chick PM at HH5 rescues a caudal mammillary-like region, and ablation at HH5^{+} rescues relatively normal morphology and *Nkx2.1* expression in the hypothalamus (Patten *et al.* 2003; García-Calero *et al.* 2008). In contrast, surgical ablation of the notochord during these stages does not severely disrupt forebrain morphology or expression of forebrain and hypothalamic markers (Patten *et al.* 2003; García-Calero *et al.* 2008). The PM, therefore, is required for the induction of the hypothalamus and for its continued development.

By contrast, a second organiser structure, the anterior neural ridge (ANR, Shimamura and Rubenstein 1997) at the anterior border of the neural plate, appears dispensable for hypothalamic induction; surgical ablation of the ANR demonstrates its requirement for induction of an essential telencephalic gene, *Foxg1*, but reveals that it is not required for induction of the hypothalamus (Shimamura and Rubenstein 1997). In summary, these ablation studies indicate that the PM is required for induction of the DVM, including the hypothalamus.

1.4.3. *Shh* and Nodal act cooperatively to induce the hypothalamus

Both mice *shh*$^{-/-}$ mutants and patients with mutations in the SHH gene recapitulate the cyclopic and holoprosencephalic phenotypes detected in PM ablation studies (Roessler *et al.* 1996; Belloni *et al.* 1996; Chiang *et al.* 1996) and appear to lack a hypothalamus. This suggests that *Shh* is required for induction of the hypothalamus. In support of this, *Shh* is produced by the

PM (Martí *et al.* 1995). However, since studies show that *Shh* is required as a survival factor for PM cells (Aoto *et al.* 2008; Aoto *et al.* 2009; Ellis *et al.* 2015), it raises the possibility that *Shh* operates indirectly, i.e. controlling expression of an unknown factor X in the PM. *Shh*-null mice do indeed show an excessive apoptosis of PM cells indicating that *Shh* is required for PM survival (Aoto *et al.* 2009). However, while the PM can be rescued in *Shh*$^{-/-}$ *Gli3*$^{-/-}$ double mutants, the ventral hypothalamus is not rescued and no *Nkx2.1* expression is detected. This indicates that *Shh* release from the PM is directly required for induction of the hypothalamus (Aoto *et al.* 2009). Further support for this idea comes through *ex vivo* gain-of-function studies in mice and chick that have demonstrated that exposure of neural plate explants to recombinant *Shh* protein induces expression of *Nkx2.1* (Ericson *et al.* 1995; Shimamura and Rubenstein 1997; Dale *et al.* 1997). At the same time, loss-of-function studies *ex vivo* show that when the PM is treated with anti-*Shh* antibodies, it is unable to induce *Nkx2.1* expression in similar neural plate explants (Dale *et al.* 1997). It is important to note, however, that in all these studies, the neural plate is likely to have already undergone some pre-patterning, such as complementary expression of *Six3* and *Irx3* (Kobayashi *et al.* 2002). Exposure of mice anterior neural plate explants to recombinant *Shh* resulted in expression of *Nkx2.1*, but exposure of posterior explants resulted in expression of *Foxa2*, a characteristic of caudal diencephalic ventral midline and floor plate (*Shimamura and Rubenstein (1997)*. Together these studies show that *Shh* is necessary but may not be sufficient to induce the hypothalamus

A different *ex vivo* study suggests that the TGFβ family member, Nodal may co-operate with *Shh* to induce RDVM character, and hence the hypothalamus. Nodal and *Shh* are co-expressed in the PM at HH4, a time that it induces '*area a*' cells to a DVM identity. Exposure of '*area a*' explants to low levels of *Shh* is insufficient to induce *Shh* expression, However, Nodal can work synergistically with such low levels of *Shh* to induce *Shh* (Patten *et al.* 2003). Morover, unpublished studies (Placzek lab) show that BMP signalling can induce Nodal and BMPs have been previously shown to acts synergistically with *Shh* to induce the hypothalamus (Dale *et al.* 1997; Ohyama *et al.* 2005),

potentially via their indirect induction of Nodal.

In vivo studies support the idea that Nodal is required for hypothalamic induction. Analysis of zebrafish Nodal or Nodal pathway mutants, show that Nodal/Nodal signalling is required to induce expression of hypothalamic *Nkx2.1* in zebrafish (Rohr *et al.* 2001; Mathieu *et al.* 2002). In mice, loss of Nodal activity in knockout mice halts development at gastrulation stages, precluding analysis of the hypothalamus (Lowe *et al.* 2001). However, heterozygous Nodal mutant mice exhibit disrupted forebrain development and a holoprosencephaly-like phenotype (Lowe *et al.* 2001; Andersson *et al.* 2006). Similarly in chick, pharmacological blocking of both *Shh* and Nodal signalling leads to reduction or loss of *Nkx2.1* expression, and manifestation of cyclopia and holoprosencephaly (Mercier *et al.* 2013). Finally, humans with mutations in the NODAL signalling pathway display holoprosencephalic phenotypes (Gripp *et al.* 2000; Roessler *et al.* 2009). Collectively, these studies demonstrate a cooperative role of *Shh* and Nodal signalling in induction of the hypothalamus during the neural plate stage. The precise mechanism of how these components work together remains poorly understood.

1.4.4. Activation of *Shh* expression in the hypothalamus

Studies in mouse have revealed that PM-derived *Shh* can induce hypothalamic character through Gli-mediated signalling to transcriptionally activate transcription factors in the hypothalamus (Park *et al.* 2000; Geng *et al.* 2008; Aoto *et al.* 2009; Zhao *et al.* 2012). In both $Shh^{-/-}$ $Gli3^{-/-}$ mouse mutants and in double *Gli1/2* mutant mice, expression of *Shh* and *Nkx2.1* in the hypothalamus are lost (Aoto *et al.* 2009; Park *et al.* 2000). Activation of hypothalamic *Shh* appears to require synergistic activity from the *Six3* transcription factor; 70% of haploinsufficient *Six3* mutant mice exhibit holoprosencephaly, but when crossed with *Shh* heterozygous mutant mice, 100% of embryos manifest holoprosencephaly and loss of hypothalamic *Nkx2.1* expression (Geng *et al.* 2008). Further studies show that *Six3* can directly activate *Shh* expression by binding to and activating a particular *Shh* enhancer that regulates expression in the hypothalamus and diencephalon,

Shh Brain Enhancer-2 (SBE2) (Jeong *et al.* 2008). Members of the SoxB1 family, which encode high mobility group (HMG)-containing transcription factors (Pevny and Placzek 2005), have also been reported to be required for upregulation of hypothalamic *Shh* and *Nkx2.1* expression (Zhao *et al.* 2012; Ferri *et al.* 2013). Similarly to *Six3*, Sox2 and Sox3 have been shown to directly bind and activate SBE2 *in vitro*, and thus can activate SBE2-driven *Shh* expression in the hypothalamus (Zhao *et al.* 2012). Together, these studies begin to unravel a possible general mechanism of hypothalamic induction, in which Nodal is required to modulate the RDVM's response to PM-derived *Shh* to activate GLI-mediated upregulation of transcription factors that, working in co-operation with *Six3*, Sox2 and Sox3, further upregulate and maintain expression of *Shh* and *Nkx2.1* and hence hypothalamic character.

1.4.5. Further hypothalamic development requires downregulation of Shh

The expression of hypothalamic *Shh* is both spatially and temporally dynamic. As outlined above, *Shh* is initially expressed in the ventral midline of the hypothalamus. Subsequently, *Shh* is downregulated in part of this

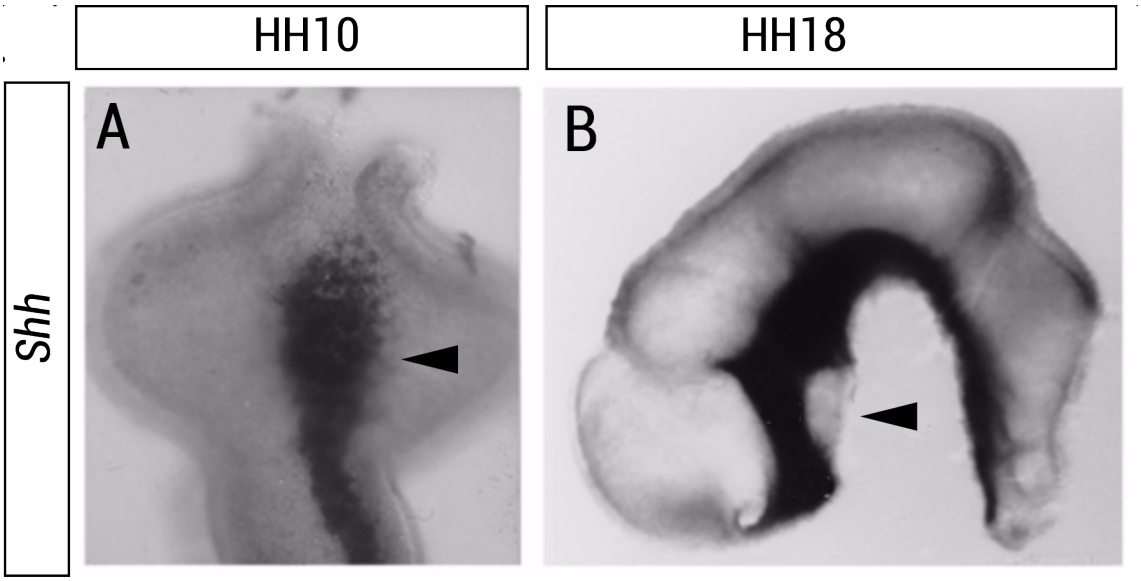

Figure 1.4 | Expression of *Shh* in the hypothalamus is dynamic
(A) Flat mount view of HH10 embryo showing expression of *Shh* in the ventral midline of the hypothalamus. (B) Wholemount side view of HH18 embryo showing expression of Shh. Between HH10 and HH18, *Shh* is downregulated in the ventral midline and induces its own expression in the adjacent basal and anterior hypothalamus. Images were taken from Manning *et al. (2006)*.

ventral midline hypothalamus; (Fig.1.4; Manning *et al.* 2006; Alvarez-Bolado *et al.* 2012). Recent studies in chick and mice shows that downregulation of *Shh* in the tuberal hypothalamus is required for the appearance of additional markers, including that of *Emx2*, a marker expressed in the mammillary hypothalamus (Manning *et al.* 2006; Trowe *et al.* 2013).

Shortly after the onset of hypothalamic *Shh* expression in the RDVM/ hypothalamic ventral midline, a variety of signals in the PM, including chordin and Nodal, are downregulated (Dale *et al.* 1997; Ellis *et al.* 2015). As a consequence, BMP signalling is now activated in the PM (Dale *et al.* 1997; Ohyama *et al.* 2008; Ellis *et al.* 2015). BMPs from the PM now downregulate *Shh* in the overlying hypothalamic ventral midline. (*Manning et al. (2006)* demonstrated that BMP does so by upregulating the transcriptional repressor, *Tbx2* in *Shh*-expressing hypothalamic ventral midline cells, which in turn leads to downregulation of *Shh* in a cell-autonomous manner. At this point, *Tbx2*$^{+}$ *Shh*$^{-}$ cells begin to define the future ventral tuberal and mammillary hypothalamus. BMP-mediated downregulation of *Shh* is important for further patterning of the hypothalamus: upregulation of the tuberal and mammillary marker genes, *Fgf10* and *Emx2* in explants requires BMP activity (Manning *et al.* 2006). Studies in mice and zebrafish suggest this process is widely conserved (Thisse *et al.* 2004; Pontecorvi *et al.* 2008; Trowe *et al.* 2013). *Tbx2* and Tbx3 are expressed in the forming ventral/basal hypothalamus of mouse, and have been shown to sequester Sox2 from binding to SBE2. In this way, Tbx repressors prevent Sox2 from maintaining expression of *Shh* (Pontecorvi *et al.* 2008; Trowe *et al.* 2013).

Intriguingly, it was also noted that cell cycle dynamics was altered by the BMP-mediated downregulation of Shh. At HH8, dividing cells in S-phase, detected through BrdU (bromodeoxyuridine) labelling, were detected in the ventral midline of the prospective ventral tuberal and mammillary hypothalamus. In contrast, at HH10, BrdU^{+} cells were minimally detected in the ventral tuberal and mammillary hypothalamus, however, this cell cycle arrest is transient as increased levels of BrdU^{+} cells were detected by HH13 (Manning *et al.* 2006). This transient cell cycle arrest and subsequent return to cell cycle was demonstrated, in vivo, to be dependent upon the BMP-Tbx2

pathway. The addition of chordin-soaked beads at HH5, an antagonist of BMP signalling, resulted in increased levels of $BrdU^+$ cells at HH10 when minimal levels of $BrdU^+$ cells were expected. Furthermore, electroporation of RNA interference vectors that target *Tbx2* in the ventral tuberal and mammillary region at HH10 resulted in maintained *Shh* expression and loss of pH3 (phospho-HistoneH3) expression, a mitotic marker, compared to loss of *Shh* expression and high levels of pH3 expression in controls (Manning *et al.* 2006). These observations suggest that downregulation of *Shh* by the BMP-*Tbx2* pathway is important to effect a transient cell cycle arrest followed by a synchronised proliferation that results in an expansion of the ventral tuberal and mammillary region.

1.4.6. Role of neuroepithelial-derived *Shh* in the hypothalamus

In vivo grafting studies and *ex vivo* studies in chick show that prior to its downregulation, *Shh* from the ventral midline of the hypothalamus induces its own expression in the adjacent basal, which encompasses the anterior and lateral hypothalamus (Fig.1.4; Ohyama *et al.* 2005; Ohyama *et al.* 2008; Manning *et al.* 2006; Alvarez-Bolado *et al.* 2012). As yet the role of *Shh* expressed in the hypothalamus is not fully understood. To study this, several studies have analysed the hypothalamus in conditional *Shh* knockout mutant mice and fish

Szabó et al. (2009) used a Foxb1-driven Cre to delete exon-2 of the *Shh* locus in Foxb1-lineage cells, resulting in expression of truncated and non-functional *Shh* mRNA (Zhao *et al.* 2007). In mice, Foxb1 is expressed in the spinal cord and extends to the diencephalon. Foxb1 is transiently and weakly expressed in the diencephalon at E8.5 including the ventral midline, and Foxb1-driven Cre recombination activity is detected in the ventral diencephalon where it extends to the eye level, a region termed suboptic (a region likely to be equivalent to the suprachiasmatic area, on the basis of relative position to the optic stalk). Analysis for *Shh* exon-2, which labels non-truncated functional *Shh* mRNA, shows that functional *Shh* mRNA is lost in the ventral hypothalamus, diencephalon, midbrain, and hindbrain as early as E8.5 (no comment was made regarding the spinal

cord). Thus, in these mice, functional *Shh* would likely be missing from the entire ventral midline of the neural tube but not from the PM. Full-length *Shh* was detected ventral to the suboptic region, and expression of *Shh* receptor, *Ptch1*, and effector, Gli1, is maintained in this region. However, as predicted through earlier studies in chick, showing that ventral midline-derived *Shh* induces its own expression in the basal hypothalamus (Ohyama *et al.* 2005; Ohyama *et al.* 2008; Manning *et al.* 2006), expression of *Shh* is lost in the basal hypothalamus and zone of intrathalamica limitans (ZLI), an organiser structure in the p2/p3 prosomere boundary. Further, *Szabó et al. (2009)* reported that mutant mice exhibited a reduction in *Nkx2.1*, a loss of markers of the mammillary hypothalamus, such as *Dlx*2 and Dbx2, and a reduced number of pro-melanin concentrating hormone (pmch)-labelled neurons and absence of hypocretin-orexin (Hcrt)-labelled neurons in the lateral hypothalamus. Together these results suggest that hypothalamic ventral midline-derived *Shh* is required for further development of the hypothalamus.

In another study, *Shimogori et al. (2010)* used *Nkx2.1*-driven Cre to delete *Shh* in *Nkx2.1*$^{+}$ hypothalamic cells from E10.5; i.e. a time when expression of *Shh* is detected in anterior and basal hypothalamus but is already downregulated in the ventral hypothalamic midline. *Shimogori et al. (2010)* report that the mutant mice exhibit a thinning of the anterior and tuberal hypothalamic neuroepithelium and absence of markers associated with anterior and tuberal neurons (*Nr5a1*, *pomc*, and *Nkx6.2*). Additionally, expression of Lef1, which labels a rostral mammillary region termed pre-mammillary hypothalamus, is reduced in size. The authors suggested that *Shh* from the anterior/basal hypothalamus is needed for late aspects of neuronal differentiation in the anterior/tuberal hypothalamus and for the maintenance of the pre-mammillary region.

Zhao et al. (2012) used a hypothalamic-specific upstream regulatory element of Shh, SBE2 (Jeong *et al.* 2006), to drive Cre expression and delete *Shh* in the hypothalamus from E9.5. As in the *Shimogori et al. (2010)* study, *Shh* has already been downregulated in the ventral hypothalamic midline and is secondarily induced in the anterior and basal hypothalamus and thus,

the phenotypes reported in this study are likely to reflect a role for basal/anterior, rather than ventral-derived SHH signalling. Moreover, since the caudal mammillary hypothalamus contains a redundant enhancer, SBE4, it suggests that functional SHH will be maintained in the caudal mammillary but deleted in the anterior and basal hypothalamus (Jeong *et al.* 2006). Loss of functional *Shh* in the mutant mice led to anteroposterior hypothalamic patterning defects. In particular, the authors noted a reduction in Six6 expression in the anterior hypothalamus at E10.5 and a concomitant increase in expression of *Fgf10* and *Bmp4*, genes whose expression normally mark the tuberal/mammillary hypothalamus. *Tcf4*, a member of the HMG-box TCF/LEF family of transcription factors involved in Wnt/β-catenin signalling (Cadigan and Waterman 2012), is also expressed in the anterior hypothalamus and shares an overlapping domain with Six6 and, in wild-type mice, is rostral to *Bmp4* and *Fgf10*. However, *Tcf4* expression domain is not affected in the mutant mice and shares overlapping expression with ectopically expanded *Fgf10* and *Bmp4* expression. On this basis, *Zhao et al. (2012)* argue that *Shh* deriving from the anterior and basal hypothalamus is required to maintain gene expression boundaries, rather than to promote the formation of anterior hypothalamic cells. However, analysis of these embryos at later stages of development (E12.5), *Zhao et al. (2012)* reveals a size reduction in an area termed the retrochiasmatic area of the hypothalamus, which lies between *Foxg1*$^{+}$ telencephalon and *Tbx2*$^{+}$ infundibulum. Additionally, the infundibulum displays dysmorphic morphology: the infundibulum fails to evaginate properly and is ectopically positioned. Together, the mouse studies show a role for neuroepithelial-derived *Shh* in further growth, patterning, and differentiation of the hypothalamus. However, the phenotypes of the hypothalamus in the conditional knock out animals are complex, and the mechanism through which *Shh* governs these remains unclear.

A recent study in our lab (Muthu *et al.* 2016) has begun to address the mechanism of how neuroepithelial-derived *Shh* may regulate growth and differentiation, through studies in the zebrafish anterotuberal hypothalamus. *Muthu et al. (2016)* report that pharmacological blocking of Shh signalling in

zebrafish embryos at 28hpf (a time when *Shh* is expressed in the anterior and basal hypothalamus) resulted in a size reduction of the anterior and tuberal hypothalamus and the loss of its resident neurons. This is consistent with mice mutants suggesting a role for *Shh* in hypothalamic growth and differentiation. *Muthu et al. (2016)* additionally show that growth and differentiation in the anterotuberal hypothalamus requires a cooperation of retinal homeobox gene 3 (Rx3) and *Shh* activity. Rx3 is required to select for *rx3*$^{+}$ progenitors that will migrate anteriorly and give rise to tuberal/ anterior hypothalamic neurons. Chokh (chk) zebrafish mutants that lack functional Rx3 (Kennedy *et al.* 2004) fail to develop anterior-most expression of *Shh* and accumulate *rx3*$^{+}$ progenitors that either fail to differentiate or undergo apoptosis (Muthu *et al.* 2016). Pharmacological blocking of Shh signalling provided evidence to suggest that Shh signalling governs growth and differentiation in the anterior hypothalamus by acting as an on-off switch for *rx3* and thus selects for *Shh*$^{+}$ *rx3*$^{-}$ progenitors and promotes their differentiation.

In summary, these studies in mice and zebrafish show that Shh signalling from the hypothalamic neuroepithelium is required for normal growth and differentiation in the anterior, tuberal, and mammillary hypothalamus. Additional studies using mouse embryos, in which WNT and BMP signalling in the hypothalamus is disrupted, suggest complex interactions between these signalling ligands and *Shh* (Brinkmeier *et al.* 2007). As yet, these are poorly understood. Nonetheless a clear conclusion is that the hypothalamus grows and develops over an extended period and requires Shh signalling for this. Further zebrafish studies demonstrate that growth of the anterior hypothalamus is driven by anisotropic growth of progenitor cells derived from *rx3*$^{+}$ territory. However, as yet, we do not know where the *rx3* cells originate. Are they hypothalamic or do they originate from re-specified telencephalic or diencephalic cells?

1.5. Development of the Pituitary

The pituitary gland links the nervous and endocrine systems, allowing the hypothalamus to control body homeostasis via the hypothalamo-

pituitary neuraxis (Pearson and Placzek 2013). The pituitary gland consists of two halves: the anterior lobe/pituitary (adenohypophysis) and posterior lobe/pituitary (neurohypophysis). The posterior pituitary is derived from the hypothalamus, specifically from the infundibulum of the tuberal hypothalamus (Pearson *et al.* 2011); the anterior pituitary is derived from an embryonic structure termed Rathke's pouch (RP), which is not neural in origins but derived from tissue anterior to the neural plate (Sánchez-Arrones *et al.* 2015).

The infundibulum develops as an outgrowth (or evagination) from the tuberal hypothalamus and throughout development, the tip of RP (the future dorsal-most part of the anterior pituitary) abuts the infundibulum (Fig.1.5). This spatial relationship is important: development of RP is dependent on signals originating from the diencephalon, initially, and from the infundibulum at later stages (Rizzoti and Lovell-Badge 2005). Here, I outline our current understanding of infundibulum development and the importance of the ventral hypothalamus and infundibulum in development of RP.

1.5.1. FGFs govern outgrowth of the infundibulum

Fate mapping in chick embryos have revealed that the infundibulum is composed of different cell types with distinct origins in the RDVM (Pearson *et al.* 2011). A relatively anterior RDVM population forms a horseshoe-shaped 'collar' around an adjacent posterior RDVM population (Fig.1.5B). The horseshoe-shaped cell population are called collar cells and the posterior cell population is termed non-collar ventral midline. Collar cells are an interesting cell population. They express Sox3, a marker which is associated with stem cells (Pevny and Placzek 2005; Sarkar and Hochedlinger 2013), and possess progenitor-like properties; *in vitro* explant studies have shown that collar cells are highly proliferative and can differentiate into neurons, glial cells, unidentified pigmented cells, as well as infundibular-like cells. *Pearson et al. (2011)* proposed a model of infundibulum morphogenesis in which outgrowth of the infundibulum is driven by collar cells: in this model, collar cells give rise to descendants that form the walls of the

developing infundibulum. This process requires FGFs. Fgfs are initially expressed in the tuberal hypothalamus, then subsequently restricted to the infundibulum in chick, mice, and zebrafish (Manning *et al.* 2006; Pearson and Placzek 2013; Ohuchi *et al.* 2000; Tsai *et al.* 2011; Herzog *et al.* 2004). *Pearson et al. (2011)* demonstrated, *in vitro*, that proliferation of $Sox3^{+}$ collar cells requires FGF signalling; thus in the absence of FGF, it is proposed that the lack of proliferation in collar cells results in failure of descendants and hence failure of infundibular outgrowth. Consistent with this idea, other studies show that loss of FGF activity results in disrupted infundibular development. In *Fgf10*-null mutant mice, the infundibulum fails to evaginate and undergoes apoptosis (Ohuchi *et al.* 2000). In zebrafish, Fgf3 is required for maintenance of an infundibulum-like structure (Liu *et al.* 2013). In addition to driving proliferation and outgrowth of the infundibulum, FGFs have also been shown to be important for guidance of axons to the infundibulum in zebrafish (Liu *et al.* 2013).

Together, these studies show the importance of FGF signalling in driving formation of the infundibulum. In addition, they suggest that cells with stem/progenitor potential form in a region of the hypothalamic ventral midline that is in close proximity to the infundibulum.

1.5.2. Development of Rathke's pouch is dependent on signals from the ventral diencephalon

Development of Rathke's pouch is a multi-step process involving (1) induction of the hypophyseal placode from the oral ectoderm, (2) invagination of the placode to become RP (Fig.1.5A), (3) fate commitment, and (4) expansion and terminal differentiation (Sheng *et al.* 1997; Rizzoti 2015). Several studies have shown that RP development is dependent on secreted signalling ligands, first from the ventral diencephalon and then from the infundibulum (Daikoku *et al.* 1982; Takuma *et al.* 1998; Gleiberman *et al.* 1999). In amphibians, ablation of the infundibular primordium results in disrupted development of RP and absence of differentiated cells (Kawamura and Kikuyama 1998). Additionally, transplant studies in chick demonstrate that ventral diencephalic tissue can ectopically induce a RP-like structure

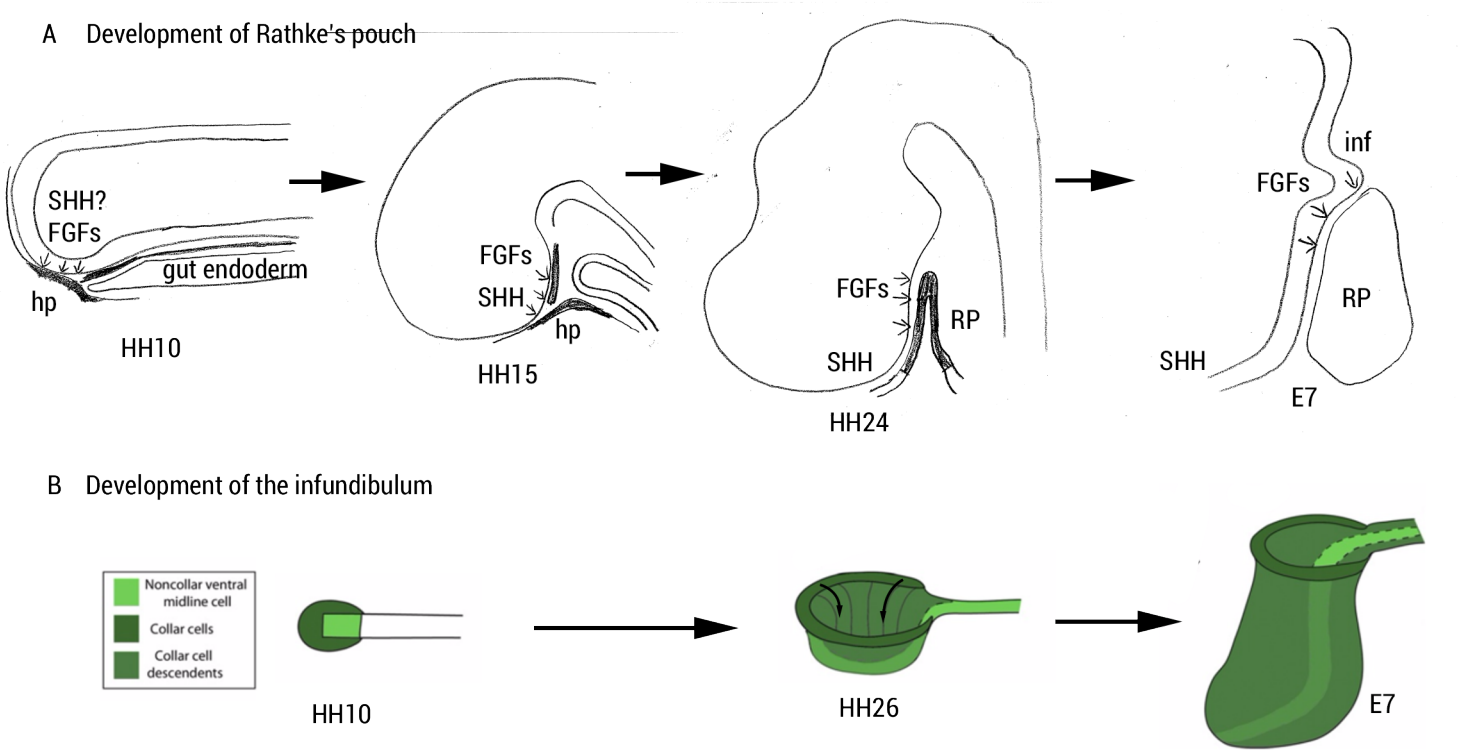

Figure 1.5 | Morphogenesis of Rathke's pouch and the infundibulum

(A) Development of Rathke's pouch (RP). The RP is initiated through induction of the hypophyseal placode (hp) in the oral ectoderm. Signals emanating from the ventral diencephalon are implicated to have RP-inducing properties over the underlying hp (small arrows). Subsequently, a hp forms a pouch rudiment and begins to invaginate towards the ventral diencephalon and future infundibulum. Eventually RP will bud off from the oral ectoderm in a process termed individualisation, an apoptotic-dependent process. Throughout development of RP, signals emanating from the ventral diencephalon are required for normal development. (B) Development of the infundibulum can be traced as early as HH10, when a population of rostral diencephalic ventral midline cells begins to surround a posterior population (light green) to form a collar (dark green). At the onset of infundibulum outgrowth/evagination, these collar cells give rise to cells that will populate the walls of the evaginating infundibulum. Schematic of infundibulum development taken from PEARSON *et al. (2013)*.

in head ectoderm, (Gleiberman *et al.* 1999). What, then, are these signals emanating from the ventral diencephalon? In both *Fgf10*-null mice, and mice that lack the FGF10 receptor (FGF receptor 2 isoform IIb (*FgfrIIIb*)), the infundibulum fails to develop, and at the same time, RP is underdeveloped and shows high levels of apoptosis (Ohuchi *et al.* 2000; De Moerlooze *et al.* 2000).

Shh is also implicated in RP development. As is the case with BMP and FGF, its precise role is difficult to dissect because it both directly and indirectly influences RP development. Loss of *Shh* at early stages results in a rostral shift of *Fgf10* and *Bmp4* and an ectopic duplication of RP (Zhao *et al.* 2012). The *Shh* receptor, *Ptch1*, and the Gli transcription factors are expressed in RP, suggesting that these cells can directly respond to Shh signalling (Treier *et al.* 2001). *Shh* is also expressed in the oral ectoderm initially, but is subsequently downregulated in RP (Treier *et al.* 2001). Nonetheless, dysregulation of the SHH pathway in human patients have proposed that Shh signalling may be required for the individualisation of RP as these human patients retain this link between the RP and oral ectoderm (Rizzoti 2015).

In summary, development of RP requires signals produced from the ventral diencephalon and infundibulum. However, the precise role of these signals has not been elucidated.

1.6. Thesis Aims

Development of the hypothalamus is a complex process. Past efforts have focused on elucidating the mechanism governing hypothalamic induction, and on the manner in which protracted Shh signalling is important in continued development of the hypothalamus. Our understanding has been informed by work in both the chick and the mouse. One of the main challenges in studying the hypothalamus is the lack of promoters that are associated with a specific region of the hypothalamus at early stages of development; this limits mouse genetic approaches to dissect early hypothalamic development. Another challenge is the complex anatomy of

the hypothalamus; since the earliest description of forebrain organisation in the 1890s, there is still much debate regarding forebrain organisation today, and much of this debate is centered around the hypothalamus. To this end, we still do not have a complete and accurate understanding of where the hypothalamus or hypothalamic progenitors are located at various stages of development, including the neural plate and early neural tube stage.

Many questions regarding hypothalamic development, therefore, still remain. In this thesis I set out to use the chick embryo as a model system. I hypothesised that systematic fate mapping of the RDMV (medial and posterior prosencephalic ventral midline) would provide a new model for hypothalamic development. Amongst the questions that I aimed to address were the following:

- Does the hypothalamus and its neighbouring structures develop as transverse compartments according to the prosomeric model?
- What is the relationship between the hypothalamus and the prechordal mesoderm after DVM specification?
- How is the hypothalamus regionalised along the rostrocaudal axis?
- What is the precise role/mechanism of action of neural-derived Shh?
- How does the infundibulum develop where it does?
- How is the formation of the infundibulum linked with development of Rathke's pouch?

I therefore set out to (1) systematically fate map the ventral midline of the prosencephalon during the early neural tube stage to identify the anteroposterior boundary of the hypothalamus. In addition, I wished to gain insight into morphogenesis of the developing hypothalamus during early stages (Chapters 3, 4). (2) With a map of the hypothalamic territory, I aimed to examine gene expression data to determine whether the hypothalamus is regionalised during early neural tube stages (Chapter 5). (3) On the

basis of my results, I proposed and tested a new model for hypothalamic development (Chapter 6).

Chapter 2
Materials and Methods

2.1. Chick husbandry and embryo techniques

Fertilised Bovan brown chicken eggs (Henry Stewart & Co, Norfolk, UK) were incubated in humidified 37˚C incubators and staged according to *Hamburger and Hamilton (1951)*. All experiments involving live chick embryos conformed to the relevant regulatory standards (University of Sheffield).

2.1.1. Fate mapping of the ventral prosencephalon

Hamburger and Hamilton stage (HH)10 (9-10 somite) embryos were accessed *in ovo* by making a small opening in the egg shell, on the side of the air sack, and removing the shell membrane. Blue food colouring dye (Dr. Oetker, discontinued) was diluted 1:5 in Leibovitz's L-15 medium (Thermo Fisher, 11415056) and injected into the yolk sac, underneath the embryo, in order to visualise the embryo and the prechordal mesoderm. The ventral prosencephalon was accessed by first surgically removing the vitelline membrane overlying the prosencephalon, then surgically incising the prosencephalon along the dorsal anteroposterior midline. To identify injection sites along the anteroposterior ventral midline, two methods were used. The first method utilised a microscope graticule to measure the distance

In the first method, the posterior and medial ventral midline was systematically fate mapped along the anteroposterior axis by using a microscope graticule to measure the distance away from the prosencephalic neck. In the second method, ventral midline cells were partitioned into four regions relative to the underlying anterior, medial, or posterior prechordal mesoderm or anterior to the prechordal mesoderm.

Fluorescent lipophilic membrane dyes were focally injected into the desired area using a picospritzer II microinjection system (Parker Instrumentation; optimal settings: 19psi, 4-9msec pulse) under a fluorescent stereomicroscope (Leica, MZ10 F). Dyes were injected through 0.78mm-thick borosilicate glass needles (Harvard Warner, GC100TF-10), which were pulled by a micropipette puller (Sutter Instrument Co., P-97; optimal settings: heat=350, pull=200, velocity=150, time=200).The fluorescent lipophilic dyes used were CellTracker CM-DiI (Life Technologies, C7000) and Vybrant DiO (Life Technologies, V22886), which were reconstituted in absolute ethanol to a final concentration of 5mg ml-1. CM-DiI is designed to retain fluorescence after the *in situ* hybridisation process and was specifically used when a subsequent fluorescent *in situ* hybridisation was required.

After injections, the dorsal incision in the neural tube was closed and embryos were imaged with a fluorescent stereomicroscope (Leica, M165 FC) to document the injection site. Eggs were then re-sealed with parafilm and tape, then placed into a humidified 37˚C incubator for 48 hours or 4 days to approximately HH20 and HH27, at which point, embryos were extracted and fixed, overnight, in 4% paraformaldehyde. Embryos were washed in phosphate-buffered saline (PBS) and hemi-dissected, or in some cases, fully dissected to reveal the neuroepithelium then imaged under a fluorescent stereomicroscope. Embryos were then processed by *in situ* hybridisation on transverse sections.

n.b. It is important to note that occasionally, the lipophilic dyes will form crystals after injections, likely due to unincorporated dye clustering together as a consequence of their hydrophobic nature; these crystals remain fluorescent and can be seen during analysis (e.g. x in Fig.4.10B).

These crystals are free-floating and often can be removed carefully. However, they have a tendency to stick to the neuroepithelium and in the interest of preserving embryo morphology, they are usually not removed. In cases where the crystals are removed, fluorescence is no longer detected in its proximity, suggesting that these fluorescent crystals do not label surrounding tissue.

2.1.2. Summary of fate maps

A summary schematic of fate maps (Fig.4.12A) was generated by collating all fate mapping experiments and measuring the position of the injection site relative to the prosencephalic neck. Injections based on measurements and underlying PM were both included. To measure the relative positions, a percentage-based method was used due to variable lengths between the prosencephalic neck and anterior neuropore.

2.1.3. EdU labelling

Proliferating cells was detected in sagittal sections using the Click-iT EdU Alexa Fluor 488 kit (Life Technologies, C10337). Embryos were treated *in ovo* with 200µl 0.5mM EdU then resealed and incubated for 90 minutes. These parameters were experimentally optimised; embryos treated with 200µl 0.5mM EdU for 1h, 1.5h, and 2h showed that a 1h treatment is insufficient time for EdU penetration into the inner layers of the embryo (n=4) and that 1.5h (n=3) and 2h (n=4) treatment showed no difference in labelling (data not shown).

Embryos were then fixed and sectioned as described below (see 2.2.1). Staining for EdU in sections was conducted in accordance with the manufacturer's protocol. Following EdU staining, slides were mounted with DAPI-containing Fluoroshield (Sigma) and imaged with a Zeiss AxioImager. Z1 using the ApoTome.2. Quantification of number of EdU-labelled cells and DAPI-labelled nuclei were carried out in Adobe Photoshop using the count tool.

2.1.4. Cyclopamine treatment of embryos

A concentration curve analysis was conducted to determine the optimal concentration of cyclopamine required to inhibit Shh signalling (Fig.2.1). Cyclopamine (reconstituted in ethanol) was diluted in PBS to a final concentration of 0.24mM, 0.48mM, and 0.6mM. Embryos treated with 0.24mM of cyclopamine exhibited weak levels of *Ptch1*, a readout of Shh signalling, and embryos treated with 0.6mM of cyclopamine exhibited absence of *Ptch1* but high death rates were observed (n=5/7 deaths). Embryos treated with 0.48mM cyclopamine displayed absence of *Ptch1* (n=7/7) and low death rates (n=2/9 deaths).

Cyclopamine was applied to embryos *in ovo* by removing the vitelline membrane overlying the prosencephalon and pipetting 5µl of 0.48mM cyclopamine over the prosencephalon. Embryos were then resealed with parafilm and tape, then incubated in a humidified 37˚C incubator until the desired stage. Embryos were then fixed in 4% paraformaldehyde and further processed by *in situ* hybridisation or immunohistochemistry.

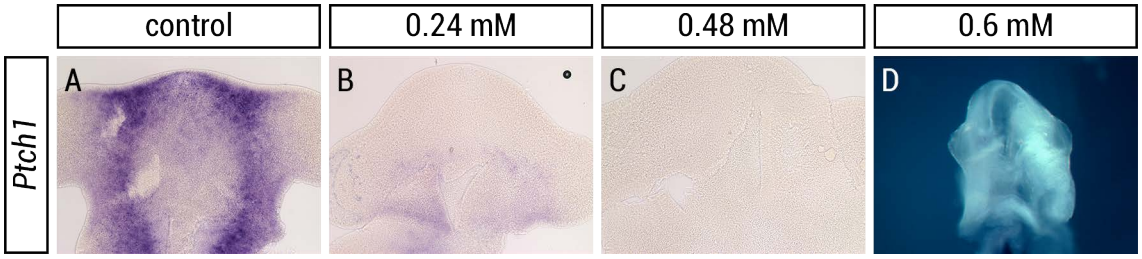

Figure 2.4 | Cyclopamine concentration curve analysis

(A-D) Ventral flat-mount view (A-C) or ventral wholemount view (D) of HH10-11 embryos showing *Ptch1* expression after treatment with PBS (control) or cyclopamine at HH9. (A) *Ptch1* is detected in control embryos (n=6/6). (B) Weak expression of *Ptch1* is detected (n=5/5) in embryos treated with 0.24µM cyclopamine. (C-D) *Ptch1* is not detected in embryos treated with 0.48µM (n=7/7) or 0.6µM cyclopamine (n=2/2).

2.1.5. Dissections and flat-mounting

In this thesis, whole mount embryos were presented as extracted neuroepithelium, hemi-dissected heads, or flat-mounted neuroepithelium. All dissections were performed using a pair of No.5 forceps (Dumont, 11251-20) and spring scissors (Vannas, 15018-10) after fixation in 4% paraformaldehyde. HH10-HH13 dissected neuroepithelium were flat

mounted by embedding the neuroepithelium ventral side up in preheated glycergel (Dako, C056330-2) on a slide, then solidified at 4˚C. To flat mount the embryo, a coverslip was placed above the solidified glycergel followed by melting of glycergel on a top of a hot plate or steam from microwaved boiling water. The coverslip is then sealed with nail varnish to prevent evaporation.

2.2. Histological techniques

2.2.1. Toluidine blue staining

Embryos were fixed in 4% paraformaldehyde overnight, sunk in 30% sucrose overnight, then cryosectioned at 15µm thickness. Slides were rehydrated in tap water, rapidly dipped in toluidine blue solution (10mg ml-1 toluidine blue and 10mg ml-1 sodium borate in deionised water) 10 times, then rinsed in tap water to remove excess toluidine solution. Slides were dehydrated in isopropanol for 20-30 dips, then dipped in 50-50 isopropanol and xylene for 10 dips, then cleared in xylene with 10-20 dips. Slides were coverslipped with DPX mountant (Sigma), then imaged with a compound light microscope (Olympus BX60).

2.2.2. Preparation of embryos for analyses in whole mount and sections

Embryos were collected at desired stages after incubation at 37˚C and fixed in 4% paraformaldehyde (PFA) at 4˚C overnight.

For analysis on sections, embryos were washed in phosphate-buffered saline (PBS; Sigma, P4417), then cryoprotected in 30% (w/v) sucrose (Sigma, S0389) in 0.2M phosphate buffer at 4˚C overnight. To further promote cryoprotection and thus, morphology of sections, two small windows were surgically incised into the neuroepithelium to promote fluid flow into the third ventricle. Tissues were orientated in optimal cutting temperature solution (OCT; VWR, 361603E) then frozen on dry ice. The frozen samples were then sectioned using a cryostat (Bright Instruments, OTF) at 15µm

thickness. Tissue was collected onto superfrost slides (Thermo Fisher, 10149870) and air dried for up to 4 hours prior to rehydration in PBS or stored in -20˚C for *in situ* hybridisation.

For analyses of whole mount embryos by *in situ* hybridisation, embryos were washed in PBS, then dehydrated through a methanol series of 25%, 50%, 75%, and stored in 100% methanol at -20˚C. For whole mount immunohistochemistry, however, embryos were washed in PBS, bleached in Dent's bleach (1:2 hydrogen peroxide:Dent's fix) overnight -20˚C, then re-fixed and stored in Dent's fix (1:4 DMSO:methanol) at -20˚C.

2.2.3. Riboprobe synthesis

DNA templates for transcription were generated either by linearising plasmids containing the template or by extracting the template using polymerase chain reaction (PCR). Linearisation of 20µg of plasmids was carried out in 100µl reactions in accordance with the manufacturer's protocols. Restriction enzymes from NEB and Promega were used. In the PCR method, M13 primers were used to isolate and amplify the template sequence. BioMix (Bioline) is a complete PCR solution that was used for PCR reactions, and 25-50ng of plasmid DNA was used in 50µl PCR reactions in accordance with the manufacturer's protocol. The PCR setting used is shown below:

1	2m	94˚C
2	30sec	94˚C
3	30sec	55˚C
4	1m	72˚C
5	GO TO 2>35 CYCLES	
6	10m	72˚C
7	END	

The resulting template DNA is purified by phenol-chloroform extraction and ethanol precipitation. DNA pellets resulting from ethanol precipitation were resuspended in double distilled (dd)H2O to a final concentration of 1µg µl-1.

Antisense digoxigenin (DIG)-labelled and fluorescein (FITC)-labelled riboprobes were synthesised by in vitro transcription. A 20µl reaction contained 1µg DNA template, 4µl 5X transcription buffer (Promega), 2µl 10X DIG or FITC RNA labelling mix, 20U RNase inhibitor (Promega), 20U of the appropriate RNA polymerase (Promega), and DEPC-treated H2O. Reaction tubes were incubated in a 37˚C water bath for 2 hours, then for a further 1 hour with added 20U RNase-free DNase I (Promega) to remove template DNA.

Riboprobes were purified using a purification column (illustra ProbeQuant G-50 Micro Columns, GE) in accordance with the supplier's protocol. The resulting 50µl riboprobe-containing elute is diluted in 5-10ml of prehybridisation solution depending on quantity of riboprobe, approximately assessed by gel electrophoresis. This 5-10ml solution was used directly for *in situ* hybridisation.

See table 2.1 for plasmids used in this thesis.

Table 2.1 | plasmids used in this study for *in situ* hybridisations

Probe name	Restriction enzyme or PCR	RNA polymerase	Source
Foxg1	XbaI	T7	gift from Lena Gunhaga (Umeå University, Sweden)
Six3	XhoI	T3	gift from Javier Lopez-Rios
Fgf10	XhoI	SP6	gift from Malcolm Logan
Tbx2	SalI	T7	gift from Malcolm Logan
p57	PCR	T7	from geneservice
p27	PCR	T3	from geneservice
Shh	SalI	SP6	gift from Thierry Lints
Ptch1	SalI	T3	gift from Phil Ingham

2.2.4. In situ hybridisation analyses on whole mount embryos and embryonic sections

Whole mount embryos were rehydrated, through a methanol series, into PBT (0.1% Tween-20 in PBS). Slides with embryonic sections were re-fixed with 4% PFA for 10 minutes, then washed with PBT.

From this point onwards, the protocol for both whole mount and section *in situ* hybridisation is the same. Samples are incubated in prehybridisation solution (see below) for 4 hours at 68˚C, followed by overnight hybridisation at 68˚C with DIG- or FITC-labelled riboprobe. This is followed by two stringency washes to dissociate non-specific hybridisations of the riboprobes: an initial wash in 50% formamide, 5X saline-sodium citrate buffer (SSC), 1% sodium dodecyl sulphate (SDS) for 1 hour and subsequently in 50% formamide, 2X SSC, 1% Tween-20 for 1 hours at 68˚C. Samples are then thoroughly washed in TBST (1X Tris-buffered saline, 1% Tween), then treated with blocking solution (1% heat-inactivated goat serum in TBST) for 90mins at room temperature followed by overnight incubation at 4˚C with anti-DIG- or anti-FITC-alkaline phosphatase (AP) antibody conjugates (1:2000 in blocking solution; Roche, 11093274910, 11426338910). Samples are then thoroughly washed in NTMT (0.1M NaCl, 0.1M pH9.5 Tris, 50mM MgCl2, and 1% Tween-20), then colourimetric reaction is initiated by incubation with 4.5µl ml-1 4-nitro blue tetrazolium chloride (NBT; Roche, 11383213001) and 3.5µl ml-1 5-bromo-4-chloro-3-indolyl phosphate (BCIP; Roche, 11383221001) in NTMT, in the dark. When staining is complete, samples were washed in PBS at room temperature for 10 minutes, then fixed with 4% PFA. Whole mount embryos were stored in 4% PFA at 4˚C. Slides of embryonic sections are dehydrated in methanol then coverslipped with glycergel (Dako, C056330-2).

The reagents to make up prehybridisation solution is shown below:

50%	Formamide
5X	SSC, pH 7.0
2% (w/v)	Blocking powder (Roche, 11096176001)
0.1%	Triton X-100
0.5%	CHAPS

1mg ml^{-1}	Yeast RNA
5mM	EDTA
50µg ml^{-1}	Heparin

2.2.5. Double chromogenic in situ hybridisation for p57Kip2 and Shh

In this thesis, the simultaneous detection of *p57Kip2* and Shh used a modified version of the wholemount *in situ* hybridisation protocol (see 2.3.3). During the overnight riboprobe hybridisation step, DIG-labelled *p57Kip2* antisense riboprobe and FITC-labelled Shh antisense riboprobe were both applied to the slide. The differentially labelled riboprobes were then detected at sequential stages. Shh was first detected through incubation with anti-FITC-AP antibody followed by staining with Fast Red solution (Sigma, F-4523) at room temperature, in the dark. This solution is made by dissolving 1 Fast Red tablet in 4 ml of staining solution (100mM pH8.5 Tris, 50mM MgCl2, 100mM NaCl2, and 0.1% Tween). The embryo were washed with PBT and the enzymatic activity of alkaline phosphatase was deactivated by treatment with 100mM glycine-HCl pH2.2 for 30 minutes. *p57Kip2* was sequentially detected by incubation with the appropriate anti-DIG-AP and stained with NBT/BCIP (see 2.3.3). Embryos were fixed and stored in 4% PFA at 4˚C.

2.2.6. Single and double fluorescent in situ hybridisation

Fluorescent *in situ* hybridisation was carried out using the TSA Plus Cyanine 3/Fluorescein System (PerkinElmer, NEL753001KT) and adapted to the protocol described for chromogenic *in situ* hybridisation (see 2.3.4). Following the riboprobe hybridisation and stringency washes, whole mount embryos or slides were washed with TNT (0.1M pH7.5 Tris-HCl, 0.15M NaCl, 0.5% Tween-20). Sample were then treated with blocking solution (0.5% blocking reagent in TNT) for 90mins at room temperature, followed by a 30 minute incubation at room temperature with anti-FITC-horseradish peroxidase (POD) antibody conjugates (1:500 in blocking solution; Roche 11207733910). Samples were fluorescently stained by a 10 minute room

temperature incubation with FITC-Tyramide (1:50 in 1X Plus Amplification Diluent from TSA kit), in the dark. Samples were thoroughly washed in TNT and whole mount embryos were stored in 4˚C; slides were mounted with DAPI-containing Fluoroshield (Sigma).

For double fluorescent *in situ* hybridisation, peroxidase activity was quenched with 3% hydrogen peroxide in PBS for 30 minutes at room temperature. The antibody and detection steps were then repeated but instead, samples were treated with anti-DIG-POD antibodies and fluorescently stained with Cy3-Tyramide.

2.2.7. Double immunohistochemistry of Lim3 and in situ hybridisation of Fgf10

In this thesis, the simultaneous detection of Lim3 protein and *Fgf10* mRNA on sections was conducted by detecting *Fgf10* first by *in situ* hybridisation (see 2.2.4) then sequentially analysed for Lim3 by immunohistochemistry.

Following *in situ* hybridisation, slides were blocked in blocking buffer (1% HINGS, 0.1% Triton X in PBS) for 2 hours. Slides were then treated with anti-Lim3 antibody in blocking buffer (see Table 2.1 for dilutions) overnight at 4˚C. Primary antibody was then poured off and washed with PBS. This was followed by treatment with secondary antibodies in blocking buffer (see Table 2.2 for dilutions) for 45 minutes at room temperature. The slides were washed with PBS then coverslipped with Fluoroshield.

2.2.8. Whole mount immunohistochemistry of Tuj1

Embryos were collected at HH20 and fixed in 4% PFA at 4˚C overnight. This was followed by PBS washes, bleaching in Dent's bleach (1:2 hydrogen peroxide:Dent's fix) overnight -20˚C, then re-fixing and storage in Dent's fix (1:4 DMSO:methanol) at -20˚C. Embryos were rehydrated in PBS and blocked in blocking solution (5% HINGS, 20% DMSO in PBS) for 60 minutes. Subsequently, embryos were treated with primary antibodies in blocking solution overnight at RT followed by treatment with secondary antibodies in blocking solution overnight at RT. Embryos were then dehydrated in

methanol followed clearing in BABB (1:2 benzyl alcohol:benzyl benzoate).

Table 2.2 | Primary antibodies used in this study

1° Antibody	Species	Dilution	Source
Lim3	Mouse IgG	1:50	DSHB
Tuj1	Mouse IgG	1:100	Covance

Table 2.3 | Secondary antibodies used in this study

2° Antibody	Dilution	Source
Alexa Fluor 488	1:500	Molecular Probes
Alexa Fluor 594	1:500	Molecular Probes

2.3. Image capture and manipulation

2.3.1. Imaging whole mount embryos

Whole mount embryos were imaged under a Leica MZ10F stereo microscope and captured using the Leica LAS X image capture software.

2.3.2. Imaging flat-mounted embryos and embryonic sections

Flat-mounted embryos (see 2.1.4) and embryonic sections were imaged under an Olympus BX60 compound light microscope. Fluorescently labelled flat-mounted embryos and embryonic sections were imaged under a Zeiss AxioImager.Z1 fluorescent compound microscope using an Apotome.2 and captured using the Zeiss ZEN 2 software.

2.3.3. Confocal imaging

To generate a Z stack composite, sequential images of the embryos along the Z axis was captured using a confocal microscope (X,X) and a composite was generated using the Olympus FluoView FV-1000 ASW 1.6 imaging software.

2.3.4. Image manipulation

All image manipulation processes, including fluorescent channel merging were performed in Adobe Photoshop CC 2015.

2.3.5. Measurements of mRNA expression and morphological features

Measurements of the length of mRNA expression domains and mammillary hypothalamus were made in ImageJ (v1.51g).

2.3.6. Statistics

Statistics were performed and graphs were generated in Microsoft Excel and R. The type of test performed was dependent on the nature of the experiment.

Chapter 3
Morphology of the Chick Hypothalamus

3.1. Introduction

As outlined in the main introduction, the origin of the hypothalamus remains a highly debated subject and there is no universally accepted model. Moreover, as yet, no study has attempted to carefully map the origins of different anteroposterior (rostro-caudal) sub-regions of the hypothalamus in the early embryo. In large part, this is because many studies on hypothalamic development are performed in mouse, where fate mapping studies at early neural plate stages is difficult.

I set out to identify (a) the origins of the hypothalamus, and (b) the origins of distinct hypothalamic subregions, using the HH10 chick as a model organism. Before doing this (Chapter 4), I first set out to identify subregions of the developed hypothalamus that would provide a reference for the entire thesis.

3.2. Results

3.2.1. Identification and subdivision of the hypothalamus on the basis of morphology at E5

At embryonic day 5 (E5; HH27), the chick hypothalamus shows a number of morphological features that crudely define its extent and its sub-regions. I found that these are best viewed in wholemount view after removal of the surrounding retina, mesenchymal and ectodermal tissue (Figs.3.1A-C show successive stages in dissection/isolation of the brain). Three morphological landmarks identify the hypothalamus. First, the rostral end of the cephalic flexure (Figs.3.1B,C,F) marks the vicinity of the caudal boundary of the hypothalamus. Second, a hole is left behind after the optic stalk is dissected; the rostral-most region of the hypothalamus is found within the vicinity of the optic stalk. Third, the hypothalamus itself appears as an outgrowth with two curvatures on either side (Figs.3.1B-D).

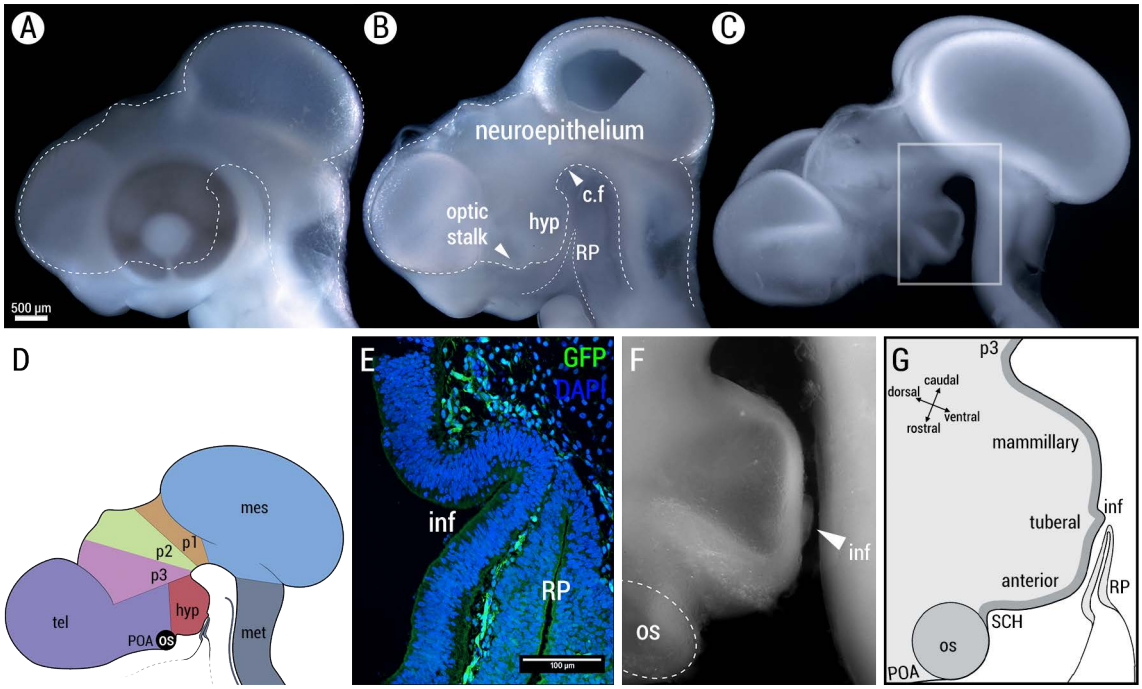

Figure 3.1 | Morphology and subdivisions of the E5 chick hypothalamus

(A-D) Serial images of an E5 chick head (A), in which the eye and mesenchyme is progressively removed to reveal a hemi-dissected chick head (B), and the neuroepithelium (C). (D) Schematic representation of the neuroepithelium, highlighting different brain regions. Dashed lines outline the neuroepithelium (A,B), and Rathke's pouch (B). (E) Sagittal section of E5 transgenic chick expressing cytoplasmic GFP counterstained with DAPI and shows infundibulum in contact with adjacent Rathke's pouch (n=3). (F, G) High power view of boxed region in (C) schematically represented in (G). hyp, hypothalamus; c.f, cephalic flexure; RP, Rathke's pouch; inf, infundibulum; tel, telencephalon; os, optic stalk; p1-3,prosomeres 1-3; mes, mesencephalon (midbrain); met, metencephalon (hindbrain)

A semi-dissected side view of the chick head shows clearly that adjacent to the hypothalamus lies Rathke's pouch, the embryonic precursor to the anterior pituitary (adenohypophysis; Figs.3.1B). Analysis of sagittal sections shows that Rathke's pouch forms immediately next to the hypothalamic infundibulum, the embryonic precursor to the posterior pituitary (neurohypophysis; Fig.3.1E; discussed in Chapter 1.4). The infundibulum can be seen as an outgrowth from the ventral hypothalamus both in sagittal sections and in a fully dissected neuroepithelium (Figs.3.1E-G).

The morphological features that can be seen at E5 (surface morphology and position of Rathke's pouch) suggest the position of three regions along the rostro-caudal axis - anterior, tuberal (medial), and mammillary (posterior) (Fig.3.1G). The anterior hypothalamus extends from the optic stalk and projects downwards towards the oral ectoderm. The tuberal hypothalamus lies above Rathke's pouch, with its thin lumen. The infundibulum serves as a key landmark to identify the caudal tuberal hypothalamus and the tip of the infundibulum aligns exactly with the tip of Rathke's pouch (Ericson *et al.* 1998; Treier *et al.* 1998; Norlin *et al.* 2000). The mammillary hypothalamus lies caudal to the tuberal hypothalamus and Rathke's pouch.

3.2.2. Identification and subdivision of the hypothalamus on the basis of morphology at E3

Similar dissection and isolation of the brain at E3 shows that, as at E5, the position of the hypothalamus at E3 (HH20) can be identified morphologically on the basis of its position between the cephalic flexure and the optic stalk (Figs.3.2A,B). The mammillary hypothalamus has a distinct convex surface anatomy, which is visible in whole mount views and sagittal sections of the embryonic brain (Figs.3.2A-D). At E3, the infundibulum has not yet formed (Pearson *et al.* 2011); its absence means that the tuberal and anterior hypothalamus are difficult to distinguish. However, in hemi-dissected view, the close positional relationship between the infundibulum and Rathke's pouch (Ericson *et al.* 1998; Treier *et al.* 1998; Norlin *et al.* 2000) predicts the position of the tuberal hypothalamus (Fig.3.2D). Rathke's pouch evaginates from the oral ectoderm and at E3 they form a contiguous structure; however,

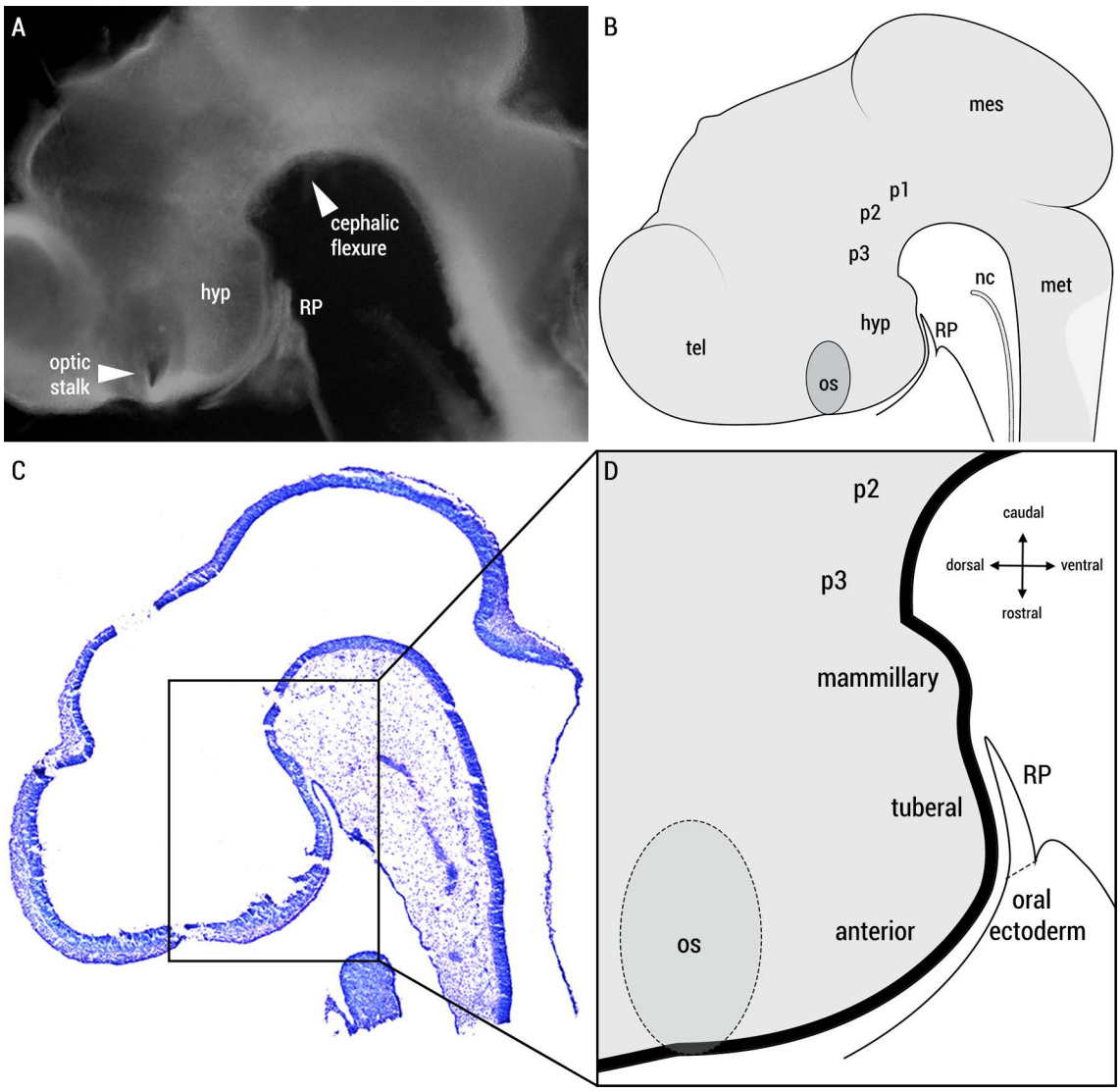

Figure 3.2 | Morphology and subdivisions of the E3 chick hypothalamus

(A,B) Wholemount side view of isolated E3 neuroepithelium and Rathke's pouch, showing the position of the hypothalamus (A); surrounding mesenchymal tissue and eye has been removed. Arrowheads point to the cephalic flexure and optic stalk. Morphology and organisation of the E3 neuroepithelium is schematically represented in (B). (C) Toluidine blue-stained sagittal section of an E3 embryonic head (n=5). (D) High power schematic view of the hypothalamus of boxed region in (C) showing the anterior, tuberal, and mammillary regions of the hypothalamus and neighbouring territories. Rathke's pouch lies adjacent to the tuberal hypothalamus. Dashed lines distinguishes Rathke's pouch from the oral ectoderm. hyp, hypothalamus; mes, mesencephalon (midbrain); met, metencephalon (hindbrain); nc, notochord; os, optic stalk; p1-3,prosomeres 1-3; RP, Rathke's pouch; tel, telencephalon

Rathke's pouch can be delineated from the oral ectoderm on the basis of Shh, which is expressed in the oral ectoderm but not in Rathke's pouch; notably, the Shh$^-$ territory correlates with the thinner lumen of Rathke's pouch (Treier *et al.* 1998; Takagi *et al.* 2008). Sagittal views show that the RP/oral ectoderm correlates with a subtle bending of the hypothalamus. I predict this to correlate with the start of the anterior hypothalamus, a region positioned rostral to the tuberal hypothalamus and Rathke's pouch, that extends to the optic stalk (Fig.3.2D).

Together, my comparative analysis of the hypothalamus in E3 and E5 shows that many of the morphological landmarks that are very clear at E5 are subtly present at E3. In addition, my analyses show that the mammillary hypothalamus is significantly smaller at E3 in comparison to the size difference of the anterior hypothalamus at these stages.

3.2.3. Topology and Morphology of the Forebrain Neuroepithelium at HH10

I next set out to determine whether any morphological landmarks are already obvious at early neural tube stages of development. At HH10 (E1.5), the neural tube is characterised by bulges and constrictions of the neuroepithelium that predict the appearance of vesicles, including the prosencephalic vesicle. The anterior-most vesicle is termed the prosencephalon and is generally believed to give rise to the forebrain (Figs.3.3A-B). As outlined in the introduction, the most widely accepted current model suggests that the secondary prosencephalon, from which the hypothalamus will arise, is located in the anterior part of this structure (Fig.3.3C). In this thesis, the prosencephalon will be referenced to as anterior, medial, or posterior prosencephalon.

To ask whether I could detect morphological landmarks that might predict the hypothalamus, I analysed sagittal sections of HH10 embryos. This analysis reveals a subtle downward turn of the ventral neuroepithelium that may indicate the beginning of the formation of the cephalic flexure (black arrowhead, Figs.3.3D,E). Other morphological landmarks are present but

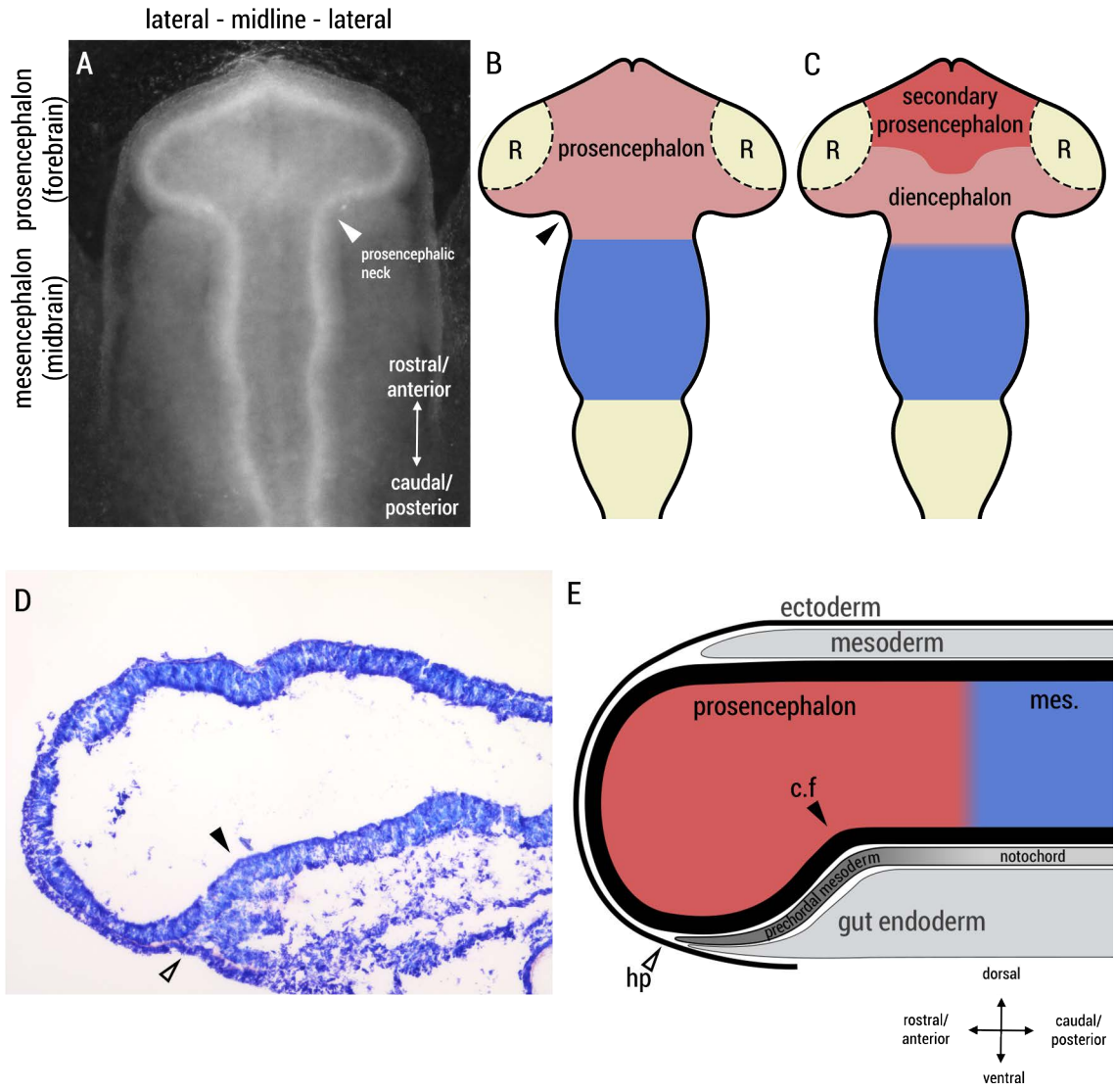

Figure 3.3 | Morphology of the prosencephalon at HH10 and neighbouring structures

(A-C) Whole mount dorsal view of an HH10 chick embryo (A). This is schematically represented in (B) and according to the prosomeric model (C). Arrowheads point to the prosencephalic neck.
(D-E) Toluidine blue-stained sagittal section of a HH10 embryo (n=5). This is schematically represented in (E). Black filled arrowheads point to a possible beginnings of the cephalic flexure. Empty arrowheads point to the hypophyseal placode, which will give rise to Rathke's pouch. c.f, cephalic flexure; hp, hypophyseal placode; mes, mesencephalon; R, retina

how they relate to the future hypothalamus at HH10 is unknown. The PM can be seen underneath the medial and posterior prosencephalon, anterior to the notochord. Underneath the PM is the gut (pharyngeal) endoderm and both the PM and gut endoderm share a similar anterior limit. Lastly, adjacent to the PM and gut endoderm lies the hypophyseal placode, which will give rise to Rathke's pouch (empty arrowhead, Figs.3.3D,E)..

3.3. Discussion

Previous studies have analysed the developing hypothalamus in mouse and chick, but have done so in wholemount brains and transverse sections (chick) or wholemount brains and sagittal sections (mouse). My approach, the analysis of hemi-dissected and/or fully dissected neuroepithelium together with analysis of sagittal sections, provides a novel way of analysing the hypothalamus. In particular, it has led me to appreciate the overall morphology of the hypothalamus and its growth over E3 to E5. Additionally, it confirms the close proximity between the infundibulum and Rathke's pouch and allows for the position of the tuberal hypothalamus to be accurately determined.

Potentially, one of the first morphological landmarks that might appear is the future cephalic flexure, a site suggested to form a boundary between p3 and hp1 (caudal hypothalamus). My studies on morphology alone, however, do not allow me to draw strong conclusions as to the position of this boundary. Nonetheless, my studies show that the cephalic flexure becomes a defining feature of the caudal hypothalamus.

Next I sought to determine where the hypothalamic regions - anterior, tuberal, and mammillary, originate.

Chapter 4
Fate mapping the ventral midline of the HH10 chick prosencephalon

4.1. Introduction

Fate mapping allows individual cells or a population of cells to be 'followed' through development and has proven invaluable in understanding the complex morphogenesis of the vertebrate brain. It generates ontogeny maps that allow the association of gene expression with a specific population of cells, and it provides insight into proliferation and cell movements.

Fate mapping studies can prove especially useful in defining regions at a time when there are few morphological landmarks. For example, at early neural tube stages, the neural tube exhibits morphological constrictions (e.g. rhombomeres) that assist in identifying the hindbrain and midbrain. In contrast, the prosencephalon lacks elaborate morphological landmarks to assist in demarcating the telencephalon, optic fields, hypothalamus, and diencephalon. As outlined in the introduction, recent studies have fate mapped the prosencephalon at HH10 in an attempt to better define the telencephalon, hypothalamus, and diencephalon, but have arrived at very different conclusions. Using quail-chick chimeras, *Garcia-Lopez et al. (2004)* suggest that the anterior and anterior-most medial prosencephalon

will give rise to the hypothalamus, including the anterior, tuberal, and mammillary regions. In contrast, studies in our lab using injection of lipophilic fluorescent dyes indicate a more posterior origin for the tuberal, infundibulum, and mammillary hypothalamus (Manning *et al.* 2006; Pearson *et al.* 2011), in a region proposed by *Garcia-Lopez et al. (2004)* to be diencephalic.

In this chapter, I use fluorescent lipophilic dyes to fate map the ventral midline of the anterior, medial, and posterior prosencephalon (a region that equates to the RDVM as defined by Dale *et al,* 1999) in an attempt to resolve these current discrepancies regarding hypothalamic origins.

4.2. Results

4.2.1. The ventral midline of the posterior prosencephalon gives rise to the hypothalamus

Previous fate-mapping studies in our lab, in which small groups of cells were labelled with DiI, have demonstrated that the ventral midline of the caudal prosencephalon of the HH10 chick embryo gives rise to ventral parts of the tuberal and mammillary hypothalamus (Manning *et al.* 2006; Pearson *et al.* 2011). Nevertheless, these studies did not perform a systematic analysis of prosencephalic ventral midline cells.

To begin, I determined that I could reproduce published studies that suggest an approximate position for future hypothalamic tuberal and mammillary regions (Manning *et al.* 2006; Pearson *et al.* 2011). DiI was focally injected into the ventral midline of the posterior prosencephalon, in a region within 0-100µm posterior to the prosencephalic neck, at HH10 (E1.5) (Figs.4.1A,G) and embryos incubated a further 4 days, until HH26-27 (E5; Fig.4.1B). As outlined in Chapter 3, at E5, the anterior, tuberal, and mammillary (posterior) regions of the hypothalamus can be recognized on the basis of their morphology and position relative to Rathke's pouch (RP). In wholemount side views, DiI fluorescence is detected in the caudal tuberal and mammillary hypothalamus (Figs.4.1B,B',C). Transverse sections

confirm that DiI-labelled cells will give rise to the ventral midline of the tuberal and mammillary hypothalamus (n=5; Figs.4.1C-E). The rostral extent of the DiI-labelled cells lies in the tuberal hypothalamus (Figs.4.1B',C). The caudal extent lies within the mammillary hypothalamus or p3 prosomere (Figs.4.1B',D,E); in the chick, the mammillary-p3 boundary has not been clearly identified (Puelles and Rubenstein 2003).

Consistently, after targeted injections to this region (Figs.4.1A,F), I observe that fluorescence is not uniform along the rostro-caudal axis: I detect a region of relatively weak fluorescence in the rostral mammillary region (empty arrowheads, Figs.4.1B',C,G,G'), between regions of strong fluorescence in the tuberal and caudal-mammillary region (n=5/5; Figs.3.1B',G,G'; filled arrowheads). This has not been reported in previous fate maps. It is widely accepted that fluorescent lipophilic dyes are diluted with each subsequent cell division (Lyons and Parish 1994), suggesting that this region of weak fluorescence may indicate local proliferation. This is consistent with my observation that the mammillary hypothalamus increases in length between E3 and E5 (see Chapter 3.2.2; Figs.3.1,3.2).

In conclusion, these results confirm the results from *Manning et al. (2006)* and *Pearson et al. (2011)* that cells in the ventral midline of the posterior prosencephalon will give rise to the hypothalamic territory. Furthermore, my results demonstrate a region of localised proliferation in the mammillary hypothalamus, caudal to the tuberal hypothalamus.

4.2.2. The ventral midline of the posterior prosencephalon extends anteriorly relative to adjacent basal cells

Fate mapping studies in New culture have shown that during neurulation (HH4-HH10), a group of midline epiblast cells anterior to Hensen's node called *area a* cells, that will give rise to the DVM (see section 1.3.2), extend anteriorly to give rise to the ventral midline of the developing neural tube (Supplementary Figs.1A-B; Schoenwolf *et al.* 1989; Patten *et al.* 2003). Neighbouring lateral epiblast cells do not show the same directed anterior extension (Fernández-Garre *et al.* 2002; Ezin *et al.* 2009). Although these

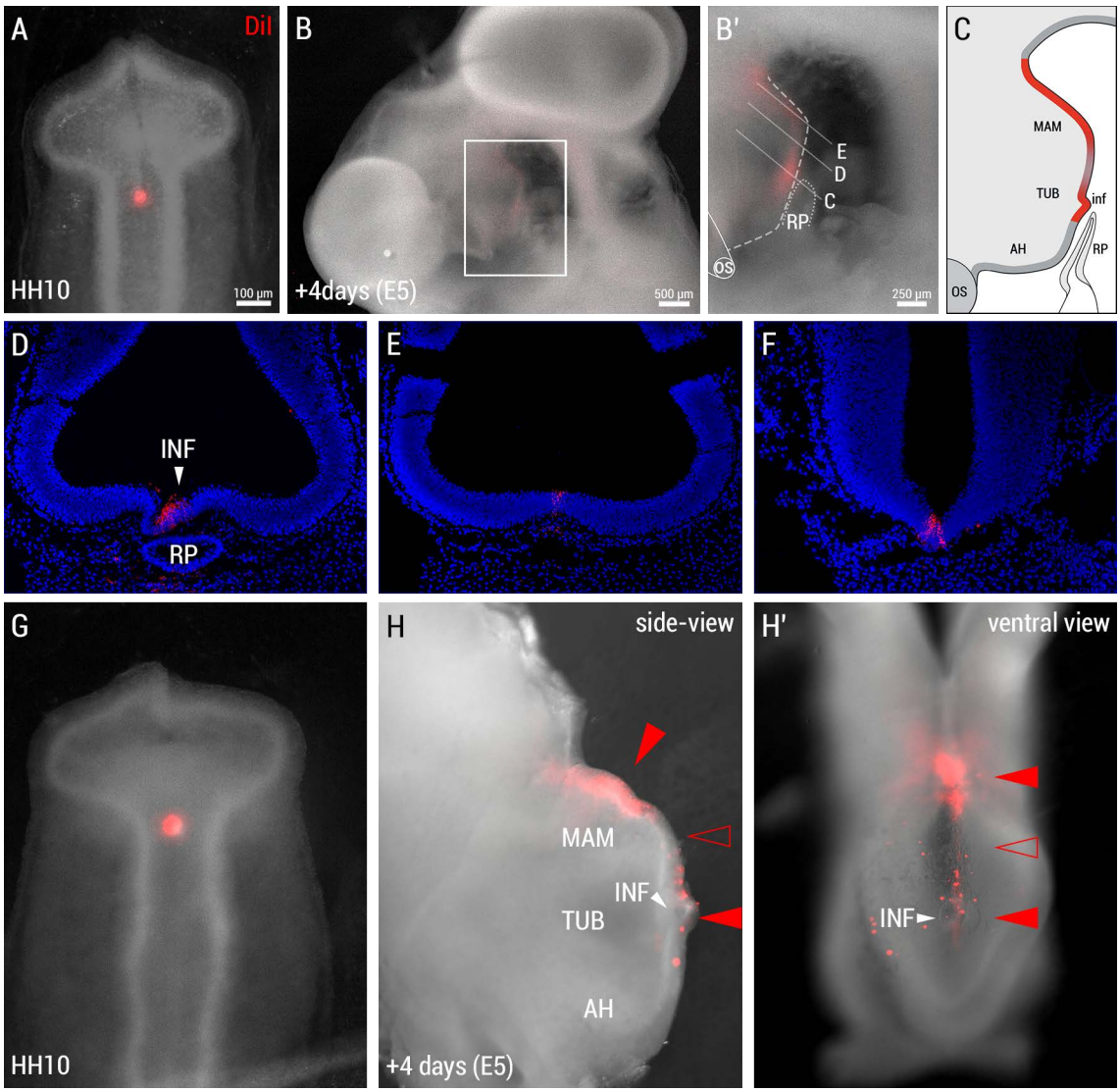

Figure 4.1 | Fate map of ventral midline of the posterior prosencephalon

(A) Representative wholemount dorsal view of 9-somite, HH10, embryo after focal DiI injection in the ventral midline of the posterior prosencephalon (n=5). (B) Hemi-dissected wholemount side view of the same embryo after 4 days of further development; boxed region is blown up in (B'). Surrounding mesenchymal tissue and eyes removed to reveal the neuroepithelium. (C) Schematic representation of DiI-labelled cells at E5. (D-F) Transverse sections relating to positions highlighted in (B') to show the caudal tuberal hypothalamus, including the infundibulum (D), rostral mammillary hypothalamus (D), and caudal mammillary hypothalamus (F). Blue, DAPI; Red, DiI. (G-H') DiI-labelled cells in the ventral midline of the posterior prosencephalon (G) gives rise to the caudal tuberal and mammillary hypothalamus as seen in the isolated neuroepithelium at E5 in side view (H) and dorsal view (H') but level of fluorescence is not consistent throughout (n=1). Filled arrowheads indicate strong fluorescence, and empty arrowheads indicate weak fluorescence. For abbreviations, see abbreviation list.

studies have not directly demonstrated that *area a* cells will give rise to the hypothalamus, *area a* cells extend as far as the presumptive prosencephalon at HH8 (Supplementary Fig.1C). On this basis, I hypothesised that hypothalamic progenitors exhibit similar migratory/extension behaviour and that cells lateral to it do not. This would predict that the ventral midline would extend further anteriorly relative to adjacent cells in the basal plate, and thus give rise to the hypothalamus; a possibility that might begin to resolve the discrepancies in defining the hypothalamic territory at HH10.

To test this, I labelled ventral midline and adjacent lateral cells in the posterior prosencephalon of a HH10 chick (n=1) using lipophilic dyes with different fluorescent emission spectra - red DiI (red) and DiO (green; Fig.4.2A), then developed the chick for a further 48 hours, until HH20 (E3). Analyses at HH20 reveals that, in keeping with my previous observations (Fig.4.1), the ventral midline of the posterior prosencephalon gives rise to the caudal tuberal and mammillary hypothalamus; by contrast adjacent lateral cells (DiO-labelled, green) do not give rise to the hypothalamus (Figs.4.2 B-C). Instead DiO-labelled cells give rise to the presumptive p2-p3 prosomeres. Transverse sections confirm this conclusion and show that DiI-labelled cells are detected in the ventral midline of the tuberal and mammillary hypothalamus but are absent in the presumptive p3 prosomere (red arrowheads, Figs.4.2D-F). DiO-labelled cells, by contrast, give rise to the ventro-lateral regions of prosomeres p2-p3 (green arrowheads, Figs.4.2D-F). Together this suggests that cells in the ventral midline and basal plates at HH10 maintain stereotypical positions along the mediolateral axis but not along the rostrocaudal axis. Conclusively, these results confirm the hypothesis that the ventral midline of the posterior prosencephalon exhibits migratory/extension behaviour and consequently gives rise to the hypothalamus, while lateral cells in the basal plate do not.

4.2.3. Fate mapping hypothalamic progenitors relative to the prosencephalic neck provides inconsistent results

Given that the widely accepted fate map of the hypothalamus is inaccurate, I next sought to extend previous fate maps and systematically fate map

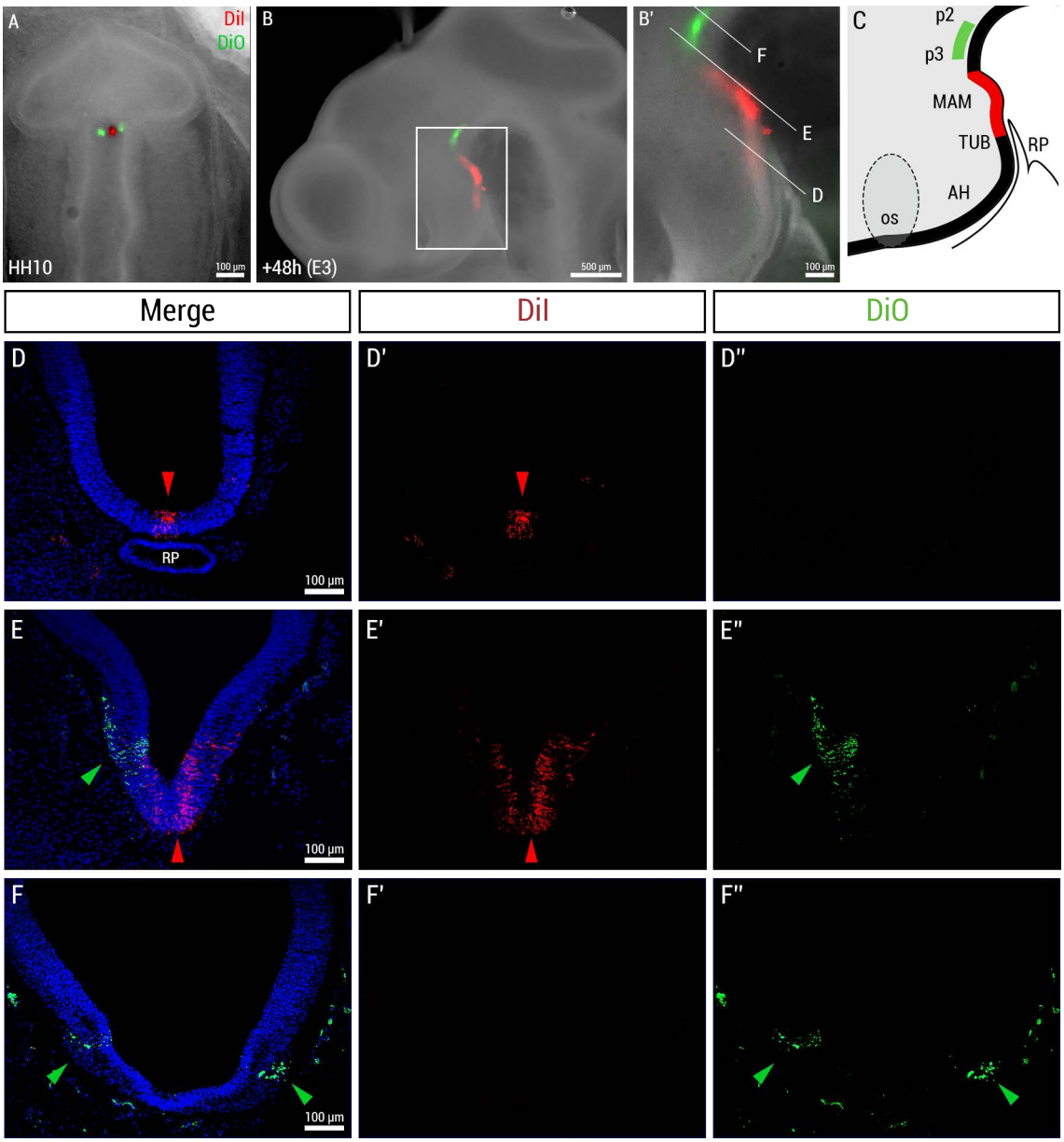

Figure 4.2 | Fate map of the ventral midline and adjacent basal plate of the posterior prosencephalon

(A) Wholemount dorsal view of HH10 embryo after focal DiI (red) injection in the ventral midline of the anterior diencephalon and focal DiO (green) injections in adjacent basal plate cells (n=1). (B) Hemi-dissected wholemount side view of the same embryo after 48 hours of further development; higher magnification of boxed region is shown in (B') and is schematically represented in (C). (D-F) Transverse sections relating to position highlighted in (B'). Red arrows point to DiI-labelled cells in the ventral caudal tuberal and mammillary hypothalamus; green arrows point to DiO-labelled cells in the basal plate of the presumptive p3 or p2 prosomeres; blue, DAPI; red, DiI; green, DiO. For abbreviations, see abbreviation list.

the ventral midline of the prosencephalon at HH10. Additionally, I sought to identify whether cells in a particular part of the prosencephalon will give rise to specific regions of the hypothalamus. In all experiments, ventral midline cells were targeted at the 9-10 somite stage (HH10; E1.5) and analysed 48 hours later, at E3 (embryos developed to various stages between HH18-20), i.e. 2 days earlier than the initial studies, but at a time I can be confident of recognising hypothalamic subdomains along the rostrocaudal axis (Chapter 3).

Published fate maps are based on studies that have imposed grids with defined measurements from the prosencephalic neck to the anterior neuropore (Manning *et al.* 2006; Garcia-Lopez *et al.* 2004). To be able to compare my fate map with published maps, I therefore initially defined the position of dye injection sites relative to their distance from the prosencephalic neck. Using this approach, I found that progenitors situated in the medial and posterior prosencephalon gave rise to the hypothalamus, again at odds with the widely accepted fate map (Fig.1.3D). Surprisingly, using this approach, it became apparent that the same equidistant population of labelled cells in different embryos did not always give rise to the same hypothalamic territory. Targeted fate mapping of cells that lie 80-100µm anterior to the prosencephalic neck (Fig.4.3A) gave rise to different regions within the hypothalamus. For example, in one embryo this region gave rise to a territory just caudal to the optic stalk (Figs.4.3B-B"). This region is the presumptive suprachiasmatic area (SCH), on the basis that published fate maps mapped the SCH to lie immediately posterior to the eye field (including optic stalk) at HH8 (Cobos *et al.* 2001). In a different embryo, however, the same area of cells gave rise to the tuberal and mammillary hypothalamus (Figs.4.3C-C"). Similar inconsistencies were observed in fate maps of ventral midline cells at the prosencephalic neck. For example, in one embryo, cells at the prosencephalic neck gave rise to the tuberal and mammillary hypothalamus (Figs.4.3D-E) while the same area in a different embryo largely gave rise to the anterior hypothalamus (Figs.4.3F-F").

These results show that the ventral midline of the medial and posterior prosencephalon (a region also known as RDVM) will give rise to the

hypothalamus but raise the possibility that these cells may not be restricted to a specific region of the hypothalamus. In other words, hypothalamic progenitors may be able to mix at HH10, i.e. an anterior population of cell does not maintain an anterior position relative to a more posterior population of cell.

To test, more conclusively, whether hypothalamic progenitors can mix or whether they maintain relative anteroposterior position, I simultaneously injected alternate DiI and DiO into 3 regions along the ventral prosencephalon at HH10 (n=1; Fig.4.4A). Analysis at HH20 demonstrated that the 3 different cell populations did maintain position relative to each other. Thus, injection points from anterior to posterior gave rise to the hypothalamus from rostral to caudal (Figs.4.4A-C). Interestingly, there appeared to be a region in the tuberal hypothalamus aligned to the tip of RP, gave rise to by DiO-labelled medial and DiI-labelled posterior cells (arrowhead, Fig.4.4B). This suggests that despite maintaining relative positions, the distance between each injection is not maintained, at least between these two cell populations. Analysis of transverse sections of this region, however, shows that DiO-labelled cells form a collar, colonising the ventral midline in the rostral tuberal hypothalamus, but more lateral regions slightly posteriorly (green arrowheads, Fig.4.4D-E). In contrast, DiI-labelled cells gave rise to the ventral midline, within DiO-labelled cells (red/green arrowheads, Fig.4.4E). In other words, DiI-labelled and DiO-labelled occupy different subregions of the ventral tuberal hypothalamus.

Conclusively, these results show that ventral midline cells of the medial prosencephalon will give rise to the hypothalamus and that hypothalamic progenitors maintain relative position during development. However it also shows that a grid reference from the prosencephalic neck results in inconsistent fate maps. Thus, I sought out a different reference point for targeted injections of lipophilic dyes.

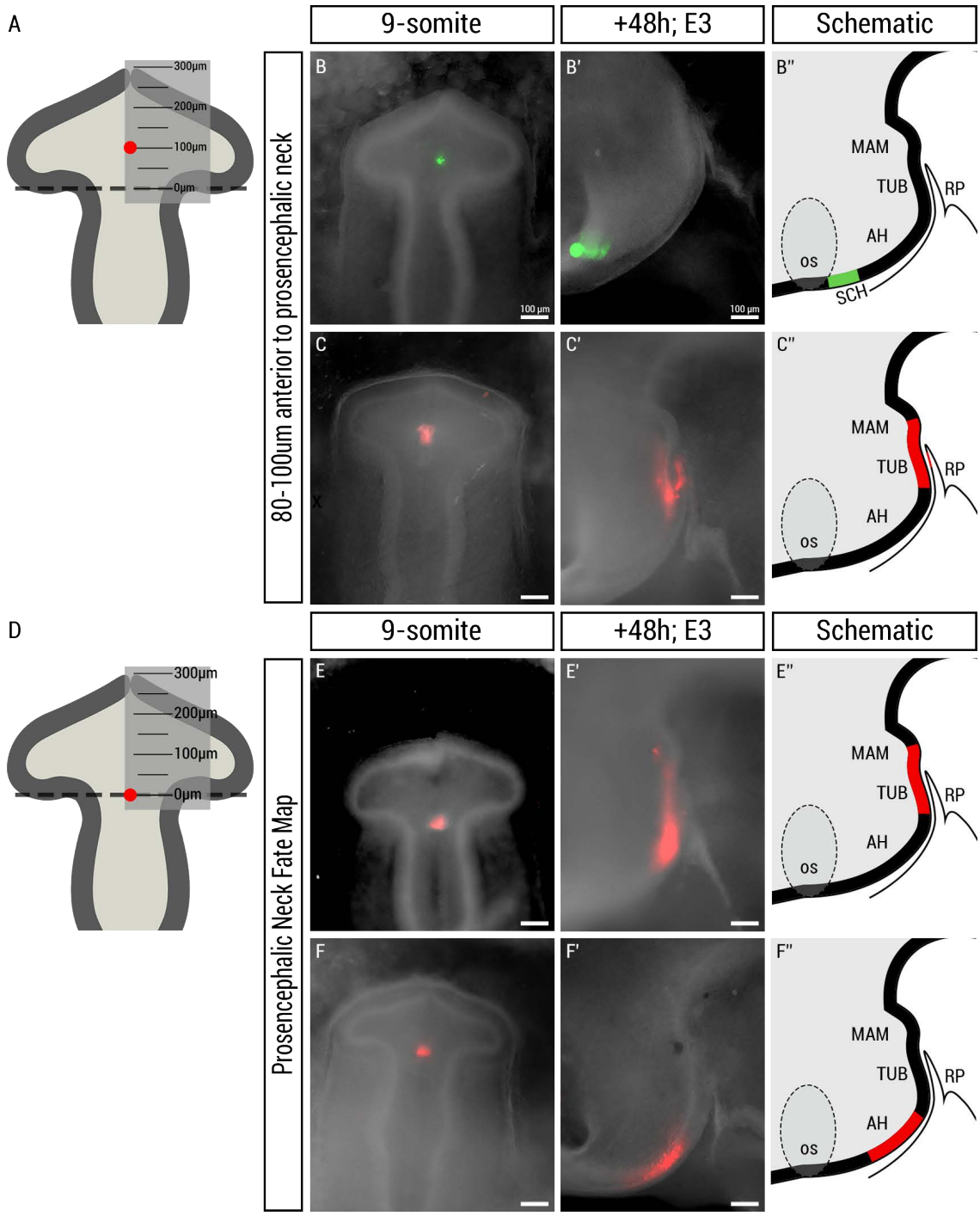

Figure 4.3 | Fate maps based on measurements from the prosencephalic neck are not replicative
(A,D) Schematic representation of regions targeted for fate mapping (red dots) based on measurements from the prosencephalic neck, indicated by the dashed line. (B-E) HH10 embryos after focal DiI (red) or DiO (green) injection in the ventral midline of prosencephalon indicated in (A,D). (B'-E') Hemi-dissected wholemount side view after 48 hours of development. (B''-E'') Schematic representation of each fate map shown. For abbreviations, see abbreviation list.

Table 4.1 | Summary of measurement-based fate maps

injection site	SCH	anterior	tuberal	tubero-mammillary
80-100µm anterior to PN	1	3	1	1
prosencephalic neck (PN)	1	3	2	4

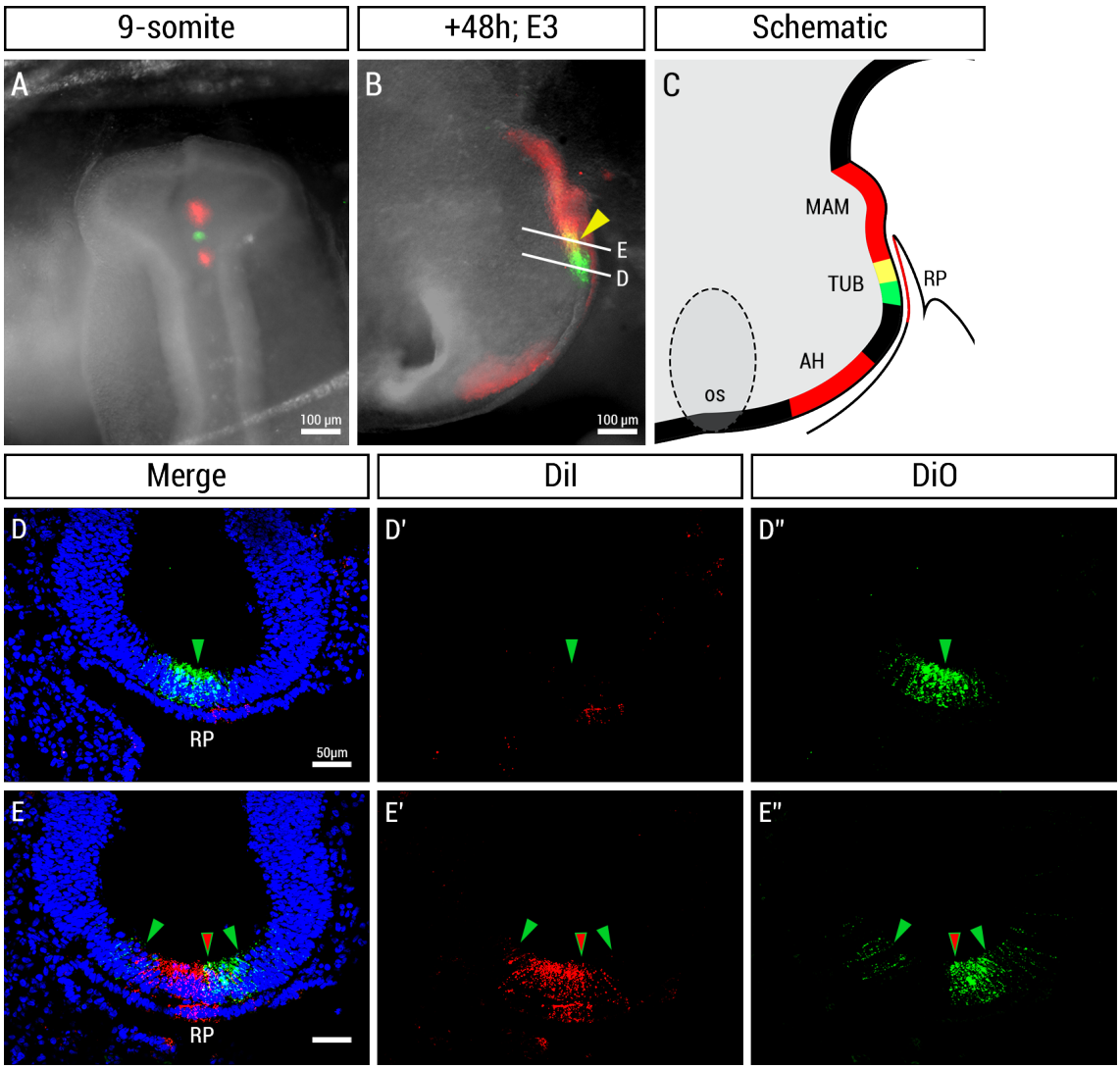

Figure 4.4 | Triple fate map of the ventral midline of the prosencephalon along the anteroposterior axis

(A) Wholemount dorsal view of HH10 embryo after focal DiI (red) and DiO (green) injections in the ventral midline of the prosencephalon at different regions along the anteroposterior axis (n=1). (B) Hemi-dissected wholemount side view of the same embryo after 48 hours of further development; fate map is schematically represented in (C). (D-E) Transverse sections relating to positions highlighted in (B). Green arrows point to DiO-labelled cells in the ventral midline (D) and more lateral regions (E). Red/green arrows point to region DiI-labelled cells and DiO-labelled cells overlap. For abbreviations, see abbreviation list.

4.2.4. Neuroepithelial cells overlying different sub-regions of the prechordal mesoderm can be accurately targeted

The prechordal mesoderm (PM) is instrumental in inducing the hypothalamus and then directing its subsequent development (see Chapter 1.3.2 and 1.3.3; Burbridge *et al.* 2016). In the early neural tube, the PM is visible under a microscope, allowing targeted injections to the overlying neuroepithelium based on position relative to the PM.

At HH10, the PM underlies a region of the neuroepithelium that extends from the medial to posterior prosencephalon, ie a region that my fate maps show to be composed of hypothalamic progenitors, and is visible when the dorsal neural tube is incised and opened (dashed lines, Fig.4.5A). I therefore asked whether I could target DiI to the ventral midline, using the PM as a reference point, and specifically targeting neuroepithelium above anterior (A), medial (B), and posterior (C) portions of the PM (Fig.4.5B). Analysis of embryos immediately after injection revealed that I can accurately target the different regions with lipophilic dyes at HH10 (Figs.4.5C-E). Transverse sections confirm that I can accurately target the ventral midline (Fig.4.5F). Moreover, to confirm the accuracy of targeting relative to the PM, I conducted a *region C* injection and subsequently analysed sagittal sections for *Shh* expression, which labels prechordal mesoderm, notochord, and ventral neural tube (Supplementary Fig.2). Sagittal sections show the position of *region C*. On the basis of this, *region B, A*, and a region anterior to *A* can be deduced on the basis of relative position to the PM (Figs.4.9B,C).

Importantly, these embryos show that the position of the prechordal mesoderm relative to the prosencephalic neck is not consistent in each embryo. For example, a DiI-labelled cells at the level of the prosencephalic neck can overlie the anterior, medial, or posterior PM (Figs.4.4C-E). These differences between individual embryos could begin to explain why my previous fate mapping using a measurement-based method led to inconsistent results.

In summary, I have shown that I can accurately target the ventral midline of the neuroepithelium overlying the anterior, medial, and posterior PM (i.e.

region A, B, and *C*, respectively). Next, I tested whether accurate targeting of hypothalamic progenitors at HH10 is possible using the PM as a reference point. Specifically, can ventral midline cells that will populate the anterior, tuberal, and mammillary hypothalamus be identified based on their relative position to the PM?

4.2.5. Ventral midline cells above the anterior prechordal mesoderm gives rise to the caudal anterior and rostral tuberal hypothalamus

Similar focal injections, targeted relative to anterior, medial or posterior portions of the PM were then conducted and embryos developed a further 48 hrs, to E3 (HH18-20) (n=10 embryos in total). Embryos were analysed in wholemount side view and after hemi-dissection, and then sectioned transversely. Targeting relative to the PM produced consistent fate-maps.

Neuroepithelial cells above the anterior PM (*Region A*) gave rise to the anterior and rostral tuberal hypothalamus (n=4/4; Fig. 4.6A-C). Transverse sections confirmed that DiI was detected in the anterior hypothalamus, and extended into the rostral tuberal hypothalamus: label was detected in rostral, but not caudal parts of the tuberal hypothalamus (FIG. 4.6D',D"). No labelled cell were detected in the mammillary hypothalamus (data not shown). Prior to the use of the PM as a landmark, my previous fate maps of the medial prosencephalon showed that some cells gave rise to the rostral-most region of the hypothalamus - the suprachiasmatic area of the anterior hypothalamus (Fig.4.3B). *Region A* fate maps did not give rise to this region, suggesting that the population of cells that gives rise to the suprachiasmatic area is anterior to *region A* and the underlying PM. DiI is also detected in Rathke's pouch. The ectodermal tissue that gives rise to Rathke's pouch touches the anterior-most PM and may even contact the neuroepithelium at the PM/ectoderm boundary. Since DiI is lipophilic, this may explain why, occasionally, these cells are labelled during dye injection (Jacobson *et al.* 1979; Sánchez-Arrones *et al.* 2015).

In summary, neuroepithelial cells overlying the anterior PM at HH10 fate

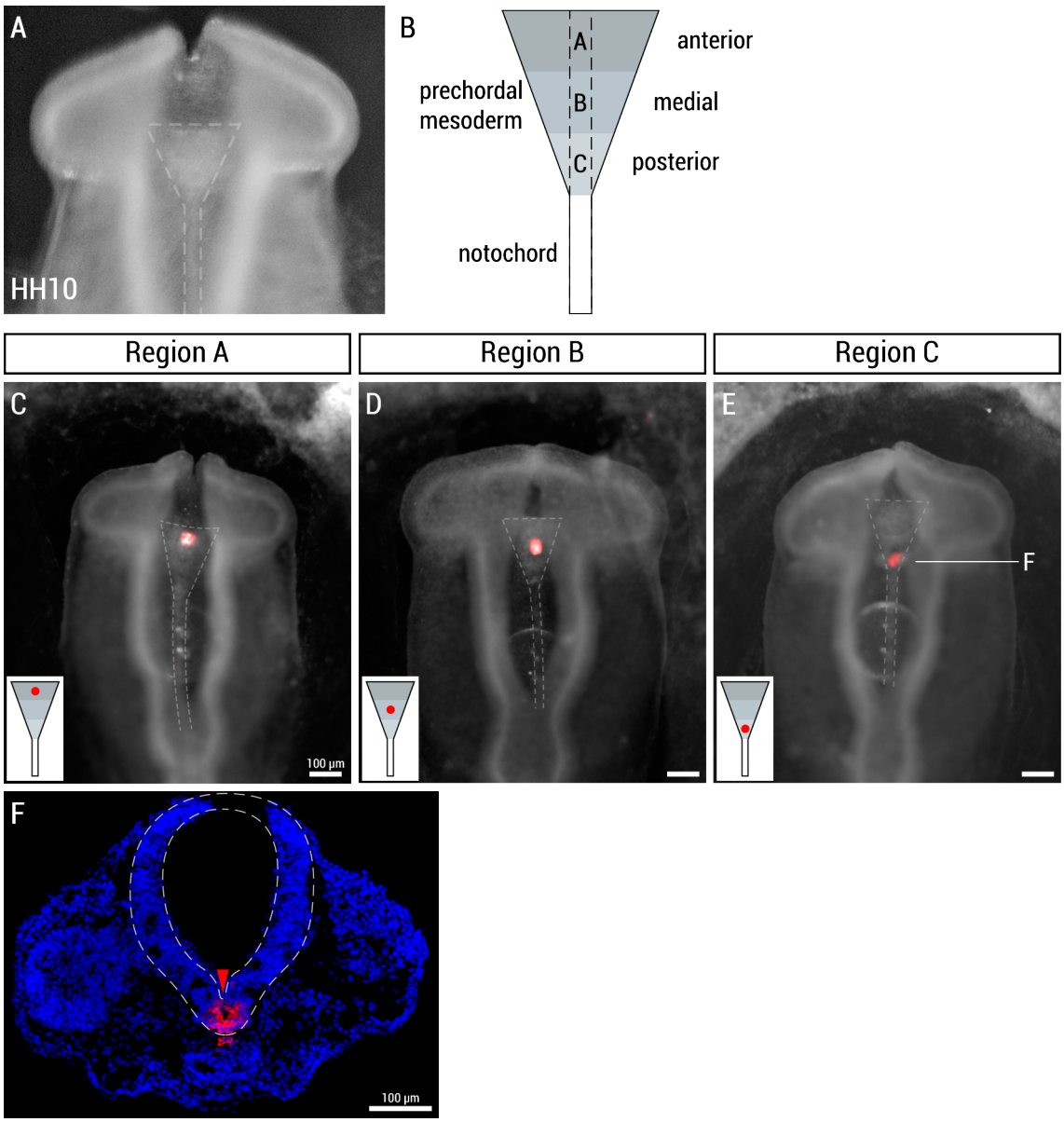

Figure 4.5 | Focal injections into different subregions of the prechordal mesoderm

(A) Wholemount dorsal view of HH10 embryo after incision of dorsal neural tube to reveal the prechordal mesoderm (dashed lines). (B) The prechordal mesoderm is subdivided into 3 regions and the ventral midline of these regions correlate with *region A* (anterior), *region B* (medial), and *region C* (posterior). (C-E) Wholemount dorsal view of HH10 embryos after focal DiI injection into *region A* (C), *region B* (D), and *region C* (E); inset shows position of injection site relative to the underlying PM, outlined by dashed lines. (F) Transverse section of highlighted position in (E) shows DiI injection in the ventral midline of the neural tube (n=1).

map to the caudal anterior hypothalamus. These cells did not populate the rostral anterior hypothalamus, suggesting that the rostral anterior hypothalamus originates from the neuroepithelium anterior to *region A* and the underlying PM.

4.2.6. Ventral midline cells above the medial prechordal mesoderm gives rise to the tuberal hypothalamus

Focal injections targeted to neuroepithelial cells above the medial PM (*Region B*) reveal that this region will give rise to the tuberal hypothalamus (n=4/4; Figs.4.6E-G). Transverse sections show that DiI is detected in the ventral midline of the rostral and caudal tuberal region. At the very posterior end of Rathke's pouch, DiI is detected in bilateral stripes in the ventral lateral tuberal hypothalamus (n=3/4). Together, these sections suggest that DiI-labelled cells form a horseshoe-shaped collar in the tuberal hypothalamus. These results are consistent with previous studies in the lab that show formation of a collar zone that surrounds and contributes to the future infundibulum (Pearson *et al.* 2011).

In summary, neuroepithelial cells overlying the medial PM at HH10 will give rise to the tuberal hypothalamus. This study also confirms earlier studies, showing that a subset of cells in the prosencephalon form a collar adjacent to RP, but extend these studies by pinpointing their origins in *region B*.

4.2.7. Ventral midline cells above the posterior prechordal mesoderm gives rise to the caudal tuberal and mammillary hypothalamus

Focal injections targeted to neuroepithelial cells above the posterior PM (*Region C*) reveal that cells in this region gave rise to the caudal tuberal and mammillary hypothalamus (n=2/2; Figs.4.6I-L). DiI fluorescence is observed at consistent levels throughout, in contrast to the observations where embryos developed to HH27 (see Chapter 4.2.1; Fig.4.1). As mentioned earlier, the mammillary-p3 boundary has not been established in chick

Figure 4.6 | Representative fate maps of *regions A*, *B*, and *C*

Representative results, showing fate of neuroepithelial cells, after focal DiI injections to *region A* (n=4; A-D), *region B* (n=4; E-H), and *region C* (n=2; I-L). (A,E,I) Wholemount dorsal view of HH10 embryo showing DiI (red) injection site in *regions A* (A), B, (E) and C (I). Inset shows injection site relative to the prechordal mesoderm. (B,F,J) Wholemount side view of isolated neuroepithelium and Rathke's pouch, after 48 hours of development, showing position of DiI-labelled cells, schematically represented in (C,G,K). (D-D'',H-H'',L) Transverse sections of position highlighted in (B,F,J). Red arrows indicate DiI-labelled cells in the neuroepithelium. For abbreviations, see abbreviation list.

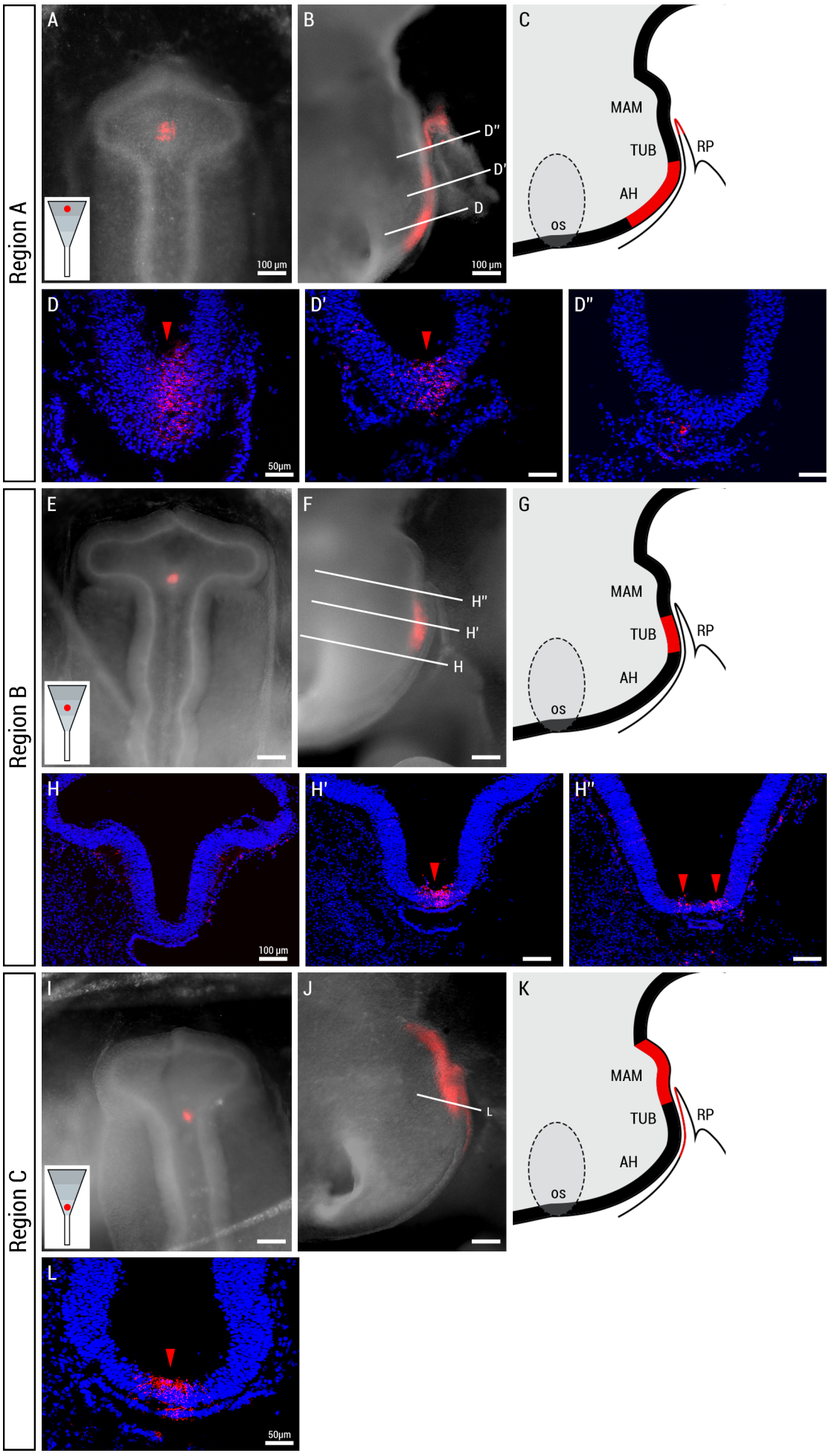
Region A
A
B
C
D''
D'
D
MAM
TUB
RP
AH
os
100 µm
100 µm
D
D'
D''
50µm
Region B
E
F
G
H''
H'
H
MAM
TUB
RP
AH
os
H
H'
H''
100 µm
Region C
I
J
K
L
MAM
TUB
RP
AH
os
L
50µm

and thus it is difficult to determine if *region C* also gives rise to the p3 prosomere. These results, together with similar fate maps that survived to a later stage at HH27, suggest an anisotropic growth of the rostral mammillary hypothalamus between E3 and E5.

Together, my fate map experiments of *region A,* B, and C, show that cells in the ventral midline of the medial and caudal prosencephalon at HH10 maintain their relative position along the rostrocaudal axis during development, and populate the anterior, tuberal and mammillary hypothalamus at HH18-20 (E3). It also shows that cells expand in number over this time, and that growth is mainly along the rostro-caudal axis.

4.2.8. Ventral midline cells anterior to *region A* and underlying prechordal mesoderm gives rise to the rostral anterior hypothalamus

As previously mentioned, fate maps of *Region A* gave rise to the caudal anterior hypothalamus and I predicted that cells anterior to this region will give rise to the rostral anterior hypothalamus, where the suprachiasmatic area is located. I have also previously shown that in the posterior prosencephalon, ventral midline cells exhibit anterior migrational/extension behaviour relative to lateral neighbours in the basal plate. I therefore, asked whether cells anterior to *Region A* and the PM will give rise to the rostral anterior hypothalamus and at the same time, I also asked whether ventral midline cells in this region will exhibit migration/extension behaviour.

To test this, I conducted a triple fate map of ventral midline cells and lateral cells on either side (n=1; Fig.4.7A). Analysis at HH19 confirmed that ventral midline cells anterior to the PM will give rise to the rostral anterior hypothalamus and additionally showed that cells lateral to the midline also gave rise to the rostral anterior hypothalamus in an overlapping transverse domain (i.e. from a side view; Figs.4.7B-C). This suggests that the ventral midline cells of this region does not exhibit similar migration/extension behaviour observed in the posterior prosencephalon. Transverse sections reveal that the ventral midline and lateral cells do not mix and maintain relative mediolateral position (Fig.4.7D-D'').

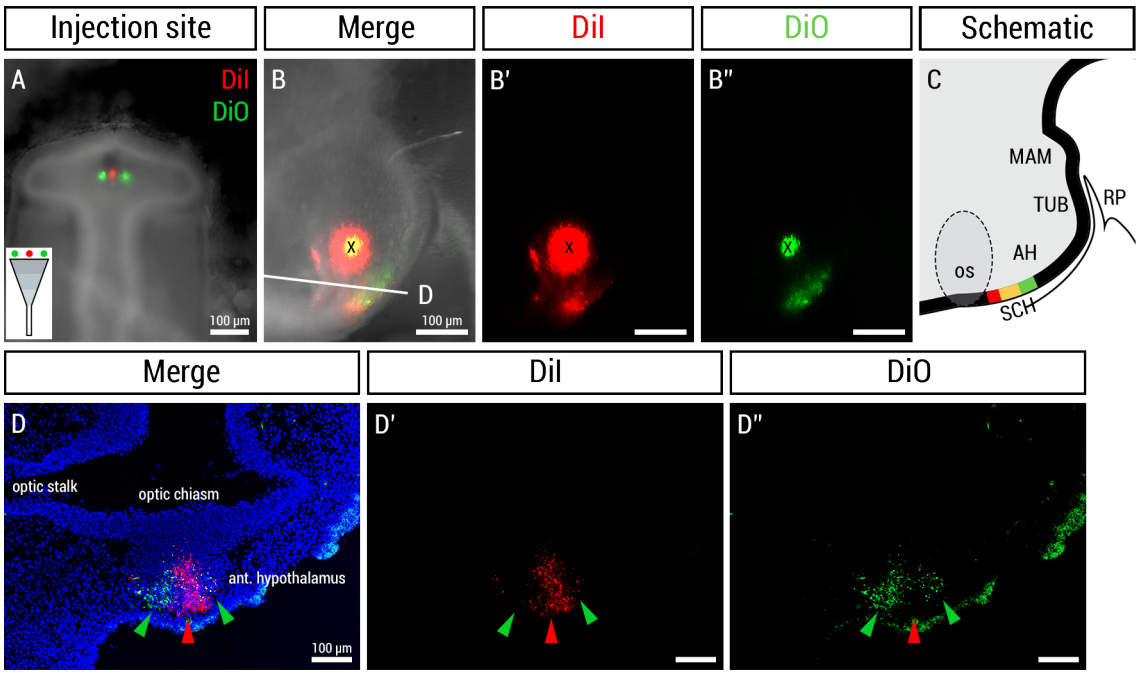

Figure 4.7 | Fate map of ventral midline and adjacent basal plate anterior to *region A* and the prechordal mesoderm

(A) Wholemount dorsal view of HH10 embryo after focal DiI (red) injection into the ventral midline and DiO (green) injection in the adjacent basal plate of region anterior to *region A* and the underlying prechordal mesoderm (n=1). Inset shows injection sites relative to the prechordal mesoderm. (B-B'') Hemi-dissected wholemount side view of the same embryo after 48 hours of further development showing position of DiI- and DiO-labelled cells, schematically represented in (C). (D-D'') Transverse section of region highlighted in (B). Red arrows indicate DiI-labelled cells and green arrows indicate DiO-labelled cells. For abbreviations, see abbreviation list.

In summary, I confirmed that cells anterior to *Region A* and the PM will give rise to the rostral hypothalamus and report that the ventral midline and cells lateral to it maintain both mediolateral and rostrocaudal positions relative to each other. In other words, the ventral midline of this region does not exhibit the migrational/extension behaviour observed in the posterior prosencephalon.

4.2.9. Ventral midline cells anterior to *region A* and underlying prechordal mesoderm does not extend anteriorly relative to adjacent basal cells

I next sought to examine the migratory/extension behaviour in *Region A* cells with a similar fate mapping strategy (n=1; Fig.4.8.A). Consistent with previous fate maps, the ventral midline of *Region A* gave rise to the ventral midline of the rostral hypothalamus (red/green arrowhead, Figs.4.8B-C). The cells lateral to the midline gave rise to an extensive region of the lateral hypothalamus along the rostrocaudal axis and extended from the caudal anterior to the mammillary hypothalamus (green arrowhead, Figs.4.8B-C), thus relative rostrocaudal position is not maintained. Additionally, both midline (red) and lateral (green) cells gave rise to a common transverse region in the caudal anterior/rostral tuberal region (red/green arrowhead, Figs.4.8B-C). The embryo was not sectioned, however, extrapolation from similar fate maps anteriorly (Fig.4.7) and in the posterior prosencephalon

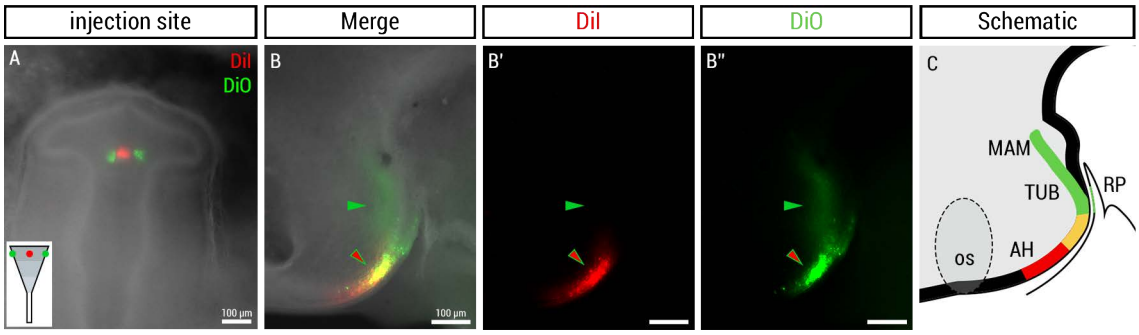

Figure 4.8 | Fate map of ventral midline of *region A* and adjacent basal plate cells
(A) Wholemount dorsal view of HH10 embryo after focal DiI (red) injection into the ventral midline of *region A* and DiO (green) injection in the adjacent basal plate. Inset shows injection sites relative to the prechordal mesoderm (n=1). (B-B'') Hemi-dissected wholemount side view of the same embryo after 48 hours of further development showing position of DiI- and DiO-labelled cells, schematically represented in (C). Red arrows indicate DiI-labelled cells and green arrows indicate DiO-labelled cells. For abbreviations, see abbreviation list.

(Fig.4.2), predicts that the midline and lateral cells maintain mediolateral position.

In summary, ventral midline cells overlying the PM and their lateral neighbours display a dynamic positional relationship, in which midline cells migrate/extend anteriorly and consequently gives rise to a more rostral position relative to lateral cells. However, ventral midline cells anterior to the underlying PM do not exhibit this behaviour.

4.3. Discussion

A schematic representation of all my fate mapping analyses is shown in Figs.4.9A-C (see Methods 2.1.2). Conclusively, I have confirmed earlier fate map studies in the lab (Manning *et al.* 2006; Pearson *et al.* 2011) that the ventral midline of the posterior and medial prosencephalon ('RDVM') will give rise to the floor of the hypothalamus. In addition I have extended these studies to show, for the first time, the position and extent along the anteroposterior axis, of the progenitors that will form the ventral regions of the future anterior, tuberal, and mammillary hypothalamus. Finally, I

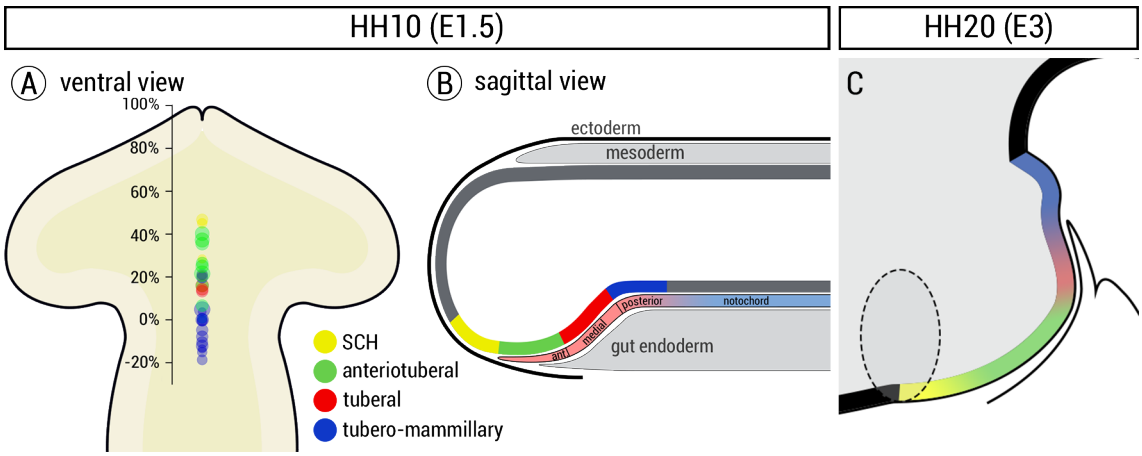

Figure 4.9 | Summary of fate map experiments

(A) Schematic of HH10 prosencephalon, from a dorsal view, showing injection sites of all fate map experiments relative to the prosencephalic neck (n=33). The distance of each injection site away from the prosencephalic neck is measured as a percentage of the total distance between the prosencephalic neck and the anterior neuropore. The diameter of each injection site represents the relative size of each injection. Colour of injection sites represent which region of the hypothalamus they will give rise to in (C). (B) Schematic of HH10 embryo, from a sagittal view, showing presumptive regions of the future hypothalamus relative to the underlying prechordal mesoderm. The colours in the neuroepithelium corresponds to the hypothalamic region, which it will give rise to in (C). (C) Schematic of E3 hypothalamus and Rathke's pouch showing the subdivisions of the hypothalamus and where they originate from at HH10 in (A,B). For abbreviations, see abbreviation list.

have shown that these can be identified precisely at HH10 on the basis of their position relative to subregions of the PM. Specifically, cells lying above the anterior, medial, and posterior PM will give rise to the caudal anterior, tuberal, and mammillary hypothalamus. Anterior to the PM, ventral midline cells of the neuroepithelium will give rise to the rostral-most anterior hypothalamus, the SCH. My fate maps suggest therefore, that the widely-accepted fate map of the HH10 embryo (Fig.1.3D) is incorrect and that, instead, hypothalamic progenitors are found more posteriorly.

4.3.1. Predictive morphological landmarks for the hypothalamus at HH10

My results show that at HH10, the prechordal mesoderm underlies the future caudal anterior, tuberal, and mammillary hypothalamus, and show that the rostral anterior hypothalamus lies anterior to the PM at HH10. Thus, the PM is a morphological feature that can predict the position of the future hypothalamus in a wholemount embryo. The PM is also visible in sagittal sections at HH10. On this basis, it is possible to map the relative position of the different regions of the hypothalamus on a sagittal plane (Fig.4.9C). This shows that the caudal anterior hypothalamus lies above the anterior PM, anterior tip of the gut endoderm, and the RP placode. The future tuberal hypothalamus lies posterior to this above the medial PM. The future caudal tuberal and mammillary hypothalamus lies above the posterior PM at a junction where there is a depression of the neural tube that may correlate with the rostral end of the cephalic flexure at later stages.

As outlined in Chapter 3, at E3-E5, a number of morphological features can be used to define the hypothalamus and its subregions (anterior, tuberal, mammillary) along the anteroposterior axis, including the tip of Rathke's pouch, the infundibulum, the cephalic flexure, the optic stalk, and the general surface morphology of the hypothalamus. By contrast, as I outlined in chapter 3, other than the rudimentary cephalic flexure-like structure there were few definitive morphological features that allowed identification of the future hypothalamus and its subregions.

My findings, show that the position of the PM at HH10 accurately predicts the position of hypothalamic ventral midline progenitors. In turn, this shows the position of other tissues, relative to the forming ventral hypothalamus. At HH10, Rathke's pouch placode and the anterior end of the gut endoderm are in close contact with *region A* of the PM. At present, we do not know whether these tissues play a role in hypothalamic induction or development. Their close proximity to progenitors that will ultimately form the anterior and rostral tuberal hypothalamus suggests it would be worth investigating, in future, if they play a role in anterior/tuberal development.

4.3.2. Anisotropic growth of the mammillary hypothalamus between E3 and E5

In chapter 3, I observed that the mammillary hypothalamus grew rapidly in size relative to the anterior and tuberal hypothalamus over E3-E5 (i.e. anisotropic growth), as assessed by gross surface morphology. My fate mapping studies confirm this. At E5, the rostral mammillary hypothalamus exhibits extensive dilution of DiI labelling relative to the tuberal and caudal mammillary regions, which suggests anisotropic proliferation in the rostral mammillary compared to the tuberal and caudal mammillary hypothalamus. In contrast, at E3, cells labelled with DiI fluorescence are detected at similar levels through the caudal tuberal and mammillary hypothalamus. Taken together, this suggests that the rostral mammillary hypothalamus undergoes rapid proliferation between E3 and E5, resulting in cell division-dependent dilution of DiI fluorescence. This is consistent with unpublished studies in our lab suggesting that localised rapid growth between E3 and E7 to is required to build a new territory in the rostral mammillary hypothalamus. In particular, these studies show that expression of Sox3 in the infundibulum and *Bmp4* in the mammillary hypothalamus are initially adjacent but their expression domains become separated from each other over E3 to E7. The region in which DiI is diluted correlates with the Sox3^{-} *Bmp4*$^{-}$ rostral mammillary territory at E5. Thus, my fate map extends these studies to provide indirect evidence that the rostral mammillary hypothalamus undergoes rapid proliferation between

E3 and E5.

4.3.3. The ventral midline of medial and posterior prosencephalon is hypothalamic and not diencephalic

My fate mapping experiments is in direct conflict with the widely accepted fate map proposed by *Garcia-Lopez et al. (2004)*, shown schematically in Figs.1.3C,D, which argues that the hypothalamus is located in the anterior prosencephalon. I have shown that the ventral midline of cells overlying the PM extend anteriorly/rostrally relative to their basal neighbours. Specifically, ventral midline cells in the posterior prosencephalon will give rise to the hypothalamus, while adjacent basal cells will give rise to the presumptive p3 and/or p2 prosomere. This migration/extension behaviour of ventral midline cells could begin to explain the discrepancy in results between fate maps in our lab and the *Garcia-Lopez et al. (2004)* study. However, it does not explain why they do not find that cells in the posterior prosencephalon give rise to the hypothalamus. A likely explanation is that they did not actually fate map the ventral midline, as I explain below:

In this chapter, I accurately targeted cells in the ventral midline and overlying different subregions of the PM with injections of fluorescent lipophilic dyes. In contrast, the *Garcia-Lopez et al. (2004)* study used quail-chick chimeras to fate map the prosencephalon. This technique involves the grafting of quail donor tissue into a host chick embryo of the equivalent stage. Quail cells can be distinguished from chick cells at the cellular level on the basis of their distinct condensed nuclear heterochromatin (Le Douarin 1993). This allows the generation of fate maps by immunohistochemically staining and following quail cells at different developmental stages. *Garcia-Lopez et al. (2004)* report that they isolated ventral prosencephalic tissue that included both ventral midline and basal tissue, then grafted this into the host chicken by replacing the chick-equivalent tissue. However, due to the nature of this technique, it is difficult to confirm (a) that the isolated tissue contains ventral midline cells and (b) that the donor quail tissue is grafted into an exact equivalent region. Due to this less precise technique, it is likely that fate maps of the posterior and medial prosencephalon in

Garcia-Lopez et al. (2004) did not give rise to the hypothalamus because ventral midline cells were not included in the grafts.

Nonetheless, to be absolutely certain of the accuracy of my results, I next examined fate-mapped cells within the context of defined molecular markers of the hypothalamus, and hypothalamic subregions.

Chapter 5
Gene expression analysis of the anterior and tuberal hypothalamus

5.1. Introduction

The experiments outlined in Chapter 4 suggests the origins of the ventral anterior, tuberal, and mammillary hypothalamus, as assessed by morphological criteria outlined in Chapter 3. To extend this analysis, I further characterised the ventral anterior and tuberal hypothalamus, by analysis of signalling molecules and transcription factors, then cross-referenced this expression pattern to the fate maps. In part, this was an attempt to verify my fate map. In addition, I wanted to test whether the hypothalamic regions I identified at HH10 are already regionalised into anterior and tuberal hypothalamic domains, i.e. whether the HH10 prospective hypothalamus already expresses markers that define anterior and tuberal regions at later stages of development.

5.2. Results

5.2.1. Subdivision of the anterior and tuberal hypothalamus on the basis of *Six3* and *Fgf10* expression

I analysed the expression pattern of *Tbx2*, *Six3*, *Foxg1* and *Fgf10* at HH27 (E5). Each has been shown to be expressed in the chick hypothalamus (see below), but no study has yet analysed them at a time when the anterior, tuberal, and mammillary hypothalamus can be recognised on the basis of morphology and relative position to Rathke's pouch (discussed in Chapter 3).

A previous study in the lab shows that the T-box transcription factor, *Tbx2*, is initially expressed in the ventral hypothalamus, from HH11 and is subsequently downregulated in the mammillary region (Manning *et al.*, 2005), becoming restricted to the anterotuberal region by HH20, E3 (Pearson *et al.* 2011). Thus, this suggests that expression of *Tbx2* could be used as a marker for the anterotuberal hypothalamus from HH20. However, expression of *Tbx2* at later stages has not been reported. In situ hybridisation for *Tbx2* at HH27 (E5) in sagittal sections show that *Tbx2* is now detected in the infundibulum and mammillary hypothalamus (Fig.5.1A). This is in stark contrast with its expression at earlier stages (HH20, E3) in the anterotuberal region (Fig.5.1B). Due to this dynamic expression pattern between E3 and E5, I concluded that *Tbx2* is an unsuitable definitive marker for the anterotuberal hypothalamus.

Another candidate marker for the anterotuberal hypothalamus is *Six3*, which has been reported to be expressed in the rostral hypothalamus (Bovolenta *et al.* 1998). *Six3* expression was analysed by *in situ* hybridisation on sagittal embryonic brain sections at HH27 (E5). *Six3* is expressed in a domain that includes the dorsal and ventral telencephalon, the anterior hypothalamus, and that extends into the tuberal hypothalamus where it ends in the caudal infundibulum (n=2; green arrowhead, Figs.5.2A',B,C). *Six3* is also detected in the baso-lateral p2/3 prosomeres and RP. To distinguish hypothalamic from telencephalic expression, (i.e. to identify the hypothalamic portion of

Six3 expression) I conducted double fluorescent *in situ* hybridisation for *Six3* and *Foxg1*, the latter a marker of the telencephalon (n=3). Expression of *Foxg1* is restricted to the telencephalon and ends caudally at the optic stalk (yellow arrowhead, Figs.5.2A,A''). Thus, on the basis of *Foxg1* expression, the *Six3*$^{+}$ *Foxg1*$^{-}$ territory marks the anterotuberal hypothalamus (Fig.5.2C).

Analysis of *Fgf10* expression pattern at HH27 (E5) in sagittal sections (n=6) shows that it is expressed in the infundibulum and, additionally, a region that I defined, morphologically, as the tuberal hypothalamus (Figs.5.3A,C). Transverse sections of this region confirm that *Fgf10* is expressed in the ventral tuberal hypothalamus and infundibulum (n=3; Fig.5.3B,B').

Comparison of the expression pattern of *Fgf10* and *Six3* reveals that they share a common caudal limit in the caudal infundibulum. More importantly, *Fgf10* is expressed in the tuberal but not in the anterior hypothalamus. Thus, I conclude that the *Six3*$^{+}$ anterotuberal hypothalamus can be further subdivided into *Six3*$^{+}$ *Fgf10*$^{-}$ anterior and *Six3*$^{+}$ *Fgf10*$^{+}$ tuberal hypothalamus.

I next asked whether the expression of *Six3* and *Fgf10* also distinguishes the anterior and tuberal hypothalamus at an earlier stage when the hypothalamus is less morphologically distinct. Double fluorescent *in situ* hybridisation for *Six3* and *Foxg1* in E3 sagittal sections (n=5) show that *Six3* is expressed in the *Foxg1*$^{+}$ telencephalon and anterotuberal hypothalamus. In the absence of the infundibulum, expression of *Six3* in the tuberal hypothalamus is determined on the basis of morphology: the caudal limit of *Six3* expression is aligned to the tip of RP (green arrowhead, Figs.5.4A-A''). Additionally, *Six3* expression is detected in the oral ectoderm and RP. Fluorescent *in situ* hybridisation for *Fgf10* in E3 sagittal sections (n=5) shows that *Fgf10* is expressed in the tuberal hypothalamus and its expression domain correlates with the tip of RP (future dorsal R) caudally, and the future ventral RP, rostrally (green arrowheads, Figs.5.4B,B').

Conclusively, the expression pattern of *Foxg1*, *Six3*, and *Fgf10* is comparable between E3 and E5 and subdivides the anterotuberal hypothalamus into *Six3*$^{+}$ *Fgf10*$^{+}$ tuberal and *Six3*$^{+}$ *Fgf10*$^{-}$ anterior hypothalamus (Fig.5.4C).

5.2.2. *Region A* cells give rise to the caudal anterior and rostral tuberal hypothalamus

My fate maps showed that *region A,* B, and C will colonise the caudal anterior/rostral tuberal, tuberal, and caudal tuberal/mammillary hypothalamus, respectively (summarised in Figs.5.5A-B). The regional identity of these fate mapped cells was determined on the basis of morphology. I next sought to extend these fate mapping studies to determine, firstly, whether *region B* cells are restricted to *Six3*$^{+}$ *Fgf10*$^{+}$ tuberal hypothalamus, and secondly whether *region A* cells colonise the *Six3*$^{+}$ *Fgf10*$^{+}$ tuberal hypothalamus, the *Six3*$^{+}$ *Fgf10*$^{-}$ anterior hypothalamus, or both. To test this, I conducted either *region A* or *region B* fate maps then subsequently analysed expression of *Six3* and *Fgf10* in serial adjacent transverse sections taken through the rostral tuberal and caudal anterior hypothalamus.

Region A cells gave rise to *Six3*$^{+}$ *Fgf10*$^{-}$ anterior hypothalamic cells but also gave rise to a small region of *Six3*$^{+}$ *Fgf10*$^{+}$ tuberal hypothalamic cells that spanned 15-35µm in length along the rostrocaudal axis (estimated based on 15µm-thick transverse sections) (n=2/3; Figs.5.5C-F''). *Region B* cells were restricted in their fate, and gave rise to *Six3*$^{+}$ *Fgf10*$^{+}$ tuberal hypothalamic cells: DiI-labelled cells were not detected in *Six3*$^{+}$ *Fgf10*$^{-}$ anterior hypothalamus (n=3; Figs.5.6).

Conclusively, I extend previous morphological observations by showing, molecularly, that *Region A* cells give rise the caudal anterior and rostral tuberal hypothalamus.

5.2.3. Analysis of expression patterns in the chick hypothalamus at E1.5 (HH10)

In previous fate mapping experiments, I showed that the ventral hypothalamic territory can be identified in the early neural tube stage, at HH10 (E1.5), on the basis of its position relative to the underlying PM (see section 4.2.4-7; Fig.4.6). However, it is not clear whether the hypothalamic progenitors, at this stage, are regionalised. I therefore asked whether progenitors of the anterior hypothalamus or tuberal hypothalamus can be identified,

at HH10, on the basis of the gene expression patterns that define them at later stages of development. To ask this, I analysed the expression of *Foxg1*, *Six3*, and *Fgf10* at HH10.

At HH10, *Six3* is expressed in the ventral prosencephalon, including the telencephalon, retina, and hypothalamus. In a ventral whole mount view of the isolated neuroepithelium at HH10, *Six3* expression is detected in a wide domain in the anterior prosencephalon and in a progressively narrower domain in the medial and posterior prosencephalon (n=4; Fig.5.7A). Analysis of *Fgf10* expression shows that *Fgf10* is expressed in the ventral medial and posterior prosencephalon (n=6, Fig.5.7B). Its expression in this regions is similar to that of *Six3* – i.e. it is expressed in a broad domain in the medial prosencephalon, and tapers to a narrow domain in the posterior prosencephalon. Comparison of the expression patterns of *Six3* and *Fgf10* with my fate mapping studies suggests that hypothalamic progenitors, at HH10, express both *Six3* and *Fgf10* (Figs.5.7A-C).

As outlined in chapter 4, anterior and tuberal hypothalamic cells can be distinguished from E3 on the basis of *Six3* and *Fgf10* expression: anterior cells are *Six3*$^{+}$ *Fgf10*$^{-}$, whereas tuberal cells are *Six3*$^{+}$ *Fgf10*$^{+}$. Further, anterior cells do not express *Foxg1*. I therefore set out to test if I could recognise 'anterior' and 'tuberal' like cells at HH10

To do so I examined expression of *Six3* and *Fgf10* in sagittal sections of HH10 embryos (where morphological features can be recognised – see chapters 3 and 4), and relative to expression of the telencephalic marker, *Foxg1*. Double fluorescent labelling of *Six3* and *Foxg1*, followed by sagittal section analysis, shows the position of the telencephalic/hypothalamic boundary. This lies above the surface ectoderm. I predict this region of the surface ectoderm to mark the anterior-most point of invagination of the pouch i.e. the future ventral part of RP (red arrowhead, Figs.5.7D-D"). The telencephalic/hypothalamic boundary lies approximately 100µm anterior to the tip of the pharyngeal endoderm and the PM (empty red arrowhead, Fig.5.7D). Posteriorly, strong expression of *Six3* is detected as far back as the proposed cephalic flexure. However, weaker expression is detected

more posteriorly to this, i.e. into midline regions of presumptive prosomere p3 that overlie the notochord (green arrowhead, Figs.5.7D-D").

Analysis of *Fgf10* reveals that its anterior limit appears to match the telencephalic/hypothalamic boundary. Thus, expression extends beyond the PM/pharyngeal endoderm (red arrowhead, Figs.5.7D-E). This means that I cannot detect a *Six3*$^{+}$*Fgf10*$^{-}$ cell population at HH10. Thus, although I can identify cells with 'tuberal' characteristics (*Six3*$^{+}$ *Fgf10*$^{+}$), I cannot distinguish 'anterior' cells (*Six3*$^{+}$ *Fgf10*$^{-}$). Caudally, strong *Fgf10* expression extends to the proposed cephalic flexure (black arrowhead, Figs.5.7D-E).

Together, these findings suggest while 'tuberal' *Six3*$^{+}$*Fgf10*$^{+}$ cells can readily be identified, 'anterior' *Six3*$^{+}$*Fgf10*$^{-}$ cells are not obviously present.

5.3. Discussion

Here, I report for the first time that *Fgf10* is expressed in the hypothalamus at HH10. Along the anteroposterior axis, expression of *Fgf10* closely correlates with progenitors that will contribute to the anterior, tuberal and posterior hypothalamus. Moreover, comparison of *Fgf10* expression with underlying morphological features suggests that *Fgf10* extends beyond the PM up to the telencephalic boundary. Thus, although I have not yet been able to perform double fluorescent analyses with *Fgf10* and *Foxg1*, I predict that *Fgf10* and *Foxg1* will form a sharp boundary at HH10, marking a telencephalic/hypothalamic boundary. This, and the co-expression of *Six3* and *Fgf10* in cells that will give rise to the anterior, tuberal, and mammillary hypothalamus leads me to conclude that the hypothalamus cannot be subdivided into *Six3*$^{+}$ *Fgf10*$^{+}$ tuberal and *Six3*$^{+}$ *Fgf10*$^{-}$ anterior hypothalamus at HH10. Instead, only tuberal-like cells can be detected at HH10. This raises the possibility that the newly induced hypothalamus is tuberal in character. This idea forms the basis of my next chapter.

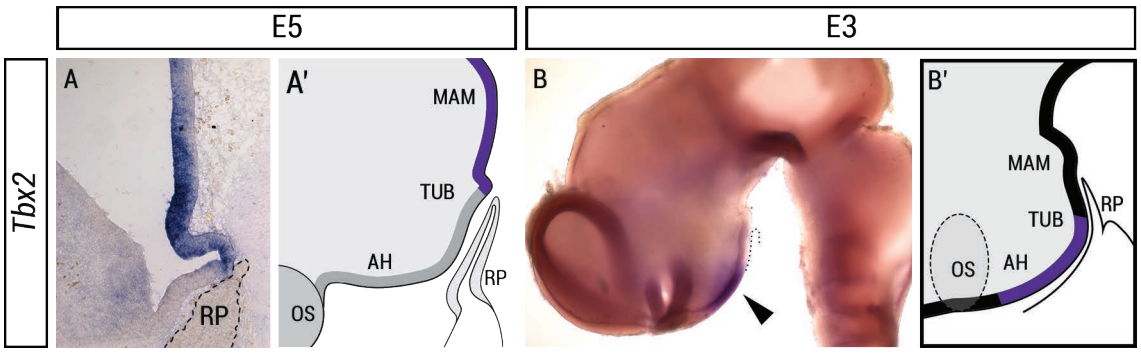

Figure 5.1 | Expression profile of *Tbx2* in E5 and E3 chick hypothalamus

(A) Sagittal section of an E5 hypothalamus showing expression of *Tbx2* in the caudal half of the infundibulum and mammillary hypothalamus (n=4). This is schematically represented in (A'). Dashed lines outline Rathke's pouch. (B) Isolated wholemount side view of E3 neuroepithelium showing expression of *Tbx2* in the anterior and tuberal hypothalamus (n=3; arrowhead); this is schematically represented in (B'). Dotted lines outline Rathke's pouch. For abbreviations, see abbreviation list.

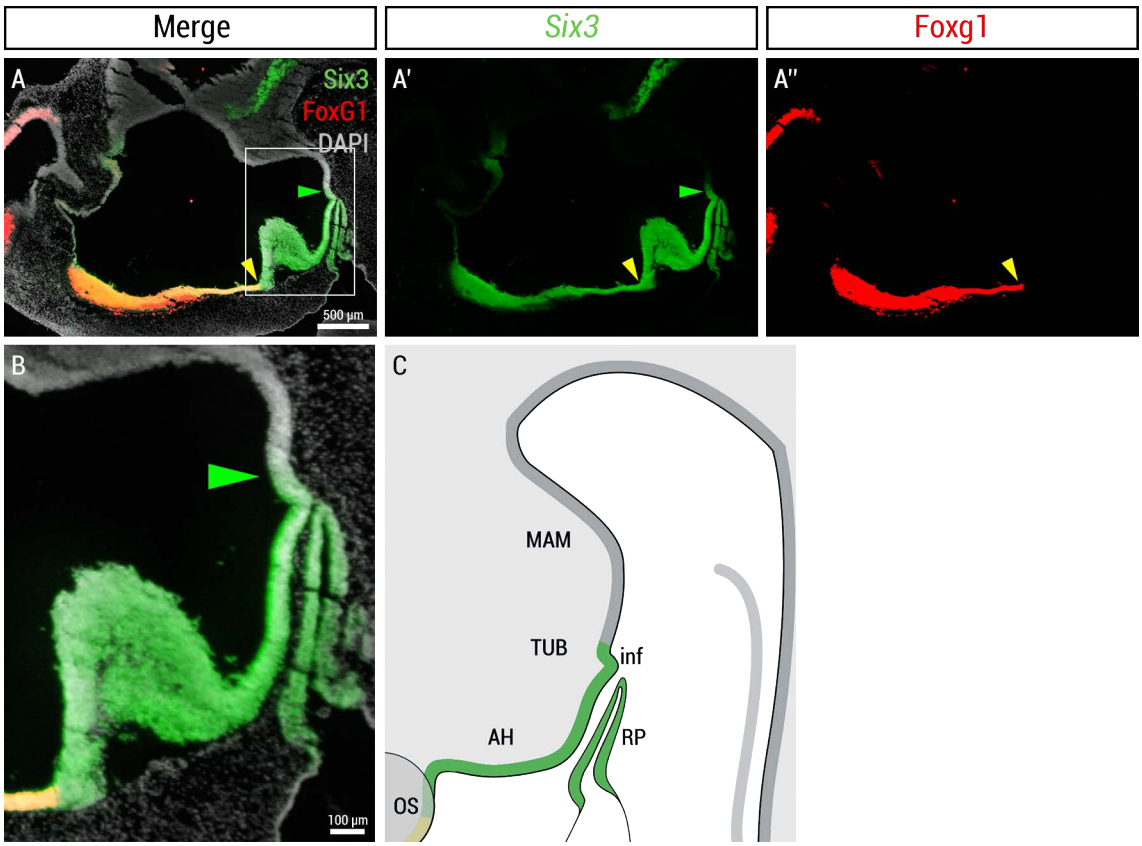

Figure 5.2 | Expression profile of *Six3* and *Foxg1* in the E5 chick hypothalamus

(A) Sagittal section of an E5 chick head, processed by fluorescent *in situ* hybridisation for *Six3* and *Foxg1* (n=2). (B) Blow up of the hypothalamus from boxed region in (A), schematically represented in (C). *Six3* is detected in the caudal infundibulum and extends to the telencephalon, and is additionally detected in the baso-lateral p3-p2 prosomere (A'). Green arrowheads point to the caudal extent of *Six3* expression domain in the caudal infundibulum. *Foxg1* is detected in the telencephalon. Yellow arrowheads point to the caudal extent of *Foxg1* expression domain, identifying the telencephalic-hypothalamic border. For abbreviations, see abbreviation list.

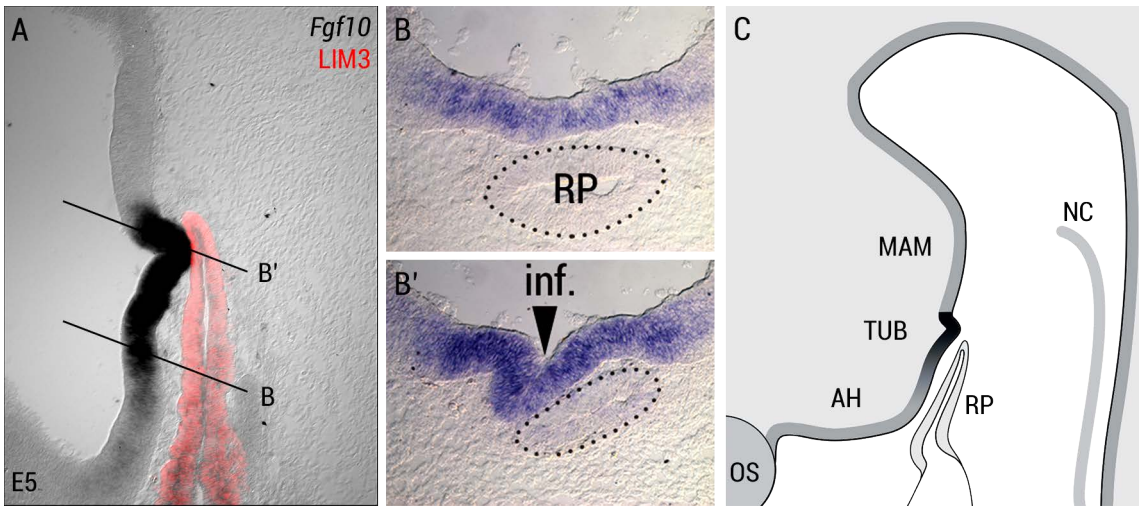

Figure 5.3 | *Fgf10* expression in the E5 chick tuberal hypothalamus

(A) Sagittal section of an E5 chick head, processed by simultaneous *in situ* hybridisation for *Fgf10* and immunolabelling for LIM3 (n=6). *Fgf10* expression is detected in the tuberal hypothalamus, adjacent to dorsal LIM3$^+$ Rathke's pouch. *Fgf10* expression in the tuberal hypothalamus is schematically represented in (C). (B-B') Transverse sections of positions highlighted in (A) show *Fgf10* expression in the ventral tuberal (B) and infundibulum (B'; n=3). For abbreviations, see abbreviation list.

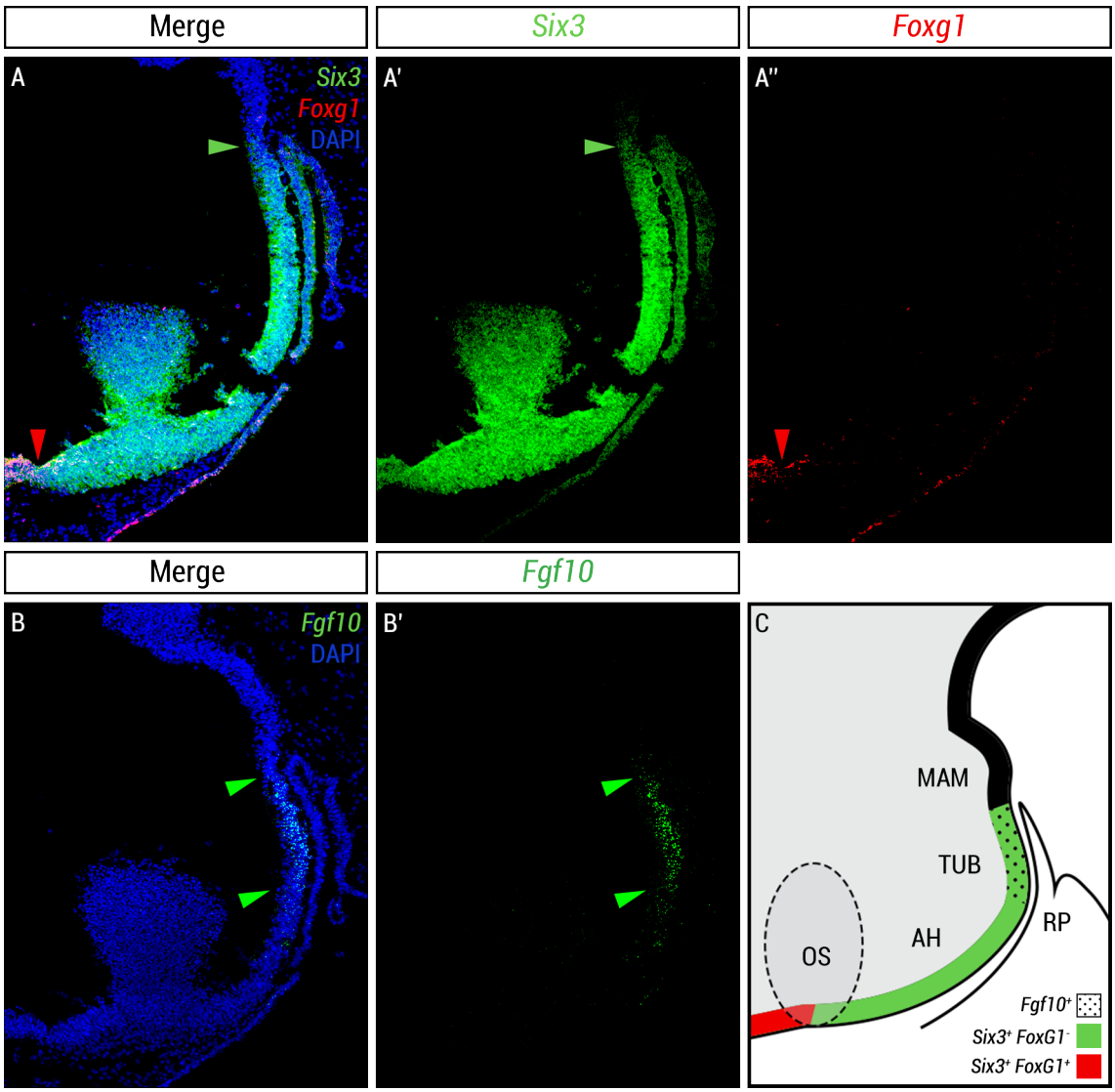

Figure 5.4 | Expression profile of *Six3*, *Foxg1*, and *Fgf10* in the E3 chick hypothalamus

(A) Sagittal section of an E3 embryo processed by fluorescent *in situ* hybridisation for *Six3* (green, A') and *Foxg1* (n=5; red, A''). *Six3* expression is detected in the tuberal hypothalamus, as defined by the adjacent dorsal Rathke's pouch tip (green arrowhead), and extends to the telencephalon (A'). Caudal expression of *Foxg1* identifies the caudal telencephalon and the telencephalic-hypothalamic boundary (red arrowhead, A''). (B) Sagittal section of an E3 embryo processed by fluorescent *in situ* hybridisation for *Fgf10* (n=5). *Fgf10* expression is detected in the tuberal hypothalamus and corresponds with the dorsal tip of Rathke's pouch and the Rathke's pouch-oral ectoderm junction (green arrowheads). (C) Schematic representation of *Six3*, *Foxg1*, and *Fgf10* expression in the E3 chick hypothalamus. For abbreviations, see abbreviation list.

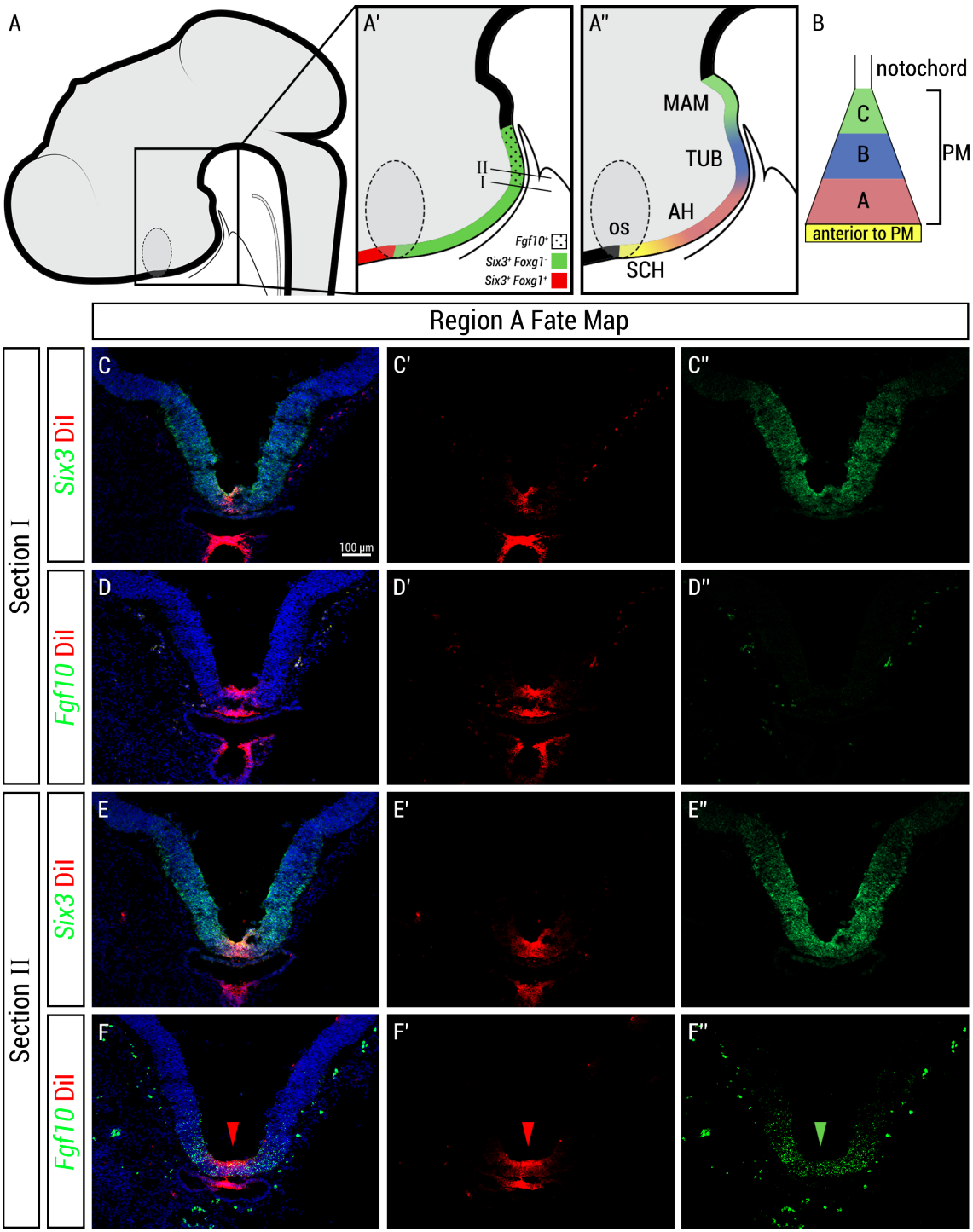

Figure 5.5 | *Region A* cells give rise to *Fgf10*+ rostral tuberal hypothalamus

(A-B) Schematic summary of *Fgf10*, *Six3*, and *Foxg1* expression in E3 hypothalamus (A') and fate maps of *region A*, B, and C (A'',B). (C-F'') Fluorescent *in situ* hybridisation for *Six3* (C-C'', E-E'') and *Fgf10* (D-D'', F-F'') on E3 embryonic transverse sections after DiI injection into *region A* at HH10. Transverse sections relate to position highlighted in (A') and correspond to anterior (Section I) and tuberal (Section II) on the basis of *Fgf10* expression. Red and green arrowheads show DiI-labelled cells and *Fgf10* expression in the rostral tuberal hypothalamus. *Region A*-derived DiI-labelled cells are detected in *Fgf10*- anterior and *Fgf10*+ tuberal hypothalamus (n=2/3). For abbreviations, see abbreviation list.

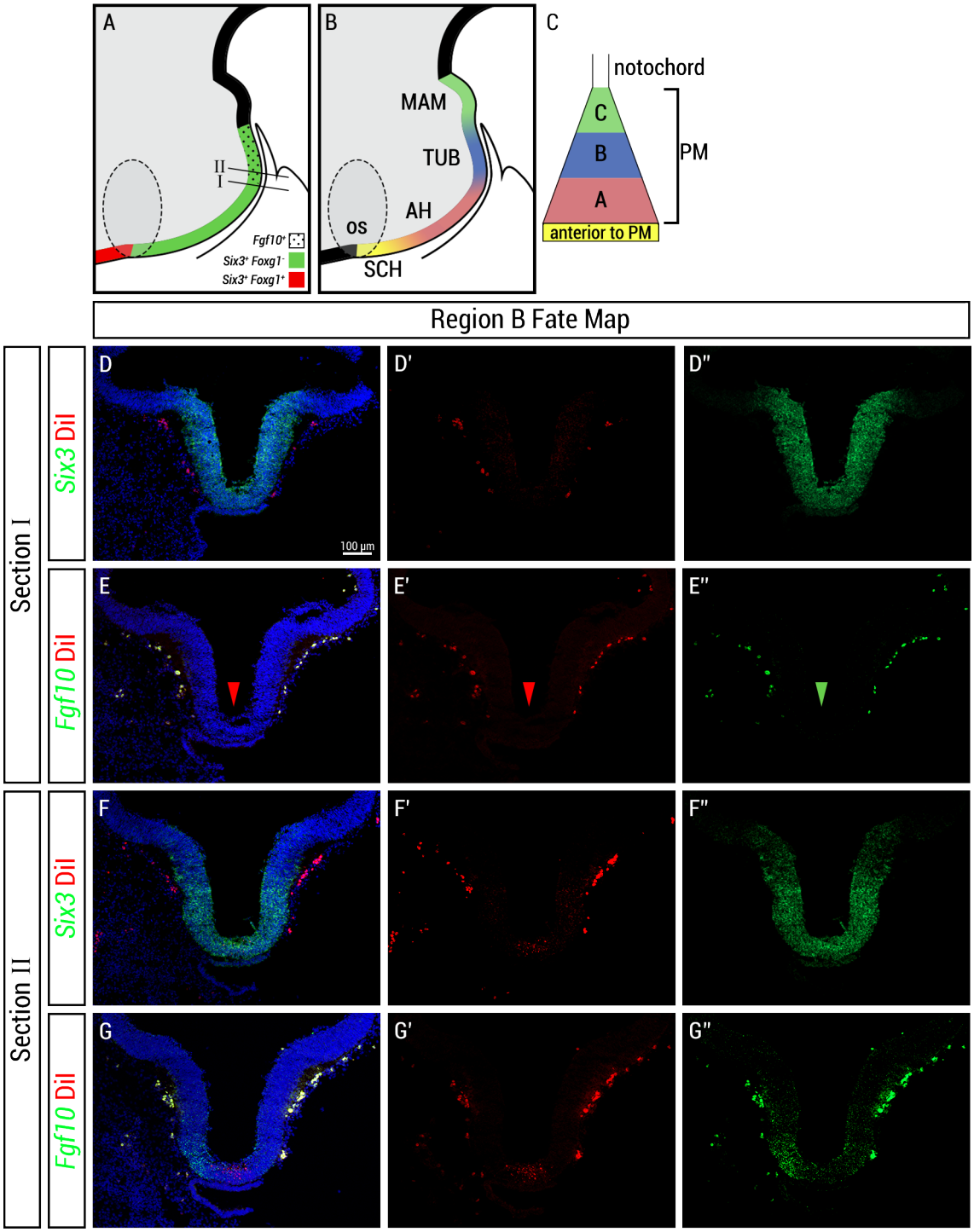

Figure 5.6 | *Region B* cells are restricted to *Fgf10*+ tuberal hypothalamus

(A-C) Schematic summary of *Fgf10*, *Six3*, and *Foxg1* expression in E3 hypothalamus (A) and fate maps of *region A*, B, and C (B,C). (D-G'') Fluorescent *in situ* hybridisation for *Six3* and *Fgf10* on E3 embryonic transverse sections after DiI injection into *region B* at HH10. TTransverse sections relate to position highlighted in (A) and correspond to anterior (Section I) and tuberal (Section II) on the basis of *Fgf10* expression. Red and green arrowheads show absence of DiI-labelled cells and *Fgf10* expression in the anterior hypothalamus. For abbreviations, see abbreviation list. *Region B*-derived DiI-labelled cells are detected in *Fgf10*+ tuberal but not *Fgf10*- anterior hypothalamus (n=3/3). For abbreviations, see abbreviation list.

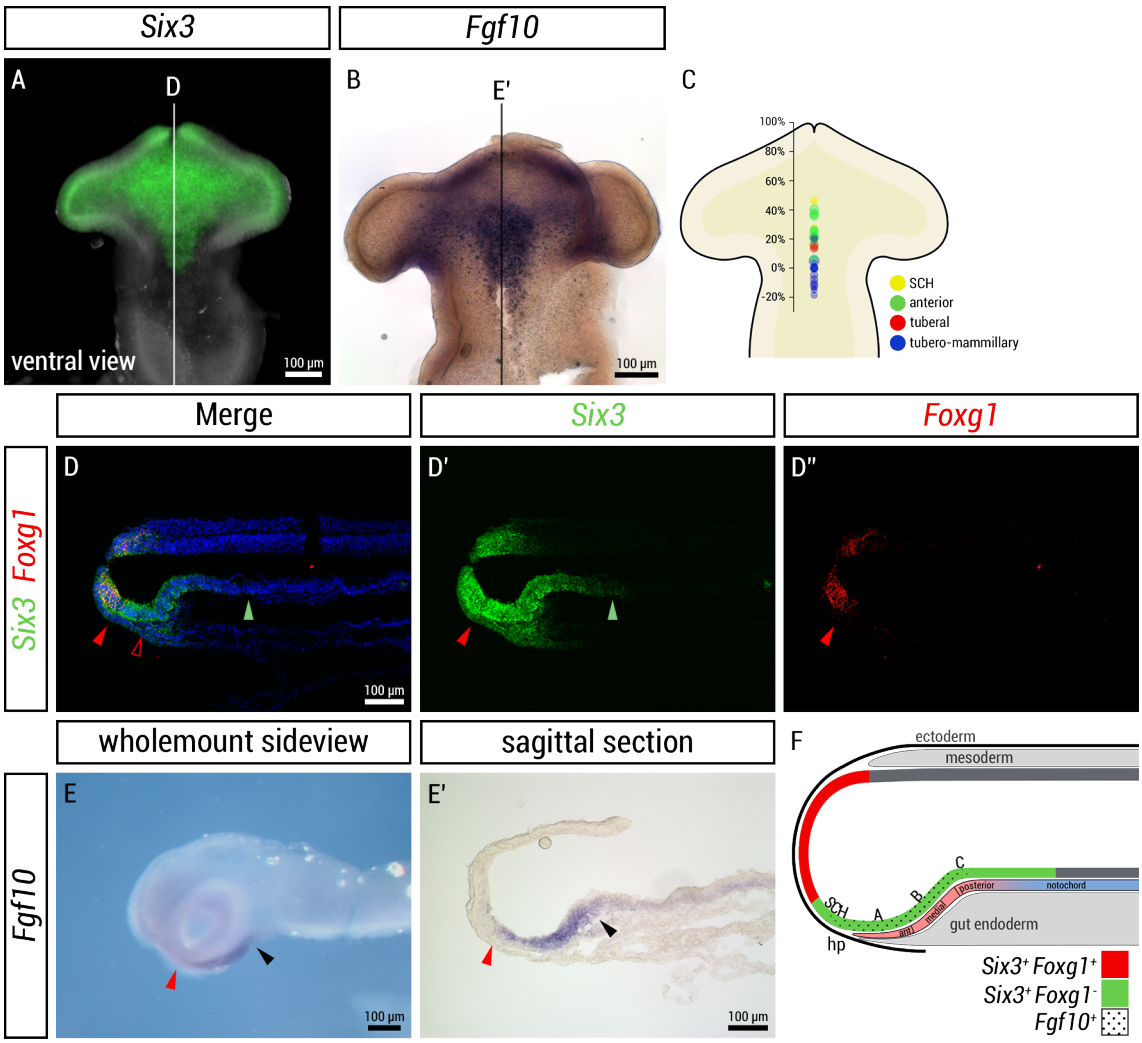

Figure 5.7 | Expression profile of *Six3*, *Foxg1*, and *Fgf10* in the HH10 chick prosencephalon

(A) Ventral flat-mount view of HH10 neuroepithelium processed by fluorescent *in situ* hybridisation for *Six3* (n=4). *Six3* is detected in the ventral anterior, medial, posterior prosencephalon, and eye fields. (B) Ventral flat-mount view of HH10 neuroepithelium showing expression of *Fgf10* (n=6). *Fgf10* is strongly detected as an oval shape in the ventral prosencephalon. (C) Schematic summary of fate map experiments; each dot represents an injection site and are colour coded based on which region of the hypothalamus it will give rise to. The position of these injection sites correlates with *Six3* and *Fgf10* expression. (D-D'') Sagittal sections of HH10 embryo fluorescently hybridised *Six3* and *Foxg1* (n=3). In the neuroepithelium, *Six3* is detected in the telencephalon and extends to the presumptive p3/p2 prosomere (green arrowhead); it is also detected in the anterior surface ectoderm, including the hypophyseal placode, prechordal mesoderm, and anterior tip of the gut endoderm (D'). *Foxg1* is detected in the telenephalon (D''). Red filled arrowheads indicate the telencephalic-hypothalamic boundary; empty red arrowheads indicate the anterior tip of the gut endoderm and prechordal mesoderm. (E-E') Wholemount view of isolated neuroepithelium processed by *in situ* hybridisation for *Fgf10* (n=6) shows expression of *Fgf10* in the ventral prosencephalon and extending to the cephalic flexure rudiment (black arrowhead). (E') Sagittal sections show that *Fgf10* is strongly expressed from the cephalic flexure rudiment to the presumptive telencephalic-hypothalamic boundary (n=3; red arrowhead). (F) Schematic representing the relationship between *Six3, Foxg1, Fgf10*, fate mapping data, and surrounding morphological features. For abbreviations, see abbreviation list.

Chapter 6
Model of anterior hypothalamic development

6.1. Introduction

My findings in Chapter 5 raise the possibility that when it first develops, the hypothalamus is tuberal in character, and can be characterised by *Fgf10* expression; i.e. that newly-induced hypothalamic progenitors express tuberal character. The implication of this is that the anterior and mammillary hypothalamus are derived from *Fgf10*$^{+}$ tuberal-like progenitors and this is supported by my findings in Chapter 4 showing that cells that will give rise to the anterior and mammillary hypothalamus will also give rise to parts of the tuberal hypothalamus. In this chapter, I focus on the anterior hypothalamus and ask how the anterior hypothalamus is built through a 'tuberal-by-default' model of hypothalamic development. In addition, I began to investigate the possible role of Shh signalling in development of the anterior hypothalamus within this model.

6.2. Results

6.2.1. Proposed models of development of the anterior hypothalamus

Here, I propose two different possible models for development of the anterior hypothalamus.

In the first model, anterior hypothalamic identity is specified by a change in fate of cells in a subregion of the *Fgf10*$^{+}$ tuberal hypothalamus, which subsequently proliferate to drive the rapid expansion of the anterior hypothalamus (Fig.6.1A). In the second model, *Fgf10*$^{+}$ tuberal hypothalamus proliferates to give rise to *Fgf10*$^{-}$ cells that populate the anterior hypothalamus. In this model, the *Fgf10*$^{-}$ cells undergo rapid transit amplification close to the tuberal region and then migrate anteriorly to populate the anterior hypothalamus. In this model, a continued supply of tuberal-derived cells fuel the growth of the anterior hypothalamus (Fig.6.1B).

In both of these models, predictions can be made regarding cell proliferation. In the first model, based on the differential rates of expansion between the anterior and tuberal hypothalamus, the anterior hypothalamus would exhibit higher levels of proliferation. In the second model, in which proliferation in the tuberal hypothalamus drives expansion of the anterior hypothalamus, the tuberal hypothalamus is predicted to display higher levels of proliferation. I therefore set out to test whether the driving force for anterior hypothalamic growth lies in anterior or tuberal cells.

6.2.2. Growth of the Anterior, Tuberal, and Mammillary Hypothalamus is Anisotropic

To assess the relative growth of the anterior, tuberal, and mammillary hypothalamus, I measured the length of each region in sagittal sections at HH10, HH15, HH20, and HH27 (Fig.6.2A). The tuberal hypothalamus was defined through length of *Fgf10* expression. The anterior hypothalamus was defined by the total length of *Six3*$^{+}$ *Foxg1*$^{-}$ anterotuberal territory, from

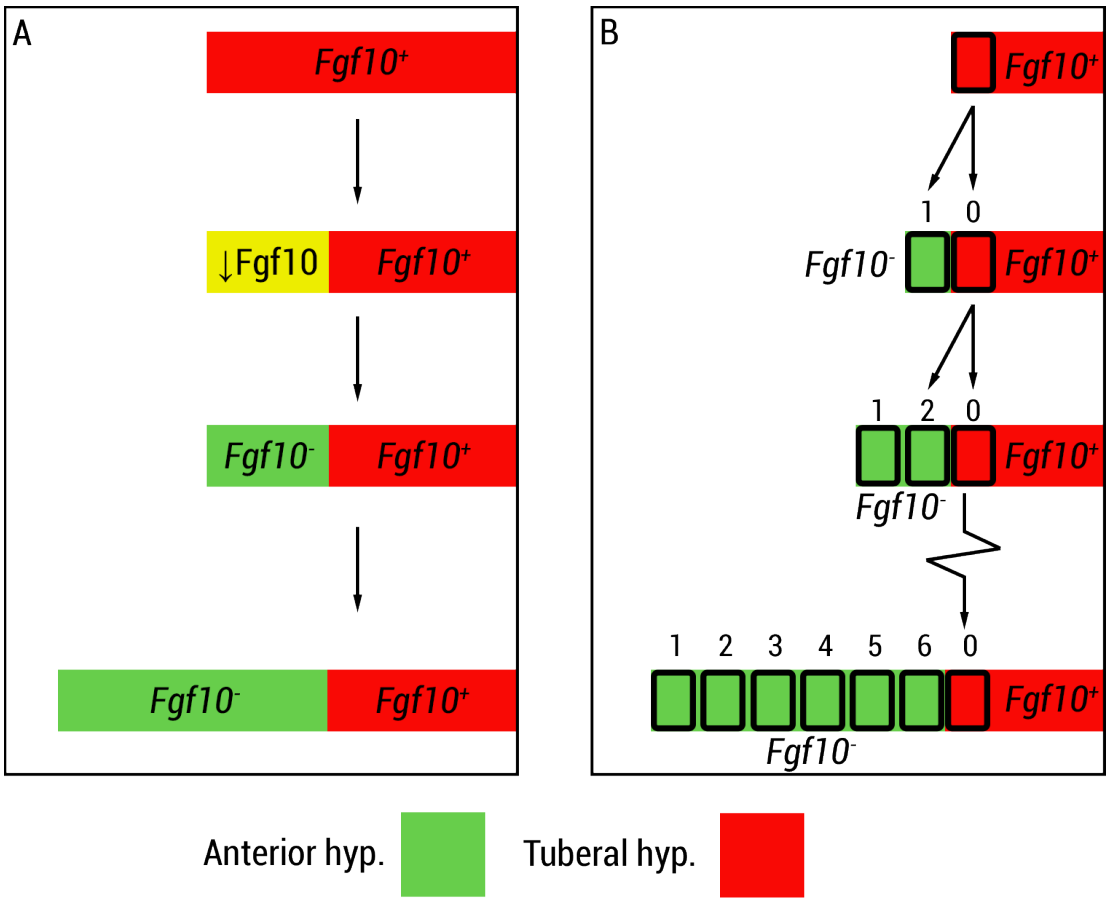

Figure 6.1 | Models of development of anterior hypothalamic development

(A) Anterior hypothalamic identity is specified by a change in fate of an anterior subregion of *Fgf10*+ tuberal hypothalamic cells to give rise to *Fgf10*- anterior hypothalamic cells that subsequently proliferate to drive growth of the anterior hypothalamus. (B) The anterior hypothalamus is built by a proliferating front of *Fgf10*+ tuberal hypothalamic cells that give rise to *Fgf10*- anterior hypothalamic cells.

which was subtracted the length of *Fgf10*$^{+}$ territory (analysed in serial adjacent sections). The mammillary hypothalamus was measured on the basis of morphology outlined in Chapter 3: from the rostral cephalic flexure to the caudal tuberal hypothalamus, identified through the dorsal tip of RP. At HH10, however, the anterior and mammillary hypothalamus is not recognisable through such molecular and morphological markers; but the correlation of my fate mapping data and the expression of *Fgf10* at HH10 suggests that the hypothalamus at this stage is not yet regionalised but expresses tuberal characteristics (Chapter 5).On this basis, the length of anterior and mammillary hypothalamus, at HH10, were given a value of 0.

The tuberal hypothalamus initially reduces in size between HH10 and HH15, then gradually increases in size (Fig.6.2A-B). However, this growth rate is relatively low compared to that of the anterior and tuberal hypothalamus. Growth of the anterior hypothalamus follows a logarithmic growth curve: growth rate is highest between HH10 and HH20 but slows down between HH20 and HH27. In contrast, growth of the mammillary hypothalamus is exponential: growth rate increases over time and is greatest between HH20 and HH27.

On the basis of this, a prediction is that at HH20, the anterior hypothalamus is a highly proliferative population compared to the tuberal and mammillary hypothalamus.

6.2.3. The anterior hypothalamus is less proliferative than the tuberal hypothalamus

To test whether anterior hypothalamic cells are highly proliferative, I assayed cell proliferation by EdU analysis. 5-ethynyl-2'-deoxyuridine (EdU) is a thymidine analog alternative to 5-bromo-2'-deoxyuridine (BrdU) that is incorporated into *de novo* DNA and is visualized by "click" chemistry - the tagging of EdU molecules with fluorescent azides (Salic and Mitchison 2008). I treated HH15 (E2.5) embryos with EdU *in ovo* for 90 minutes, then fixed and stained for EdU-labelled cells. EdU staining of sagittal sections shows that the anterior hypothalamus contains lower numbers of EdU-labelled

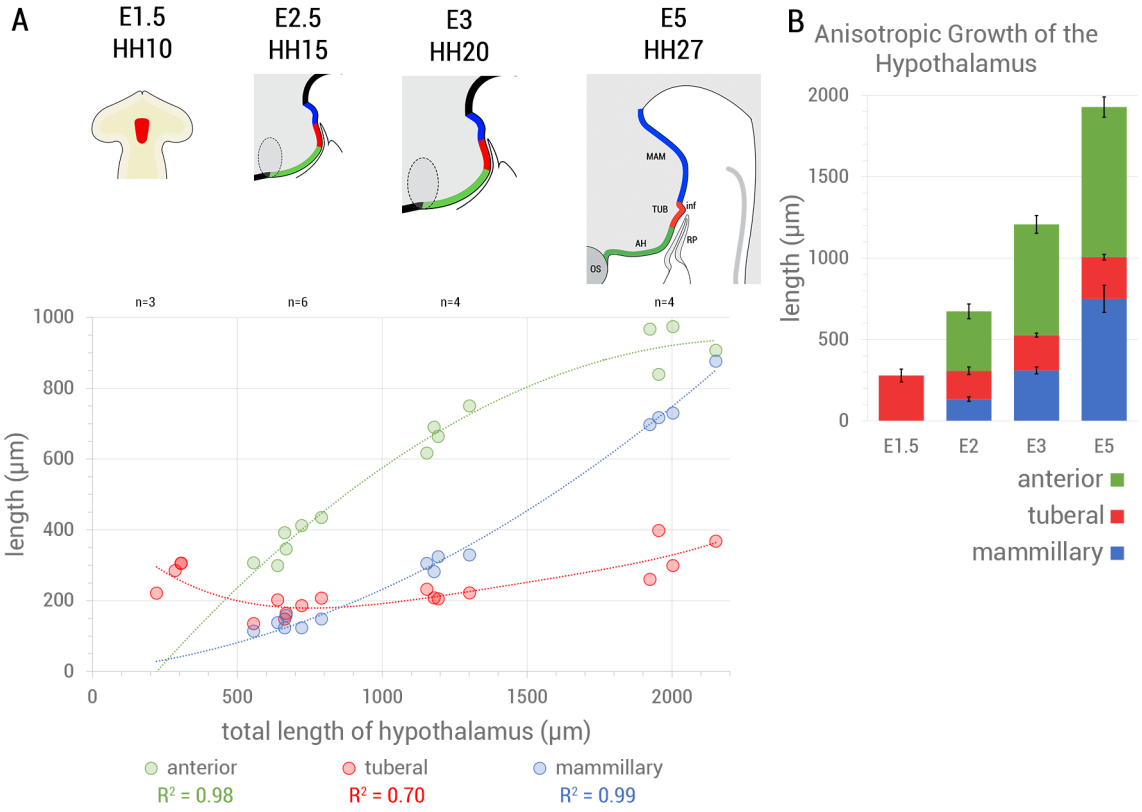

Figure 6.2 | Growth of the hypothalamus over E1.5 and E5 is anisotropic

(A) Scatter plot showing growth of anterior, tuberal, and mammillary hypothalamus over E1.5 and E5. (B) Bar chart representing relative sizes of anterior, tuberal, and mammillary over E1.5 to E5. . Line of best fit (coloured lines) were generated in Microsoft Excel to represent growth of the anterior (logarithmic), tuberal (polynomial), and mammillary hypothalamus (exponential) over time. Error bars represent 95% confidence intervals.

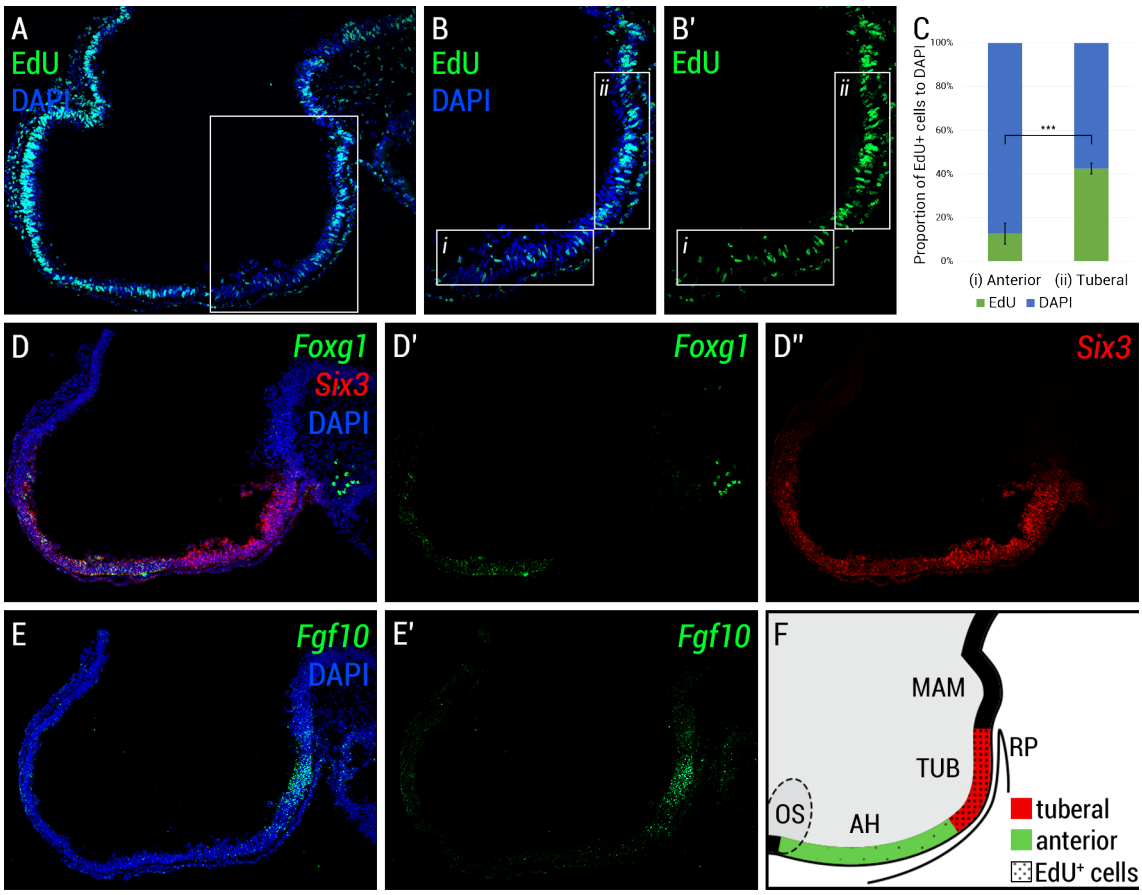

Figure 6.3 | EdU analysis of HH15 anterior and tuberal hypothalamus

(A-B') Sagittal sections of HH15 embryo showing EdU+ proliferating cells in the anterior and tuberal hypothalamus. (B-B') Blow up of boxed region in (A). Labelled boxed regions i and ii corresponds to the anterior and tuberal hypothalamus, respectively. (C) Mean proportion of EdU+ cells and DAPI-labelled nuclei are quantified in 15µm-thick sagittal sections in the boxed anterior (i) and tuberal (ii) regions. The anterior hypothalamus contains statistically significantly less EdU+ proliferating cells than the tuberal hypothalamus (n=4, p<0.001 = ***; t-test, unpaired, 2-tailed). Error bars represent 95% confidence interval. (D-E) Fluorescent *in situ* hybridisation analysis of *Foxg1*/*Six3* and *Fgf10* on serial adjacent sagittal sections of HH15 embryos (n=3). *Foxg1* is detected in the telencephalon (D') and *Six3* is detected in the telencephalon and extends to the caudal tuberal hypothalamus, and adjacent to the dorsal tip of Rathke's pouch (D''). *Fgf10* is detected in the tuberal hypothalamus, adjacent to Rathke's pouch (E-E'). (F) Schematic showing relationship of *Foxg1*, *Six3*, and *Fgf10* expression in an HH15 hypothalamus. For abbreviations, see abbreviation list.

cells compared with the tuberal hypothalamus (Figs.6.3A-B'). Comparison of the EdU profile with markers of anterior and tuberal hypothalamus show that the *Six3*$^{+}$ *Fgf10*$^{+}$ tuberal hypothalamus has high levels of EdU staining while the *Six3*$^{+}$ *Fgf10*$^{-}$ anterior hypothalamus has low levels of EdU staining (Figs.6.3D-F). Quantification of the number of EdU-labelled cells proportional to the number of DAPI-stained nuclei confirm this observation, showing that only 15% anterior nuclei are EdU^{+}, compared to 40% tuberal nuclei (Fig.6.3C).

In summary, the EdU profile of the hypothalamus at HH15 shows that the anterior hypothalamus has lower numbers of proliferating cells compared to the tuberal hypothalamus. This is in stark contrast with the observation that the anterior hypothalamus is undergoing rapid growth during this time point. This result favours the second model of anterior hypothalamic development and suggests that the reason the anterior hypothalamus expands rapidly between HH10 and HH20 (Fig.6.2) is due to a proliferating front driven from the tuberal hypothalamus.

6.2.4. *p57^{Kip2}* is expressed in the anterior hypothalamus at E1.5

The lower levels of EdU detected in the anterior hypothalamus predicts that cells here may already be differentiating. To investigate this, I analysed the expression of the Cip/Kip family of cyclin-dependent kinase inhibitors (CKIs), including *p57^{Kip2}*, *p27^{Kip1}*, and *p21^{Cip1}*. These genes are negative cell cycle regulators of the G1-to-S-phase. The G1-to-S phase transition is a critical cell cycle event that determines whether a cell will commit to cell division, remain in G1-phase, or exit the cell cycle (Sherr and Roberts 1999). *p57^{Kip2}* and *p27^{Kip1}* promote cell cycle exit and have been shown to be important for differentiation (Zhang *et al.* 1999; Quaroni *et al.* 2000; Galderisi *et al.* 2003).

In situ hybridisation for *p57^{Kip2}* and *p27^{Kip1}* at HH15 (E2.5) shows that *p57^{Kip2}* is detected at strong levels in the ventral anterior hypothalamus, while *p27^{Kip1}* is detected at minimal levels (black arrowheads, Figs.6.4A,B). Expression of *p21^{Cip1}* likewise is not detected in the ventral hypothalamus

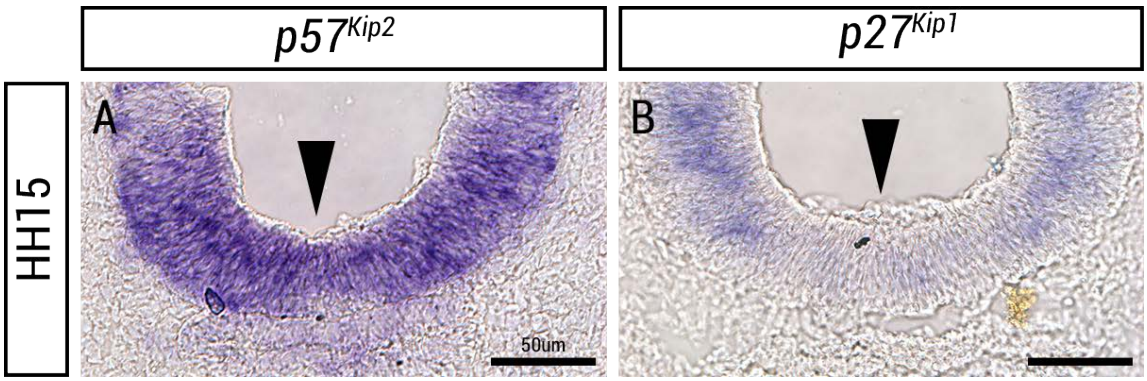

Figure 6.4 | Expression of *p57Kip2* and *p27Kip1* in the ventral anterior hypothalamus
In situ hybridisation analysis of *p57Kip2* (n=2) and *p27Kip1* (n=3) on transverse sections of the anterior hypothalamus at HH15. *p57Kip2* is detected in the ventral midline and basal regions (A). *p27Kip1* is detected strongly in basal regions but minimal levels are detected in the ventral midline (B). Black arrowheads point to the ventral midline.

at a later stage of development (HH27) and thus I did not analyse for *p21Cip1* at HH15. Together, this suggests that *p57Kip2* may govern the behaviour of anterior hypothalamic cells.

I therefore next extended my analysis of *p57Kip2* expression to earlier stages (HH9 to HH13, E1.5) and to a later stage (HH18, E3). No expression was detected in the forming hypothalamus at HH9 (data not shown). At HH10, I began to detect *p57Kip2* in the hypothalamus. Expression appeared as punctate spots that formed an arc shape (black arrowheads in Figs.6.5A,A'). *p57Kip2* was also detected in lateral regions more posteriorly in the presumptive p1, p2, or p3 prosomeres (white arrowheads in Figs.6.5A,A'). Comparison with my fate mapping experiments at HH10 suggest that *p57Kip2* expression in the hypothalamus correlates with the anterior hypothalamus (Chapter 4; Fig.4.6). Over HH11, HH12, and HH13, the expression of the hypothalamic *p57+* territory expands in length along the anterior-posterior axis (Figs.6.5B-D'). This expansion of *p57+* territory coincides with the rapid expansion of the anterior hypothalamus. Analysis at HH18, when divisions of the hypothalamus can be recognised morphologically, confirms that *p57Kip2* is expressed in the anterior hypothalamus and reveals that expression extends into the tuberal hypothalamus as a continuous domain, with a caudal boundary adjacent to the posterior tip of Rathke's pouch (Figs.6.5E-E'). I showed in Chapter 4 that expansion of the anterior hypothalamus exhibits a logarithmic growth pattern, with a high rate

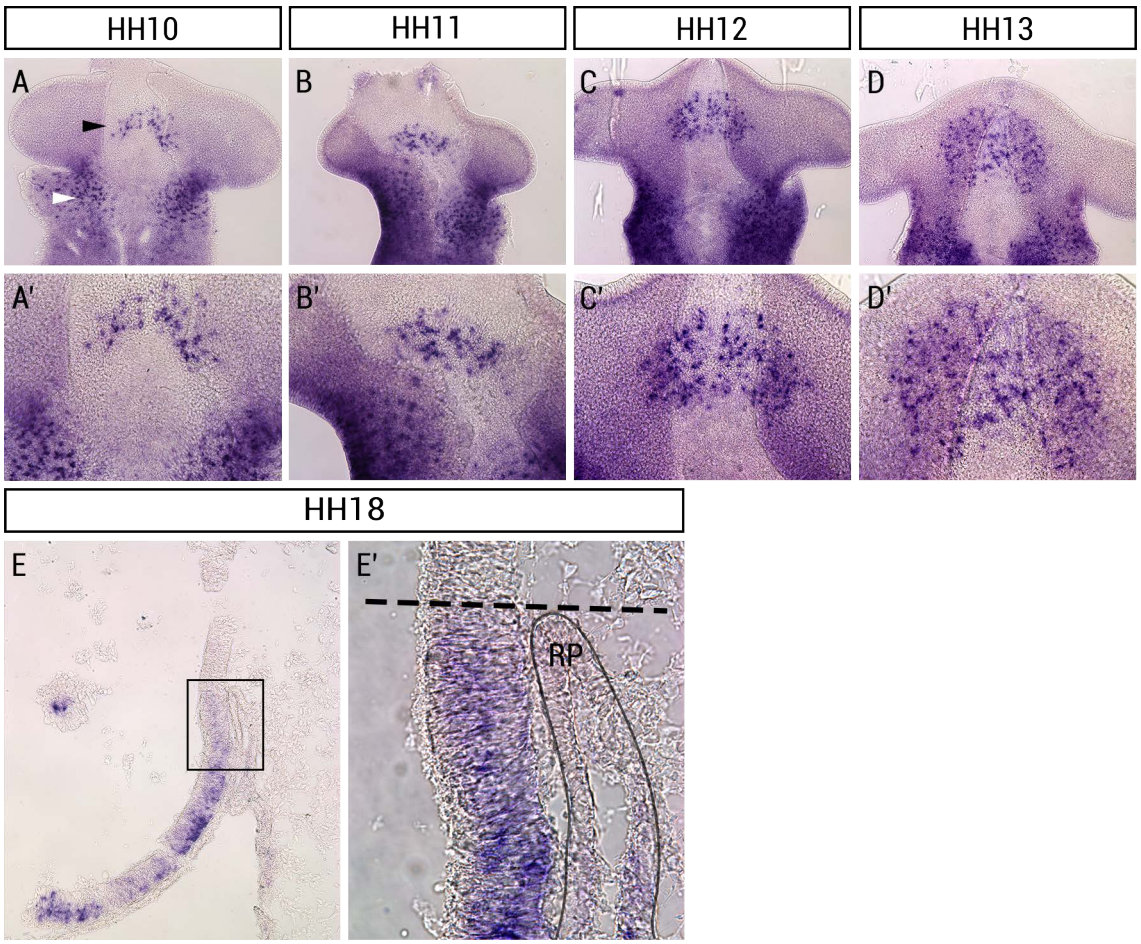

Figure 6.5 | Expression of *p57^{Kip2}* in the hypothalamus between HH10 and HH18

In situ hybridisation analysis of *p57^{Kip2}* in wholemount embryos and sagittal sections. (A-D) Ventral views of flat-mounted neuroepithelium at HH10 (n=4), HH11 (n=1), HH12 (n=6), and HH13 (n=1). (A'-D') High magnification images of the anterior hypothalamus. *p57^{Kip2}* is detected in the anterior hypothalamus and its expression domain increases over HH10 and HH13. Black arrowhead points to *p57^{Kip2}* expression in the anterior hypothalamus. *p57^{Kip2}* is also detected in the presumptive baso-lateral p2/p3 regions. (E) Sagittal section of HH18 hypothalamus. *p57^{Kip2}* is detected in the anterior and tuberal hypothalamus (n=4). (E') High magnification image shows expression of *p57^{Kip2}* in the tuberal hypothalamus, in line with adjacent to the dorsal tip of Rathke's pouch (dashed lines). RP, Rathke's pouch.

between HH10 (E1.5) and HH20 (E3) and at a low rate afterwards (Fig.6.2). My model suggests that the tuberal hypothalamus provides daughter cells that populate the anterior hypothalamus. The expression of *p57*, a cell cycle inhibitor, in the tuberal hypothalamus at E3 suggests that the tuberal hypothalamus has a lower proliferative capacity at this stage and thus correlates with the reduced rate of growth observed in the anterior hypothalamus from E3 onwards.

The role of $p57^{Kip2}$ in the hypothalamus may be to promote cell cycle exit and thus initiate cell differentiation, including neuronal differentiation. Previous studies have shown that the earliest neurogenic region in the hypothalamus is the anterior hypothalamus, which generates neurons whose axons form part of a major axonal scaffold, the tract of the postoptic commissure (Ware and Schubert 2011). Analysis of HH18 chick embryos by wholemount TUJ1 immunolabelling confirms that $TUJ1^+$ neurons first differentiate in the anterior hypothalamus, form a commissure, and extend axons posteriorly (Fig.6.6). This tract, together with the medial longitudinal fascicle (MLF) forms the ventral longitudinal tract, which extends from the anterior hypothalamus to the spinal cord. These neurons appear to differentiate in the $p57^+$ anterior hypothalamus (FIG.6.5). Based on this, I conclude that as tuberal-derived daughter cells leave the tuberal

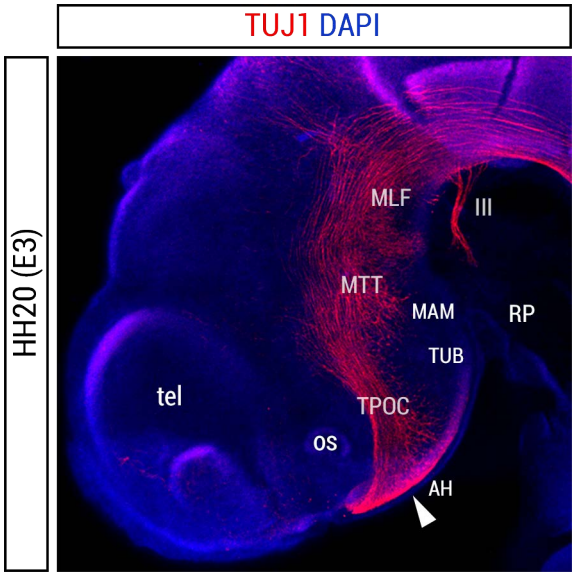

Figure 6.6 | Immunostaining for Tuj1 in the anterior hypothalamus at HH20

Isolated HH20 neuroepithelium immunostained for neuron-specific Class III β-tubulin (Tuj1; n=1). $Tuj1^+$ neurons are detected in the anterior hypothalamus and their axons form part of the tract of the postoptic commissure, a major axonal scaffold. $Tuj1^+$ neurons is not detected in the tuberal and mammillary hypothalamus. Arrowhead points to the anterior hypothalamus. III, oculomotor nerve; MTT, mamillo-tegmental tract; MLF, medial longitudinal fascicle; TPOC, tract of the postoptic commissure. For rest of abbreviations, see abbreviation list.

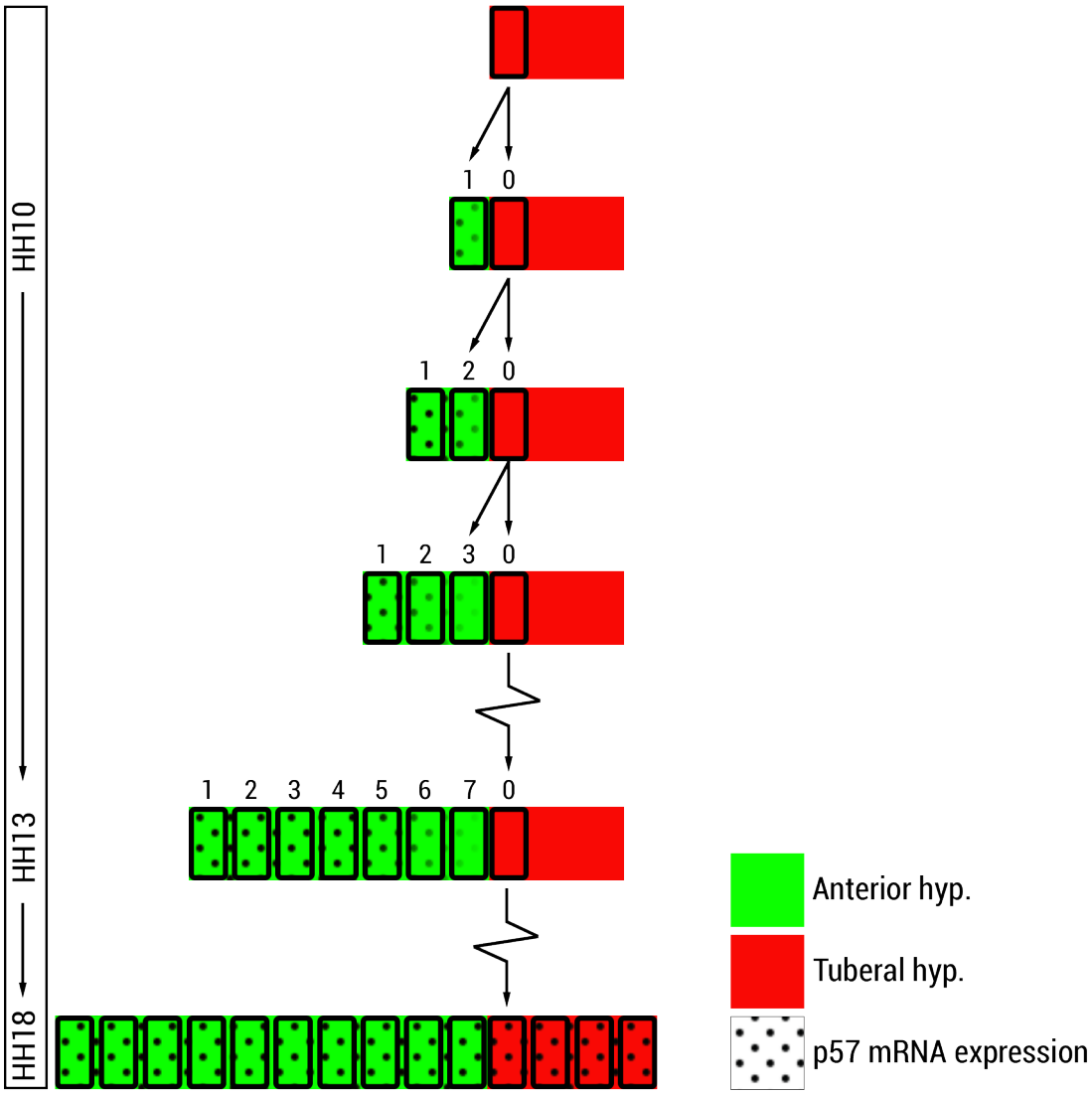

Figure 6.7 | Updated model of anterior hypothalamic development

The anterior hypothalamus is built over HH10 and HH18 through a proliferating front of tuberal hypothalamic cells that give rise to anterior hypothalamic cells. As anterior hypothalamic cells are produced, they begin to change in fate. They upregulate *p57^{Kip2}*, which in turn promotes cell cycle exit for differentiation. At HH18, the tuberal hypothalamus begins to express *p57^{Kip2}*, at which point, growth of the anterior hypothalamus slows down.

hypothalamus, they upregulate *p57^{Kip2}* which in turn promotes cell cycle exit for differentiation (Fig.6.7).

6.2.5. *p57^{Kip2}* expression in the anterior hypothalamus requires Shh signalling

As outlined in the Introduction (section 1.3.6), studies in chick, mouse and zebrafish have shown that Shh deriving from the hypothalamus is required for continued development and differentiation of the hypothalamus, including the anterior hypothalamus(Shimogori *et al.* 2010; Zhao *et al.* 2012; Muthu *et al.* 2016). The mechanism of action of Shh in anterior hypothalamic development, however, has not been studied. In particular, none of these studies were able to determine whether Shh stimulated the growth/development of the anterior hypothalamus by acting on 'tuberal' hypothalamic cells – i.e. analysed the effect of Shh within the context of a 'tuberal progenitor' model. I therefore asked whether inhibition of Shh signalling affected the development of tuberal-derived progenitors that give rise to the anterior hypothalamus. I hypothesised that Shh is required to promote anterior hypothalamic development from tuberal hypothalamic cells.

Previous studies have shown that *Shh* is expressed in, and defines, the RDVM cells that I have now shown will give rise to the hypothalamus (Dale *et al.* 1999). Analysis of *Shh* in at HH10 confirms that *Shh* expression has a similar overall expression to that of *Fgf10* in the prosencephalon (Fig.6.8A,B). Double fluorescent *in situ* hybridisation with the telencephalic marker, *Foxg1*, on sagittal sections, shows that *Shh* abuts the *Foxg1*$^{+}$ telencephalic territory (arrowhead, Figs.6.8C-C''). Together, this suggests again that at HH10, the hypothalamus is tuberal in character. However, close analysis of the fluorescent *in situ* hybridisation suggest that the highest levels of *Shh* expression are detected around the periphery of *Fgf10*$^{+}$ cells, including those in the anterior-most hypothalamus (arrowhead, Fig.6.8A'). This raises the possibility that an anterior border emerges, composed of *Shh*$^{strong+}$ *Fgf10*$^{+}$ cells, that will drive growth of the anterior hypothalamus.

To test this further, I performed double *in situ* hybridisation for *Shh* and *p57*, asking if *Shh*$^{+}$ cells correlated with the emerging anterior hypothalamus. My results show that at HH10, *p57*^{Kip2}expression coincides with the strong expression of *Shh* at the anterior border. Over HH10 to HH13, this domain expands in size along the antero-posterior axis. From HH12 onwards, *p57*^{Kip2}expression is additionally detected anterior to the *Shh*$^{+}$ territory (arrowhead, Figs.6.8A',D-F). This expression suggests a model, in which anterior hypothalamic cells begin to express *Shh* and *p57*^{Kip2}, and as they undergo further maturation, downregulate Shh.

I next asked whether *Shh* is required for development of the anterior hypothalamus. As a first step, I asked whether expression of *p57*^{Kip2} is dependent on Shh signalling. *Shh* was pharmacologically inhibited with cyclopamine. Cyclopamine was added to HH9 embryos which were then analysed at stages HH10 to HH13 for *p57*^{Kip2} expression. Cyclopamine inhibits Shh signalling by binding to Smoothened (Smo), which prevents *Ptch1* binding and thus blocks cellular responses to Hedgehog signalling (Chen *et al.* 2002), including transcriptional upregulation of *Ptch1* itself (Ingham 2012). To test that cyclopamine effectively inhibited Shh signalling, I analysed expression of *Ptch1*. At HH10 and HH13, expression of *Ptch1* was not detected in the forebrain of cyclopamine-treated embryos while it was detected in control embryos (arrowheads, Figs.6.9A,B,D,E). At HH15, expression of *Ptch1* was detected in cyclopamine-treated embryos (arrowheads, Figs.6.9C,F). This suggests that cyclopamine treatment of HH9 embryos results in downregulation of Shh signalling between HH10 and HH13, but by HH15 the inhibitory effects of cyclopamine is alleviated. Whole mount *in situ* hybridisation for *p57*^{Kip2} between HH10 and HH12 shows that *p57*^{Kip2} cannot be detected in the hypothalamus at these stages (arrowheads, Figs.6.10A-F).

In summary, my results show that *p57*^{Kip2} is downstream of Shh signalling and suggest that Shh is involved in differentiation in the anterior hypothalamus. This is in keeping with other studies in mice and zebrafish which have reported that Shh from a hypothalamic source is required for growth and differentiation of the anterior hypothalamus (Shimogori *et al.* 2010; Zhao *et*

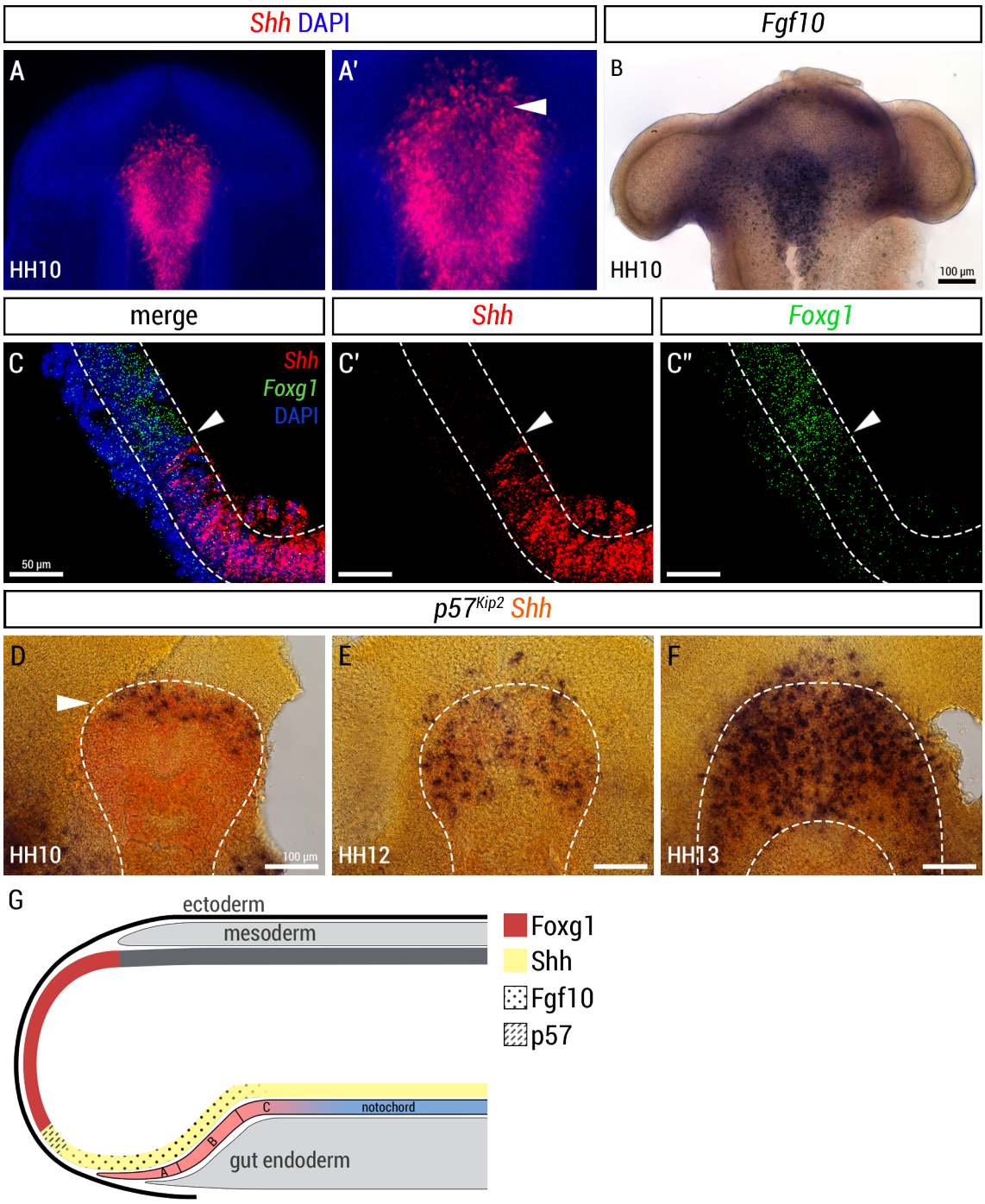

Figure 6.8 | Expression of *Shh* relative to *Fgf10*, *Foxg1*, and *p57Kip2*

(A-A') Ventral view of flat-mounted HH10 embryo fluorescently hybridised for *Shh* (n=2). *Shh* is detected strongly around the periphery (arrowhead, A'). (B) Ventral view of flat-mounted HH10 embryo hybridised for *Fgf10* (n=6). *Fgf10* is detected in the ventral prosencephalon in a similar region to *Shh* expression. (C-C'') Fluorescent *in situ* hybridisation of *Shh* and *Foxg1* on HH10 sagittal sections showing the telencephalic-hypothalamic boundary. *Shh* abuts the caudal expression of *Foxg1* telencephalon. White arrowheads point to *Shh-Foxg1* border. (D-F) Ventral view of flat-mounted prosencephalon at HH10 (n=2), HH12 (n=3) and HH13 (n=2), simultaneously hybridised for $p57^{Kip2}$ and Shh. $p57^{Kip2}$ expression expands over HH10 and HH13 and is largely restricted to anterior *Shh* expression domain. At HH12 and HH13, $p57^{Kip2}$ is detected anterior to Shh^{+} territory. (G) Schematic representation of *Shh* expression relative to *Foxg1*, *Fgf10*, and p57.

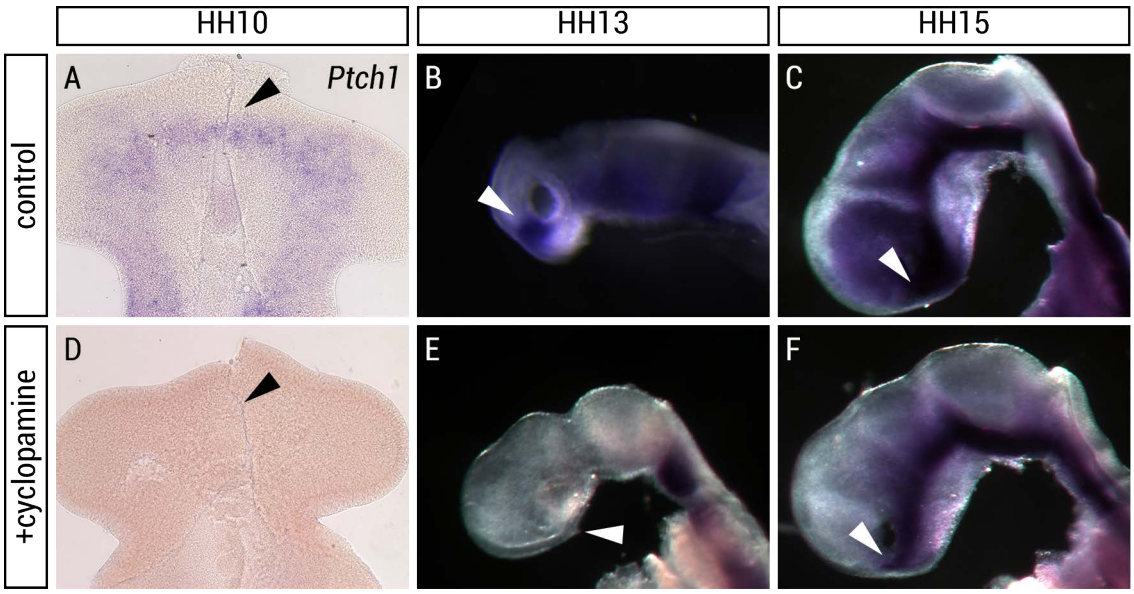

Figure 6.9 | Shh signalling is blocked between HH10 and HH15 in response to cyclopamine treatment

(A-F) In situ hybridisation analysis of *Ptch1* in wholemount embryos at HH10, HH13, and HH15 following PBS (control; HH10, n=3; HH13, n=2; HH15, n=1) or cyclopamine treatment at HH9 (HH10, n=4; HH13, n=4; HH15, n=5). Isolated neuroepithelium are presented as flat-mount (A,D) or side views (B,C,E,F). *Ptch1* is detected in the anterior hypothalamus over HH10-13 in control embryos (A-C). *Ptch1* is not detected in the anterior hypothalamus at HH10 and HH13 in embryos treated with cyclopamine (D,E) , but is detected the anterior hypothalamus at HH15 (F). *Ptch1* is also detected in the rhombomeres and spinal cord at HH13 following cyclopamine treatment. Arrowheads point to the anterior hypothalamus.

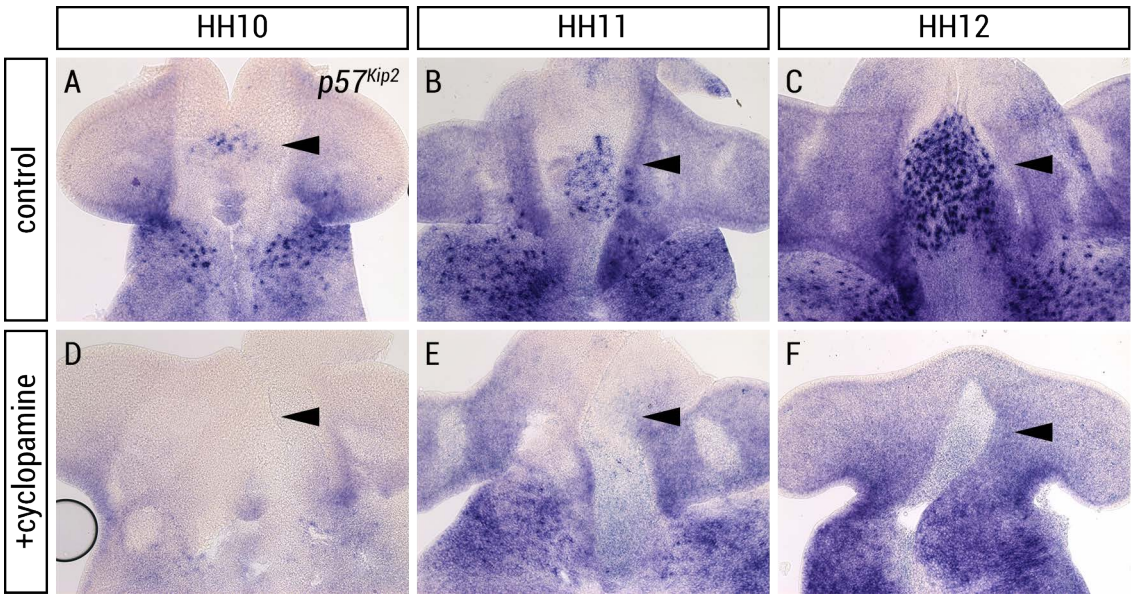

Figure 6.10 | *p57Kip2* is downstream of Shh signalling

(A-F) Ventral view of flat-mounted neuroepithelium assayed for $p57^{Kip2}$ following PBS (control; HH10, n=3; HH11, n=3; HH12, n=3) or cyclopamine treatment at HH9 (HH10, n=5; HH11, n=4; HH12, n=6). $p57^{Kip2}$ is detected in the anterior hypothalamus over HH10 and HH12 in control embryos (A-C). $p57^{Kip2}$ is not detected in the anterior hypothalamus over HH10 and HH12 following cyclopamine treatment (D-F), but is detected in the presumptive baso-lateral p2/p3. Arrowheads point to the anterior hypothalamus.

al. 2012; Muthu *et al.* 2016).

6.2.6. Shh is required for normal morphology of the anterior and tuberal hypothalamus

In my model, the anterior hypothalamus develops from the *Fgf10*$^{+}$ tuberal hypothalamus. In other words, expression of *p57*^{Kip2} is absent because development of the anterior hypothalamus is prevented in the absence of Shh signalling. To begin to ask whether inhibition of Shh signalling between HH10 and HH15 prevents development of the anterior hypothalamus, I allowed cyclopamine-treated embryos to develop to HH27 (E5). Such embryos did indeed show significant disruptions to the anterior hypothalamus.

In cyclopamine-treated embryos, the *Six3*$^{+}$ *Foxg1*$^{-}$ territory, which marks the anterior and tuberal hypothalamus, showed very unusual morphology. The contours of the ventral anterior hypothalamus that normally form a characteristic 'inverted S' shape, failed to develop. Instead, cyclopamine-treated embryos displayed a 'flattened' ventral morphology (dashed lines, Figs.6.11A,B) and only a small 'bulge' along the ventral (arrows, Figs.6.11A,B). The length of the anterotuberal hypothalamus likewise appeared to be shortened. To quantitatively measure this, I measured the length of the *Six3*$^{+}$ *Foxg1*$^{-}$ territory along the ventral surface (dashed lines, Figs.6.11A,B). Cyclopamine-treated embryos displayed a 22% reduction in length compared with control embryos (Fig.6.11C).

Analysis of *Six3* and *Foxg1* does not distinguish whether loss of territory is within the anterior or tuberal hypothalamus. To do so, I therefore analysed *Fgf10*, or *Six3*, in serial adjacent sagittal sections. This confirmed that both maintained their shared caudal boundary (Supplementary Fig.3). At first sight, the length of *Fgf10*$^{+}$ tuberal hypothalamus appeared shorter in cyclopamine-treated embryos compared to controls (Fig.6.11D,E; measurements not shown). However, I noted that in wild type embryos, *Fgf10* is expressed strongly in the tuberal hypothalamus, and is gradually weaker more rostrally. In the context of my model, I hypothesise that the high levels of *Fgf10* (filled arrowhead, Fig.6.11D) correlate with the tuberal

hypothalamus while the low levels of *Fgf10* (empty arrowhead, Fig.6.11D) mark a transition zone where tuberal-derived cells are transitioning to anterior hypothalamic cells. I subsequently compared the length of this region (high levels of *Fgf10*) in controls with the length of *Fgf10*$^{+}$ territory in cyclopamine-treated embryos (dashed lines, Figs.6.11D,E). In cyclopamine-treated embryos, the length of *Fgf10*$^{+}$ tuberal hypothalamus along the ventral surface remains unchanged compared to controls (Fig.6.11F). This result suggests that cyclopamine treatment leads to a loss of territory in the anterior hypothalamus but not a loss of tuberal territory.

Nonetheless, my experiments show that the tuberal territory is not unchanged after cyclopamine treatment. In particular, the neuroepithelium appears wider, and development of the infundibulum is disrupted. In many cyclopamine-treated embryos (n=8/10), the infundibulum is absent (Figs.6.11A-E). Specifically, the infundibulum fails to evaginate from the tuberal hypothalamus. In a minority (n=2/10), the infundibulum is present as a rudimentary evagination but does not develop properly compared to controls (filled arrowhead, Fig.6.12B).

In summary, these results suggest that Shh signalling over HH10 and HH15 is required for normal development of the anterior and tuberal hypothalamus, including the infundibulum (Figs.6.11G,H). In particular I show that in cyclopamine-treated embryos, there is a loss of anterior hypothalamic territory. In the my model, this confirms previous results to suggest that *Shh* is important for the process, in which the tuberal hypothalamus drives growth of the anterior hypothalamus.

6.2.7. Shh is required for normal anterior pituitary development

Many previous studies have suggested an important link between development of the infundibulum and development of Rathke's pouch, the precursors to the posterior and anterior pituitary, respectively. In particular, studies have suggested that signals from the ventral diencephalon are required for normal development (Daikoku *et al.* 1982; Takuma *et al.* 1998; Gleiberman *et al.* 1999). In support of this, I noted that embryos that were

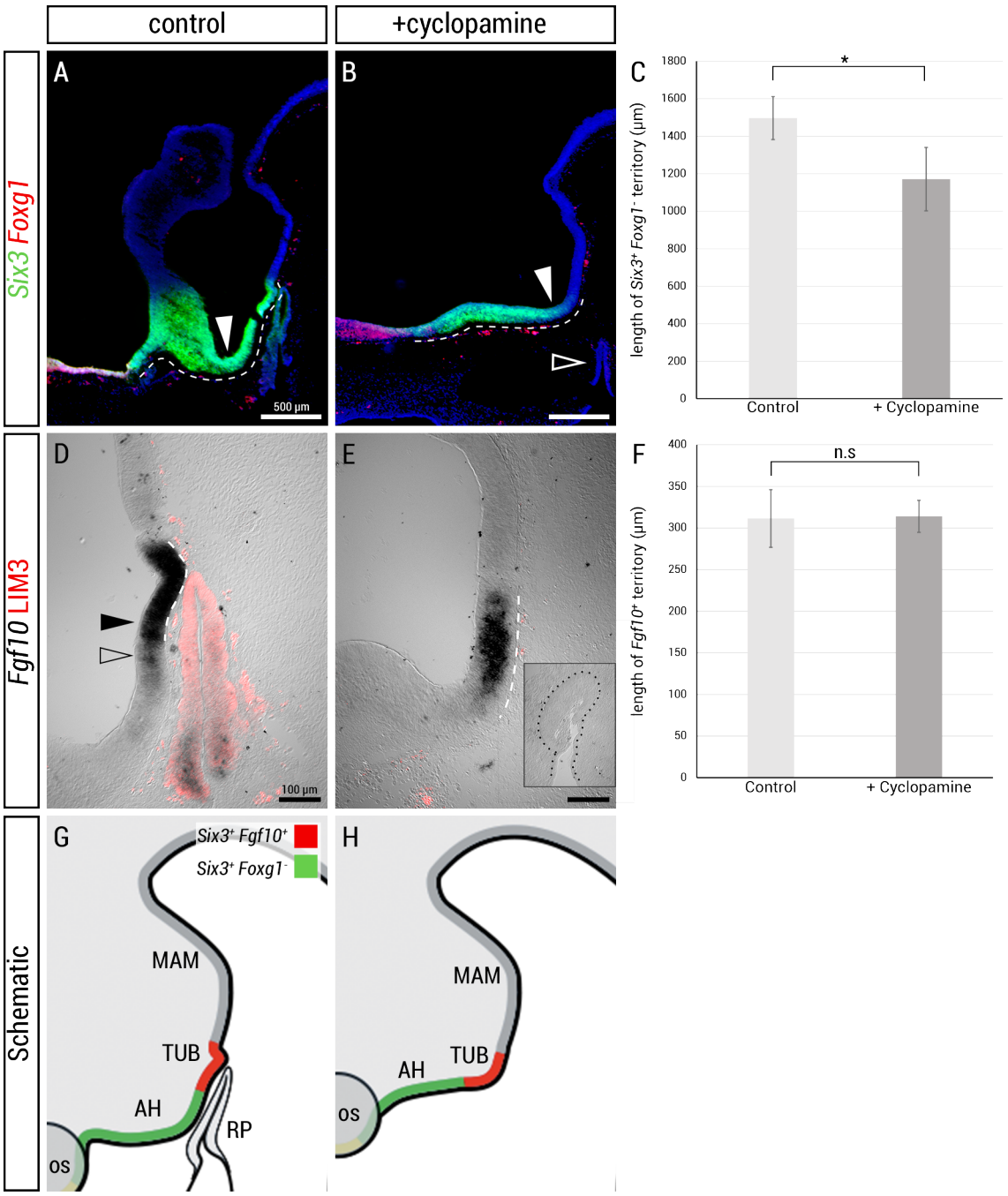

Figure 6.11 | *Shh* is required for proper growth of the anterior hypothalamus

(A,B,D,E) *in situ* hybridisation analysis of *Six3*/*Foxg1* and *Fgf10*/LIM3 on E5 serial adjacent sagittal sections following PBS (control) or cyclopamine treatment at HH9. (A-B) Morphology of *Six3*$^{+}$ *Foxg1*$^{-}$ territory is disrupted in cyclopamine-treated embryos. (D-E) The infundibulum is absent in cyclopamine-treated embryos but expression of *Fgf10* is detected. Inset in (E) shows LIM3^{-} RP-like rudiment. (C) Mean length of *Six3*$^{+}$ *Foxg1*$^{-}$ anterotuberal hypothalamus in control (n=3) and cyclopamine-treated (n=5) embryos is measured along dashed lines (A,B). The anterotuberal hypothalamus is significantly shorter in cyclopamine-treated embryos than controls ($p<0.05$ = *; t-test, unpaired, 2-tailed). (F) Mean length of *Fgf10* tuberal hypothalamus in control (n=5) and cyclopamine-treated embryos (n=5) is measured along dashed lines (D,E). Length of the tuberal hypothalamus is unaffected by cyclopamine-treatment ($p>0.05$ = ns; t-test, unpaired, 2-tailed). (G,H) Schematic representing disrupted morphology in response to cyclopamine-treatment. For abbreviations, see abbreviation list.

treated with cyclopamine displayed multiple disruptions to development of Rathke's pouch. Firstly, in cyclopamine-treated embryos, a pouch-like structure formed but did not express the anterior RP marker, LIM3 (n=4/4; SJÖDAL and GUNHAGA 2008; Fig.6.11E inset). *Six3*, which is expressed in the forming pouch, was similarly absent (n=5/6). Secondly, the close apposition of the infundibulum and RP was disrupted (n=10/10), i.e. the infundibulum and RP were no longer adjacent to each other (Figs.6.11A,B). Instead mesenchymal cells filled the intervening space. Thirdly, and finally, a subset of cyclopamine-treated embryos exhibited a second ectopic rudimentary RP-like structure (n=2/6; empty arrowheads, Figs.6.12A-C).

6.2.8. Downregulation of Shh signalling disrupts distribution of cells that populate the anterior hypothalamus

In my model for the development of the anterior hypothalamus, I predicted that directed proliferation or migration of tuberal-derived cells is required to build the anterior hypothalamus (Fig.6.7). To test if Shh signalling is involved in this process, embryos were first treated with cyclopamine or PBS at HH9; DiI is then injected into *region A* at HH10, which has been shown to populate the anterior hypothalamus (see 4.2.5; Fig.4.6); the embryo developed until HH20 and was assayed for DiI labelling and *Fgf10* expression (Fig.6.13A). I examined the distribution of DiI-labelled cells along the rostrocaudal axis, relative to *Fgf10* expression. In cyclopamine-treated embryos, 51% of sections containing DiI-labelled cells were within the *Fgf10*$^-$ anterior hypothalamus, compared to 73% in controls, i.e. a significant reduction. 49% of sections containing DiI-labelled cells were within the *Fgf10*$^+$ tuberal hypothalamus in cyclopamine-treated embryos, a significant increase compared to 28% in controls (Figs.6.13B-C). Together this shows that the distribution of *region A* cells is disrupted in response to cyclopamine. Specifically, a larger proportion of DiI-labelled cells remain in the *Fgf10*$^+$ tuberal hypothalamus, suggesting a disruption in directed proliferation and/or migration of these cells.

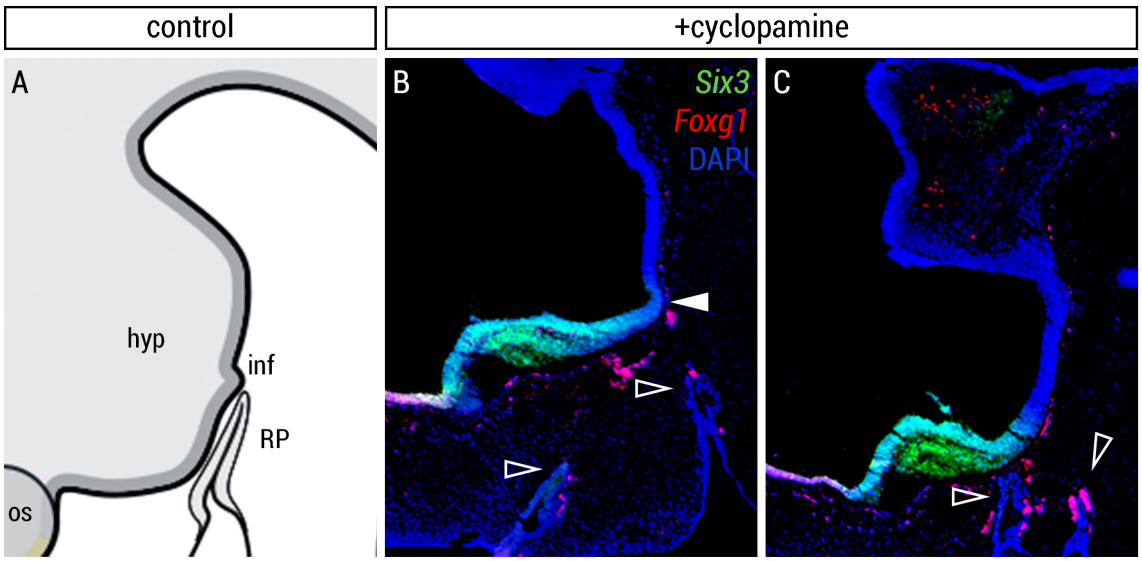

Figure 6.12 | *Shh* is required for proper morphology of the infundibulum and Rathke's pouch

(A) Schematic showing E5 hypothalamus and Rathke's pouch morphology in embryos treated with PBS (control) at HH9. (B-C) Sagittal sections of E5 embryos showing an example of a subset of embryos with rudimentary evagination of the infundibulum (n=2/10; filled arrowhead) and ectopic rudimentary Rathke's pouch-like structure (n=2/6; empty arrowheads) following cyclopamine treatment at HH9.

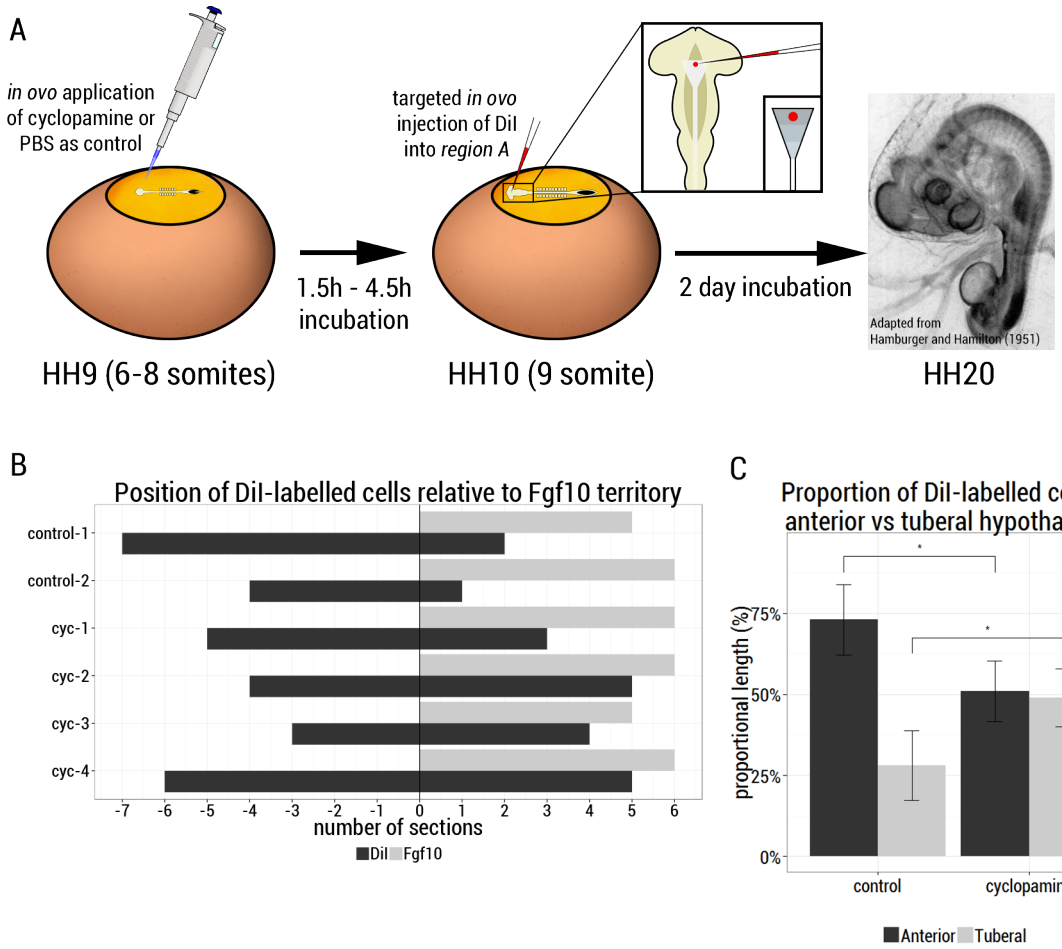

Figure 6.13 | *Shh* is required for proper distribution of *region A* cells

(A) Schematic of experimental procedure. (B-C) Bar graph illustrating individual (B) or mean (C) distribution of DiI-labelled cells relative to Fgf10⁺ tuberal hypothalamus following PBS (control, n=2) or cyclopamine treatment (n=4) at HH9 and focal injections into region A (progenitors of caudal anterior and rostral tuberal hypothalamus). (C) Higher proportion of DiI-labelled cells are retained in Fgf10⁺ tuberal hypothalamus in cyclopamine-treated embryos compared to controls ($p<0.05$ = *; t-test, unpaired, 2-tailed). .

6.3. Discussion

In the previous chapter, I showed that the hypothalamus at HH10 is not regionalised. Instead, I detect ubiquitous expression of *Fgf10* in the future anterior, medial, and mammillary hypothalamus. In this chapter, I presented two possible models to explain how the anterior hypothalamus initially forms. In the first model, *Fgf10* is downregulated in a subregion of the *Fgf10*$^{+}$ hypothalamus, which gives rise to proliferative progenitors of the anterior hypothalamus. In the second model, a proliferation front at the anterior end of the *Fgf10*$^{+}$ hypothalamus drives growth of the *Fgf10*$^{-}$ anterior hypothalamus. In support of the second model, EdU analysis suggests that cells in the anterior hypothalamus are not a proliferative population at a time when it shows substantial growth, whereas cells in the tuberal hypothalamus are proliferating highly. Furthermore, analysis of cell cycle inhibitors suggest that the reason the anterior hypothalamus is a non-proliferative population is because these cells are being instructed to differentiate.

To begin to determine which factors are involved in the growth of the anterior hypothalamus, I identified *Shh* as a candidate. *Shh* initially shows a similar expression pattern to *Fgf10* but then begins to be unregulated anterior to *Fgf10*. Its anterior boundary correlates with the expression of the cell cycle inhibitor, *p57*^{Kip2}. Preliminary data suggests that pharmacological blocking of Shh signalling between HH10 and HH15 results in (1) a shorter anterior hypothalamus, likely caused by (2) retention of anterior hypothalamic progenitors in the tuberal hypothalamus, which consequently appears wider; (3) disruption of differentiation in the anterior hypothalamus, as assessed by loss of *p57*^{Kip2} expression, and (4) failure of both the infundibulum and Rathke's pouch to develop normally. I discuss these findings more fully in the final Discussion.

6.3.1. Growth of the anterior hypothalamus is anisotropic

In this study, I have characterised the surface length of the anterior, tuberal, and mammillary hypothalamus over E1.5 to E5. This is the first report

of relative growth rates between the anterior, tuberal, and mammillary hypothalamus. It shows three key findings: (1) anterior hypothalamus grows rapidly between E1.5 and E3, (2) the tuberal hypothalamus remains relatively static, and (3) the mammillary hypothalamus grows rapidly between E3 and E5. Together, they suggest a general model of hypothalamic growth, in which initial growth occurs in the anterior hypothalamus and a second burst of growth occurs in the mammillary hypothalamus. Consistent with this finding, my fate mapping results in chapter 4 identified a highly proliferative population in the rostral mammillary hypothalamus. This raises a possibility that the rostral mammillary hypothalamus is similarly built by a proliferation front in the caudal tuberal hypothalamus.

6.3.2. Role of *p57^{Kip2}* in generation of neurons in the anterior hypothalamus

The anterior hypothalamus is an early neurogenic region in the hypothalamus, generating neurons whose axons will form part of a major axonal scaffold - the tract of the postoptic commissure (Chédotal *et al.* 1995; Chitnis and Kuwada 1990; Ware and Schubert 2011). A recent study demonstrated that Notch signalling is required for the generation of these neurons (Ratié *et al.* 2013). Notch signalling has been described as a mechanism to maintain neural progenitor identity by suppressing neuronal differentiation (Zhou *et al.* 2010). Many studies show that the Cip/Kip family of cyclin-dependent kinase inhibitors (i.e. *p21^{Cip1}*, *p27^{Kip1}* and *p57^{Kip2}*) promote cell cycle exit and differentiation (Lovicu and McAvoy 1999; Zhang *et al.* 1998; Zhang *et al.* 1999) and Notch signalling has been shown to repress the expression of these cell cycle inhibitors (Georgia *et al.* 2006; Riccio *et al.* 2008; Saravanamuthu *et al.* 2009; Zalc *et al.* 2014).

The expression pattern of the Notch effectors Hes5 and Hey1 reported in *Ratié et al. (2013)* share a similar salt-and-pepper like expression pattern with *p57^{Kip2}* in the anterior hypothalamus and correlate with the onset of *p57^{Kip2}* expression at HH10. Thus, on this basis, *p57^{Kip2}* in the anterior hypothalamus may mark neurons that have exited the cell cycle. The loss of *p57^{Kip2}* may indicate loss of these neurons.

6.3.3. Role of Shh signalling in development of the infundibulum and Rathke's pouch

Many syndromes in humans have been reported to exhibit an ectopic anterior pituitary (Bergson *et al.* 2007; Webb and Dattani 2010; Kimmell *et al.* 2014), but it is unclear how such ectopic anterior pituitaries develop. The presence of an ectopic rudimentary RP in cyclopamine-treated embryos suggests a role for Shh signalling in this aberrant developmental process and provides a starting point to further study this. Consistent with this, conditional mutant mice, in which *Shh* is deleted in the hypothalamus, report an ectopic RP (Zhao *et al.* 2012). However, there are discrepancies between the phenotypes observed in mouse and the phenotype I detect here.

Zhao et al. (2012) report that RP and the ectopic RP-like structure both express LIM3, which marks RP. In contrast, I do not observe expression of LIM3, either in RP-like structures or in ectopic RP-like structure. Moreover, *Zhao et al. (2012)* show that, in the hypothalamus, the *Fgf10*$^{+}$ tuberal hypothalamus extends rostrally, resulting in a rostral shift of an infundibulum-like structure. It has been shown that FGF signalling and other tuberal-derived signalling factors, such as BMPs, are required for RP development (Takuma *et al.* 1998; Ohuchi *et al.* 2000; De Moerlooze *et al.* 2000). It is thus possible that FGF signalling and possibly other signals derived from the tuberal hypothalamus are ectopically positioned and thus induce a second RP in the underlying oral ectoderm. In contrast, I do not observe a rostral expansion of *Fgf10* expression in cyclopamine-treated embryos.

These differences may be explained by the time point when Shh signalling is absent. In my studies, Shh signalling is blocked at a specific time point between HH10 and HH15, when *Shh* is expressed in the ventral midline. In contrast, *Zhao et al. (2012)* report that the mutant mice exhibit loss of hypothalamic Shh signalling from E9.5, a time point when *Shh* is expressed in the anterior and basal hypothalamus but not in the ventral hypothalamus. Moreover, the permanent deletion of *Shh* after E9.5 makes it difficult to determine whether the observed RP phenotype is attributed to an early or

late requirement for Shh signalling.

Nonetheless, my studies suggest that Shh signalling, acting between HH10 and HH15, is important for development of RP. However, how Shh signalling might act on development of RP remains unknown. Additionally, whether this requirement of Shh signalling is direct or indirect remains to be tested.

Chapter 7
Discussion

In the studies presented in this thesis I have,

1. identified morphological features that identify the chick hypothalamus and its subregions at E5 and E3 and shown that morphological features that define the anterior and tuberal hypothalamus correlate with expression of Six3^{+} *Fgf10*$^{-}$ (anterior) and Six3^{+} *Fgf10*$^{+}$ (tuberal) expression. Further, I have used morphological and fate mapping studies to show that the PM, gut endoderm, and cephalic flexure-like rudiment are morphological features at HH10 that can assist in identification of the future hypothalamus and its subregions.

2. shown, through fate mapping studies, that the progenitors of the ventral chick hypothalamus are situated in the anterior, medial, and posterior prosencephalon, and that progenitors that will form the anterior, tuberal and mammillary hypothalamus lie above the PM. Moreover, I have demonstrated that ventral midline cells lying above the PM exhibit anterior migration/extension behaviour relative to their neighbours in the basal plate.

3. demonstrated that the hypothalamus at HH10 is not regionalised since cells that will give rise to the anterior, tuberal, and mammillary hypothalamus all express *Fgf10*. *Fgf10* is a marker associated with

the tuberal hypothalamus at later stages and thus, I propose that the hypothalamus is initially tuberal-in-character and is multipotent: will give rise to anterior hypothalamus. To extend this, I have provided evidence that, suggests a model in which the anterior part of the tuberal hypothalamus at HH10 is a proliferation front that drives rapid growth of the anterior hypothalamus over time.

4. provided preliminary studies that pharmacological blocking of SHH results, firstly, in a smaller anterior hypothalamus and failure of the infundibulum and RP to develop normally. Secondly, I report a loss of the cell cycle inhibitor, $p57^{Kip2}$, which suggests a disruption to differentiation in the anterior hypothalamus. Thirdly, I report that a higher proportion of anterior hypothalamic progenitors are retained in the tuberal hypothalamus, suggesting a disruption to migration/ directed proliferation.

7.1. Discussion

7.1.1. Novel systematic fate mapping of the hypothalamic ventral midline and its implications

In chapter 4, I showed that the ventral hypothalamus derives from cells that occupy the ventral midline of the anterior, medial, and posterior prosencephalon. More importantly, the PM can predict the position of the future hypothalamus at HH10. This fate map of the hypothalamus is very different than the prevalent fate map model, in which the hypothalamus lies entirely within the anterior prosencephalon (Fig.1.3C,D; Garcia-Lopez *et al.* 2004; Garcia-Lopez *et al.* 2009). In chapter 4, I have discussed that the discrepancy between our studies is likely due to different fate mapping methods and that in their study, the ventral midline was not fate mapped. The new fate map that I propose,has consequential implications for understanding development of the hypothalamus compared with the old fate map model.

I demonstrate that the PM consistently lies underneath the future

hypothalamus at HH10. Preliminary analyses of my fate mapping studies suggest that the PM will largely underlie the medial and posterior prosencephalon. Thus, in the old fate model, the hypothalamus is not predicted to lie above the PM. This distinction is important as it re-emphasises that the PM may be playing an important role in specifying the hypothalamus.

It is generally accepted that the PM is initially required to induce diencephalic ventral midline (DVM) character at HH4 (Shimamura and Rubenstein 1997; Patten *et al.* 2003; Aoto *et al.* 2008). However the role and requirement of the PM at later stages is controversial and not well understood. Thus, a recent study suggests that the PM is not required for hypothalamic specification (Puelles *et al.* 2012). However, previous studies in the lab have analysed the spatial relationship between the PM and the DVM, from which the hypothalamus is thought to derive (Dale *et al.* 1999). This study shows that the future DVM, which originates from a region anterior to Hensen's node termed *area a*, is in contact with the underlying PM at HH4-4^{+}. At HH6, the DVM and PM are no longer in contact, but come into contact again around HH7-8. My findings at HH10 extend these studies to suggest that the PM is in contact with the hypothalamus between HH7 and HH10. Is the PM important for hypothalamic development over HH7 and HH10?

A possibility is that the PM is initially required for induction of DVM character (in particular *Shh* expression) at HH4-4^{+}, but at HH7-10, the PM is important for further specification of the hypothalamus, reinforcing hypothalamic identity versus caudal DVM identity. In support of this idea, isolated explants of DVM at HH5 express *Nkx2.1* only when cultured with PM (Ohyama *et al.*, 2005). At a slightly later time point (HH10) the PM appears to be required for a further specification event: studies in our lab have shown that at HH10, BMP signalling becomes the dominant signal emanating from the PM (Ellis *et al.* 2015) and it is thought this source of BMP is important for inducing *Tbx2*-mediated downregulation of *Shh* expression in the ventral hypothalamus (Manning *et al.* 2006). Thus, in conclusion, my finding that the PM predicts the hypothalamus at HH10 strongly supports the idea that the PM is required for hypothalamic development between

HH7-10.

7.1.2. The ventral midline of the posterior prosencephalon at HH10 gives rise to hypothalamic cells

The prosomeric model postulates that the adult vertebrate forebrain is organised into transverse segments. This has led to a brain segmentation paradigm, which predicts that the forebrain anlage is compartmentalised into transverse segments during early developmental stages (Puelles and Rubenstein 1993; Ferran *et al.* 2015; Puelles and Rubenstein 2015). Recent support for this has come from the *Garcia-Lopez et al. (2004)* fate mapping study, which reports that the chick diencephalon at HH10 is segmented into transverse domains that correlate with p1 (pretectum), p2 (thalamus), and p3 (prethalamus) prosomeres. Furthermore, this study reports that these diencephalic domains are lineage-restricted (i.e. a p3 cell will not colonise the p2 or p1 territory).

In contrast, my fate mapping studies demonstrate that ventral midline cells immediately adjacent to basal cells that will colonise the p3 and/or p2 prosomere, will colonise the caudal tuberal and mammillary hypothalamus and not p3 or p2 prosomeric regions. As outlined in chapter 4, this occurs because ventral midline cells migrate/extend anteriorly relative to their basal neighbours. This suggests that the ventral midline cells are not lineage-restricted to a strictly-organised transverse p3 or p2 prosomere and, thus, suggests that the diencephalon (which, I naively call posterior prosencephalon) is not organised into transverse domains at HH10, at least in the ventral midline. My study thus confirms earlier fate mapping studies in our lab (Manning *et al.* 2006).

This novel finding has implications for whether the hypothalamus is developmentally different than the diencephalon and whether it is more related to the telencephalon. This topic is highly debated in the neuroanatomy field as it has consequences for how we interpret development of the forebrain. As outlined in the Introduction, evidence for this mainly stems from expression of *Six3* in the telencephalon and hypothalamus, and the

evidence that *Six3*-null mutants show disruption to development of both the telencephalon and hypothalamus but not the diencephalon (Lagutin *et al.* 2003). On the other side of the argument, expression of markers associated with the diencephalon, that are proposed by the prosomeric model to delineate the diencephalic-hypothalamic boundary, are expressed in the hypothalamus at earlier stages of development (Shimogori *et al.* 2010; Bedont *et al.* 2015). Does my fate map provide any insight into whether the hypothalamus should be classified as diencephalic or classified together with the telencephalon in the secondary prosencephalon?

As described earlier, my fate mapping studies provides evidence to suggest that an interprosomeric boundary between p3 and the hypothalamus may not exist, at least not a boundary that exists transversely and that includes the ventral midline. Further, the finding that *Six3* expression clearly extends into the diencephalon at early stages does not provide support for its being a master regulator of hypothalamic identity. What about the hypothalamus and telencephalon? Does my fate mapping provide insight into whether they share a lineage? On the basis of morphology, in which the optic stalk approximately marks the boundary of rostral hypothalamus, caudal to the *Foxg1*$^{+}$ telencephalon, my fate mapping studies show that hypothalamic cells do not cross this boundary into the telencephalon. Instead, the rostral-most region of the hypothalamus is restricted to the rostral anterior hypothalamus, the presumptive SCH. Moreover, my fate mapping studies demonstrate that the ventral midline of this territory does not exhibit the anterior migration/extension that I observe in other regions of the hypothalamus. Together, my studies hint at the possibility of a lineage-restricted boundary between the telencephalon and hypothalamus.

Thus, my fate mapping studies, firstly, show that the diencephalon proposed by the prosomeric model is not organised into transverse segments. Secondly, there may be a lineage-restricted boundary between the telencephalon and hypothalamus. Together, they do not support the currently widely accepted model of forebrain development.

7.1.3. Insights into morphogenesis of the hypothalamus between HH10 and HH20

My fate mapping studies demonstrate that ventral midline cells overlying the PM will extend/migrate anteriorly relative to their basal neighbours. However, this behaviour is not observed in cells anterior to the PM, suggesting that these cells are static. How then, does *region A* cells, overlying the anterior PM, extend anteriorly if cells anterior to it are static? In other words, why is there not insufficient space for further migration/ extension/growth?

This problem can be illuminated if we consider the hypothalamus as an outgrowth of the neural tube. This scenario provides a means for the surface area to increase and coincidentally, allows *region A* cells to migrate/ extend anteriorly. This is schematically explained in Figs.7.1A-B. At the same time, *region C* cells, overlying the posterior PM will similarly have space to migrate/extend. In contrast, *region B* cells, overlying the medial PM will not have a lot of space to migrate/extend, possibly explaining why *region B* cells colonise a smaller region of the hypothalamus compared to *region A* and C cells.

Thus, my fate maps provide novel insights into morphogenesis of the hypothalamus. The neuroepithelium is a sheet of cells, and it is possible that growth driven from *region A* and *region C* cells creates mechanical tension that causes the hypothalamus to essentially evaginate, on a large scale. This is the first time such a model for hypothalamic morphogenesis has been proposed.

This model fits with the idea that the anterior hypothalamus is built by proliferating tuberal cells that colonise the anterior hypothalamus. Additionally, this model may provide insights into development of the infundibulum. The infundibulum develops as an outgrowth/evagination of the ventral tuberal hypothalamus and this is first observed at E4. Cells at the base of the infundibulum proliferate to give rise to cells that will

populate the walls of the infundibulum (Pearson *et al.* 2011), however, it is unclear what initiates the evagination of the infundibulum. I have shown that the mammillary hypothalamus expands rapidly over E3 and E5, and my fate mapping studies further identify a region of localised proliferation in the rostral mammillary hypothalamus. Thus, it is possible that growth in the rostral mammillary hypothalamus creates further mechanical tension that initiates infundibulum development (Fig.7.1C).

In summary, my fate mapping studies provide novel insights into morphogenesis of the hypothalamus and begins to suggest the idea that possible mechanical forces may play a role in development of the hypothalamus.

7.1.4. Shh affects differentiation and growth of the chick anterior hypothalamus

In chapter 6, I demonstrated that pharmacological blocking of Shh signalling results in a smaller anterior hypothalamus, disrupted differentiation in the anterior hypothalamus, and failure of the infundibulum and RP to develop. These results are consistent with findings in mutant mice that conditionally delete *Shh* in the ventral neuroepithelium, or hypothalamus (Szabó *et al.* 2009; Shimogori *et al.* 2010; Zhao *et al.* 2012). In mouse mutants, deletion of functional *Shh* makes its difficult to determine the developmental time points when Shh signalling is required for these processes. In contrast, in chick, I have demonstrated that Shh signalling, as measured by *Ptch1* expression, is absent between HH10 and HH15. This suggests that the phenotypes I observe can be attributed to absence of Shh signalling at these stages. Extrapolating to mice studies, this may suggest that loss of *pomc*$^{+}$ and *Nr5a1*$^{+}$ neurons may be due to absence of Shh signalling during early stages of development, rather than later.

Studies in our lab have begun to elucidate the mechanism by which Shh signalling could affect these processes. *Muthu et al. (2016)* showed that growth and differentiation in the zebrafish anterotuberal hypothalamus requires a cooperation of Rx3 and *Shh* activity, and that in the absence

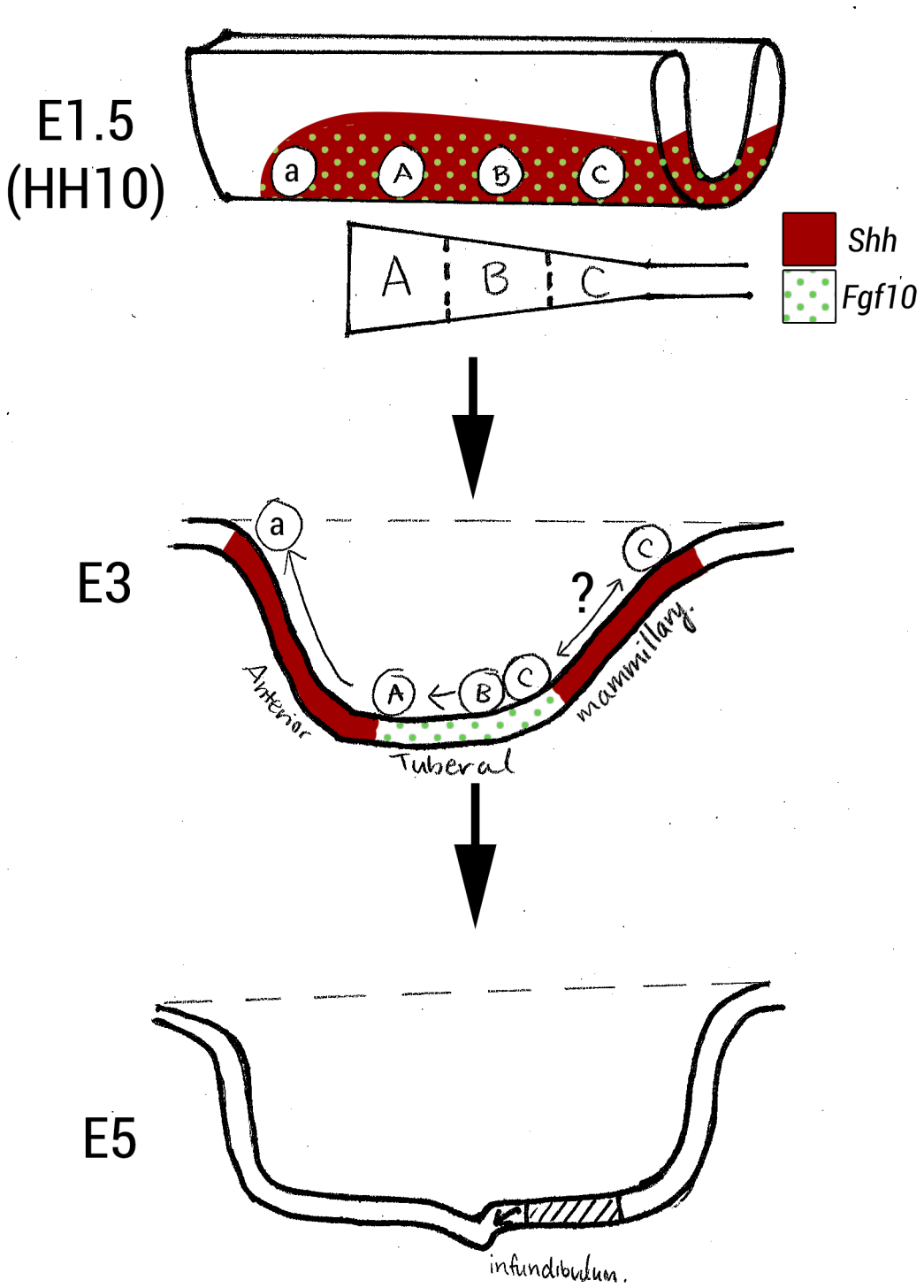

Figure 7.1 | Schematic of proposed hypothalamic morphogenesis

The proposed model of hypothalamic morphogenesis considers the hypothalamus as an outgrowth of the neural tube. Cells overlying the prechordal mesoderm are shown to extend anteriorly (labelled circles, A, B, and C), but cells anterior to the prechordal mesoderm do not extend anteriorly (labelled a). The hypothalamus develops as an outgrowth/evagination and in doing so, provides a means to increase surface *area a*nd thus, provides space for cells overlying the prechordal mesoderm to extend anteriorly. Whether initial growth of the mammillary hypothalamus is a result anterior extension or tuberal cells giving rise to mammillary cells in a posterior/caudal direction is not known as it has not been extensively studied. At E5, the rostral mammillary undergoes rapid proliferation. A consequence of this could be increased mechanical force that results in the evagination of the infundibulum.

of Shh signalling, anterotuberal hypothalamic progenitors are retained in the Rx3 territory. However, this study did not address whether $Rx3^+$ progenitors derived from the tuberal hypothalamus, the telencephalon, or another region of the diencephalon. My studies suggest that anterior hypothalamic cells derive from the tuberal hypothalamus.

To test this, future studies should be initially directed at characterising the expression of additional markers, including differentiated neurons, in the anterior hypothalamus, such as *pomc* and *Nr5a1*, and the expression of the chick homologue of Rx3, Rax and then determining whether the expression of these genes is affected by pharmacological blocking of Shh signalling in chick.

7.1.5. Implications for hypothalamic disorders

Many hypothalamic-associated disorders are reported to have abnormal levels of specific hormone production that results in the manifestation of a phenotype. For example, growth hormone deficiency has been reported in Prader-Willi syndrome and Cushing's syndrome, which suggests a dysregulation of neuroendocrine cells or the neurons that govern these cells. In chapter 6, I demonstrate that *Shh* is required for normal growth and differentiation of the anterior hypothalamus; this could begin to help us understand development of anterior hypothalamic neurons and how their abnormal development can result in dysregulation of hypothalamic function.

In addition, ectopic pituitaries have been reported in several pituitary disorders (Patkar, 1999), however, the mechanism of how an ectopic pituitary is generated remains poorly understood. My studies suggest that conditional pharmacological blocking of Shh signalling occasionally results in an ectopic Rathke's pouch (i.e. anterior pituitary) and could provide an assay to further understand the mechanism underlying the formation of ectopic Rathke's pouches.

7.2. Future directions

7.2.1. Fate mapping of the basal hypothalamus

Fate mapping is a powerful tool to help us understand the complex morphogenesis of the vertebrate embryo. For example, fate mapping studies in zebrafish, chick, and Xenopus during gastrulation have provided invaluable insights into this complex morphogenetic events and have provided an understanding of the fate of cells in each germ layer (Dale and Slack 1987; Kimmel *et al.* 1990; Schoenwolf and Sheard 1990). My fate mapping studies begin to provide a snapshot of the morphogenetic movements that occur to shape the hypothalamus, although in the absence of a systematic fate map of the entire hypothalamus, we still do not have a complete picture. Understanding the morphogenetic movements that sculpt the entire hypothalamus could provide novel insights into mechanical forces that are required for normal development of the hypothalamus. To this end, future fate mapping studies should be directed towards systematic fate mapping of the hypothalamic basal plate from a midline to lateral direction along different anteroposterior positions. An initial study could focus on mapping the *Fgf10*$^{+}$ territory, to determine if *Fgf10* expression predicts the entire hypothalamus.

7.2.2. Using pluripotent stem cells to model hypothalamic development

Through our understanding of hypothalamic development, we can provide insight into directed differentiation of human pluripotent stem cells into hypothalamic neuronal fates. Such an endeavour has the potential for novel therapies such as obesity (Merkle *et al.* 2015; Wang *et al.* 2015). To this end, I have demonstrated that *Fgf10* expression labels the hypothalamus during early stages of its development and that preliminary studies suggest that Shh signalling is required for the generation of anterior hypothalamic neuronal and glial cells. Furthermore, the ability to generate hypothalamic

progenitors from pluripotent stem cells would also provide an invaluable tool in furthering our understanding of hypothalamic development. Such pluripotent stem cells could be used to test whether *Fgf10*$^{+}$ tuberal progenitors have the ability to give rise to the different neurons and glial cells associated with different nuclei within the anterior, tuberal, and mammillary hypothalamus. Additionally, pluripotent stem cells provide an *in vitro* assay to test whether pharmacological blocking of Shh signalling results in reduction of proliferation and differentiation towards anterior hypothalamic identity such as expression of *pomc*$^{+}$ neurons.

7.2.3. Model for development of the anterior hypothalamus

In chapter 4, I identified the origins of the hypothalamus and showed that its position can be predicted by the PM. Subsequently, in chapter 5, I showed that the hypothalamus expresses *Fgf10*. At later stages in development, *Fgf10* expression is regionally associated with the tuberal hypothalamus and on this basis I hypothesise that the hypothalamus at HH10 is tuberal-by-default.

However, in this thesis, I have used the term tuberal as a regional description of the hypothalamus. This raises three important questions: (1) what is tuberal identity?, (2) is *Fgf10* sufficient for cells to adopt a tuberal identity?, and (3) is the *Fgf10*$^{+}$ hypothalamus a multipotent population rather than a population with tuberal identity?

Studies have suggested that the infundibulum, which is within the tuberal hypothalamus, will give rise to two glial cell types: tanycytes in the median eminence and pituicytes that mainly make up the neurohypophysis (Ajika 1969; Galabov and Schiebler 1978; Wittkowski 1980). Thus, future experiments should be directed at determining whether, in the absence of any further signals, the *Fgf10*$^{+}$ hypothalamus at HH10 will give rise to tuberal-specific glial cells or if it is capable of generating multiple cell types in the anterior, tuberal, and mammillary hypothalamus. This type of study will help to move forwards further our understanding of the growth and development of this critical part of the brain.

Supplementary Data

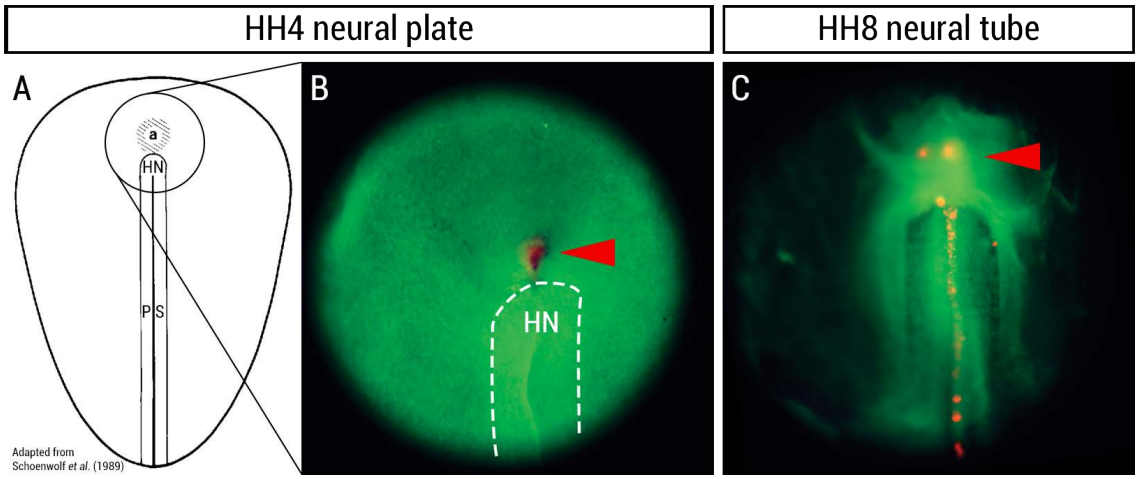

Figure S1 | Area a extends anteriorly to give rise to cells in the ventral midline of the prosencephalon

(A) Schematic of HH4 chick neural plate, highlighting position of *area a* anterior to Hensen's node (HN). Image is taken and adapted from *SCHOENWOLF (1989)*. (B) Dorsal view of neural plate showing after focal injection of DiI into *area a* and developed to HH8 (C). (C) Ventral wholemount view of HH8 neural tube. DiI is detected along the ventral midline of the neural tube and the presumptive prosencephalon. Experiments conducted by Iain Patten (unpublished).

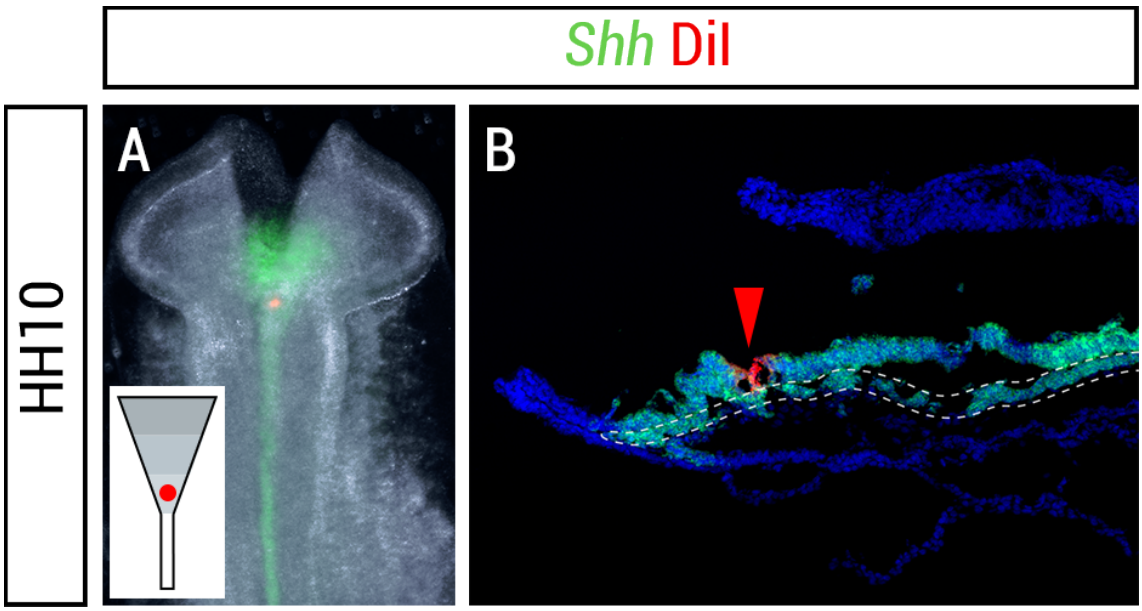

Figure S2 | Region C injection relative to prechordal mesoderm on sagittal sections

(A) Dorsal wholemount view of HH10 embryo after focal injection of DiI into *region C* (shown in inset) and flourescently hybridised for *Shh* expression (n=1). (B) Sagittal section of the same embryo shows DiI injection above the posterior prechordal mesoderm. *Shh* is detected in the ventral neural tube and axial mesoderm, including prechordal mesoderm and the notochord.

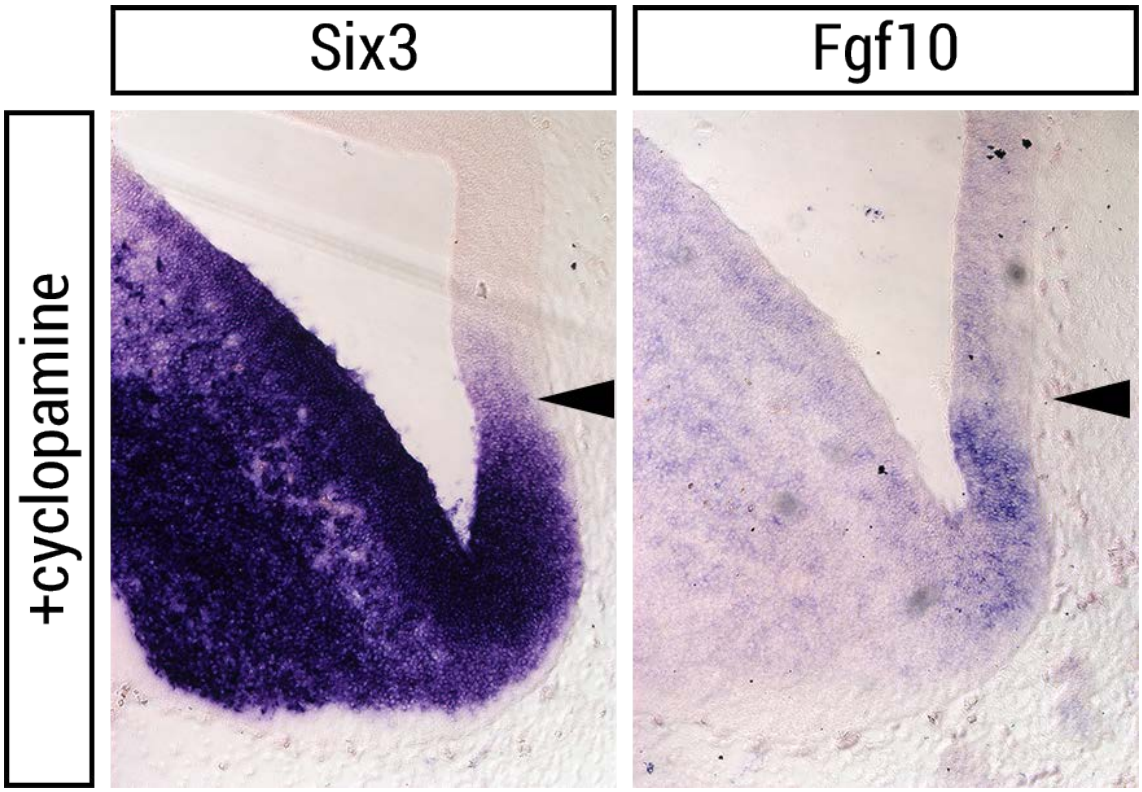

Figure S3 | Relative expression pattern of Six3 and Fgf10 unaffected in cyclopamine-treated embryos

Serial adjacent sagittal sections showing expression of *Six3* and *Fgf10* in an E5 embryo after cyclopamine treatment at HH9 (E1.5; n=5). Black arrowheads point to caudal expression domain of *Six3* and *Fgf10*.

References

Adelmann, Howard B. 1922. "The Significance of the Prechordal Plate: An Interpretative Study." The American Journal of Anatomy 31 (1). Wiley Subscription Services, Inc., A Wiley Company: 55–101.

Ajika, K. 1969. "Ultrafine Structure of the Developing Median Eminence and Pars Nervosa of the Rat." Acta Obstetrica et Gynaecologica Japonica 16 (3): 143–55.

Alvarez-Bolado, Gonzalo, Fabian A. Paul, and Sandra Blaess. 2012. "Sonic Hedgehog Lineage in the Mouse Hypothalamus: From Progenitor Domains to Hypothalamic Regions." Neural Development 7 (January): 4.

Andersson, Olov, Eva Reissmann, Henrik Jörnvall, and Carlos F. Ibáñez. 2006. "Synergistic Interaction between Gdf1 and Nodal during Anterior Axis Development." Developmental Biology 293 (2): 370–81.

Aoto, Kazushi, Yayoi Shikata, Daisuke Higashiyama, Kohei Shiota, and Jun Motoyama. 2008. "Fetal Ethanol Exposure Activates Protein Kinase A and Impairs Shh Expression in Prechordal Mesendoderm Cells in the Pathogenesis of Holoprosencephaly." Birth Defects Research. Part A, Clinical and Molecular Teratology 82 (4): 224–31.

Aoto, Kazushi, Yayoi Shikata, Hajime Imai, Daisuke Matsumaru, Tomoyuki Tokunaga, Seiji Shioda, Gen Yamada, and Jun Motoyama. 2009. "Mouse Shh Is Required for Prechordal Plate Maintenance during Brain and Craniofacial Morphogenesis." Developmental Biology 327 (1): 106–20.

Augustine, R. A., G. T. Bouwer, A. J. Seymour, D. R. Grattan, and C. H. Brown. 2016. "Reproductive Regulation of Gene Expression in the Hypothalamic Supraoptic and Paraventricular Nuclei." Journal of Neuroendocrinology 28 (4).

Balaban, E., M. A. Teillet, and N. Le Douarin. 1988. "Application of the Quail-Chick Chimera System to the Study of Brain Development and Behavior." Science 241 (4871): 1339–42.

Bedont, Joseph L., Elizabeth A. Newman, and Seth Blackshaw. 2015. "Patterning, Specification, and Differentiation in the Developing Hypothalamus." Wiley Interdisciplinary Reviews. Developmental Biology 4 (5): 445–68.

Bell, E., R. J. Wingate, and A. Lumsden. 1999. "Homeotic Transformation of Rhombomere Identity after Localized Hoxb1 Misexpression." Science 284 (5423): 2168–71.

Bellinger, Larry L., and Lee L. Bernardis. 2002. "The Dorsomedial Hypothalamic Nucleus and Its Role in Ingestive Behavior and Body Weight Regulation: Lessons Learned from Lesioning Studies." Physiology & Behavior 76 (3): 431–42.

Belloni, E., M. Muenke, E. Roessler, G. Traverso, J. Siegel-Bartelt, A. Frumkin, H. F. Mitchell, et al. 1996. "Identification of Sonic Hedgehog as a Candidate Gene Responsible for Holoprosencephaly." Nature Genetics 14 (3): 353–56.

Bergson, Jill C., Vikram K. Garg, and Jakwei Chang. 2007. "Ectopic Posterior Pituitary Lobe and Cortical Dysplasia." AJNR. American Journal of Neuroradiology 28 (2): 198–99; author reply 199.

Bovolenta, P., A. Mallamaci, L. Puelles, and E. Boncinelli. 1998. "Expression Pattern of cSix3, a Member of the Six/sine Oculis Family of Transcription Factors." Mechanisms of Development 70 (1-2): 201–3.

Boulant, J. A. 2000. "Role of the Preoptic-Anterior Hypothalamus in Thermoregulation and Fever." Clinical Infectious Diseases: An Official Publication of the Infectious Diseases Society of America 31 Suppl 5 (October): S157–61.

Brinkmeier, Michelle L., Mary Anne Potok, Shannon W. Davis, and Sally A. Camper. 2007. "TCF4 Deficiency Expands Ventral Diencephalon Signaling and Increases Induction of Pituitary Progenitors." Developmental Biology 311 (2): 396–407.

Burbridge, Sarah, Iain Stewart, and Marysia Placzek. 2016. "Development of the Neuroendocrine Hypothalamus." In Comprehensive Physiology. John Wiley & Sons, Inc.

Cadigan, Ken M., and Marian L. Waterman. 2012. "TCF/LEFs and Wnt Signaling in the Nucleus." Cold Spring Harbor Perspectives in Biology 4 (11). doi:10.1101/cshperspect.a007906.

Chédotal, A., O. Pourquié, and C. Sotelo. 1995. "Initial Tract Formation in the Brain of the Chick Embryo: Selective Expression of the BEN/SC1/DM-GRASP Cell Adhesion Molecule." The European Journal of Neuroscience 7 (2): 198–212.

Chen, James K., Jussi Taipale, Michael K. Cooper, and Philip A. Beachy. 2002. "Inhibition of Hedgehog Signaling by Direct Binding of Cyclopamine to Smoothened." Genes & Development 16 (21): 2743–48.

Chen, Li, Qiuxia Guo, and James Y. H. Li. 2009. "Transcription Factor Gbx2 Acts Cell-Nonautonomously to Regulate the Formation of Lineage-Restriction Boundaries of the Thalamus." Development 136 (8): 1317–26.

Chiang, C., Y. Litingtung, E. Lee, K. E. Young, J. L. Corden, H. Westphal, and P. A. Beachy. 1996. "Cyclopia and Defective Axial Patterning in Mice Lacking Sonic Hedgehog Gene Function." Nature 383 (6599): 407–13.

Chitnis, A. B., and J. Y. Kuwada. 1990. "Axonogenesis in the Brain of Zebrafish Embryos." The Journal of Neuroscience: The Official Journal of the Society for Neuroscience 10 (6): 1892–1905.

Cobos, Inmaculada, Kenji Shimamura, John L. R. Rubenstein, Salvador Martínez,

and Luis Puelles. 2001. "Fate Map of the Avian Anterior Forebrain at the Four-Somite Stage, Based on the Analysis of Quail–Chick Chimeras." Developmental Biology 239 (1): 46–67.

Cordero, Dwight, Ralph Marcucio, Diane Hu, William Gaffield, Minal Tapadia, and Jill A. Helms. 2004. "Temporal Perturbations in Sonic Hedgehog Signaling Elicit the Spectrum of Holoprosencephaly Phenotypes." The Journal of Clinical Investigation 114 (4): 485–94.

Couly, Gérard F., and Nicole M. Le Douarin. 1987. "Mapping of the Early Neural Primordium in Quail-Chick Chimeras. II. The Prosencephalic Neural Plate and Neural Folds: Implications for the Genesis of Cephalic Human Congenital Abnormalities." Developmental Biology 120 (1): 198–214.

Daikoku, Shigeo, Mika Chikamori, Tohru Adachi, and Yuzo Maki. 1982. "Effect of the Basal Diencephalon on the Development of Rathke's Pouch in Rats: A Study in Combined Organ Cultures." Developmental Biology 90 (1): 198–202.

Dale, J. K., C. Vesque, T. J. Lints, T. K. Sampath, A. Furley, J. Dodd, and M. Placzek. 1997. "Cooperation of BMP7 and SHH in the Induction of Forebrain Ventral Midline Cells by Prechordal Mesoderm." Cell 90 (2): 257–69.

Dale, K., N. Sattar, J. Heemskerk, J. D. Clarke, M. Placzek, and J. Dodd. 1999. "Differential Patterning of Ventral Midline Cells by Axial Mesoderm Is Regulated by BMP7 and Chordin." Development 126 (2): 397–408.

Dale, L., and J. M. Slack. 1987. "Fate Map for the 32-Cell Stage of Xenopus Laevis." Development 99 (4): 527–51.

De Moerlooze, L., B. Spencer-Dene, J. M. Revest, M. Hajihosseini, I. Rosewell, and C. Dickson. 2000. "An Important Role for the IIIb Isoform of Fibroblast Growth Factor Receptor 2 (FGFR2) in Mesenchymal-Epithelial Signalling during Mouse Organogenesis." Development 127 (3): 483–92.

Dillingham, Christopher M., Aura Frizzati, Andrew J. D. Nelson, and Seralynne D. Vann. 2015. "How Do Mammillary Body Inputs Contribute to Anterior Thalamic Function?" Neuroscience and Biobehavioral Reviews 54 (July): 108–19.

di Iorgi, N., A. Secco, F. Napoli, E. Calandra, A. Rossi, and M. Maghnie. 2009. "Developmental Abnormalities of the Posterior Pituitary Gland." In Endocrine Involvement in Developmental Syndromes, 14:83–94. Karger Publishers.

Eagleson, G. W., and W. A. Harris. 1990. "Mapping of the Presumptive Brain Regions in the Neural Plate of Xenopus Laevis." Journal of Neurobiology 21 (3): 427–40.

Ellis, Pamela S., Sarah Burbridge, Sandrine Soubes, Kyoji Ohyama, Nadav Ben-Haim, Canhe Chen, Kim Dale, Michael M. Shen, Daniel Constam, and Marysia Placzek. 2015. "ProNodal Acts via FGFR3 to Govern Duration of Shh Expression in the Prechordal Mesoderm." Development 142 (22): 3821–32.

Ericson, J., J. Muhr, M. Placzek, T. Lints, T. M. Jessel, and T. Edlund. 1995. "Sonic Hedgehog Induces the Differentiation of Ventral Forebrain Neurons: A Common Signal for Ventral Patterning within the Neural Tube." Cell 81 (5): 747–56.

Ericson, J., S. Norlin, T. M. Jessell, and T. Edlund. 1998. "Integrated FGF and BMP Signaling Controls the Progression of Progenitor Cell Differentiation and the Emergence of Pattern in the Embryonic Anterior Pituitary." Development 125 (6): 1005–15.

Ezin, Akouavi M., Scott E. Fraser, and Marianne Bronner-Fraser. 2009. "Fate Map and Morphogenesis of Presumptive Neural Crest and Dorsal Neural Tube." Developmental Biology 330 (2): 221–36.

Fernández-Garre, Pedro, Lucia Rodríguez-Gallardo, Victoria Gallego-Díaz, Ignacio S. Alvarez, and Luis Puelles. 2002. "Fate Map of the Chicken Neural Plate at Stage 4." Development 129: 2807–22.

Ferran, José L., Luis Puelles, and John L. R. Rubenstein. 2015. "Molecular Codes Defining Rostrocaudal Domains in the Embryonic Mouse Hypothalamus." Frontiers in Neuroanatomy 9 (April): 46.

Ferri, Anna, Rebecca Favaro, Leonardo Beccari, Jessica Bertolini, Sara Mercurio, Francisco Nieto-Lopez, Cristina Verzeroli, et al. 2013. "Sox2 Is Required for Embryonic Development of the Ventral Telencephalon through the Activation of the Ventral Determinants Nkx2.1 and Shh." Development 140 (6): 1250–61.

Fraser, S., R. Keynes, and A. Lumsden. 1990. "Segmentation in the Chick Embryo Hindbrain Is Defined by Cell Lineage Restrictions." Nature 344 (6265): 431–35.

Galabov, P., and T. H. Schiebler. 1978. "The Ultrastructure of the Developing Neural Lobe." Cell and Tissue Research 189 (2): 313–29.

Galderisi, Umberto, Francesco Paolo Jori, and Antonio Giordano. 2003. "Cell Cycle Regulation and Neural Differentiation." Oncogene 22 (33): 5208–19.

García-Calero, Elena, Pedro Fernández-Garre, Salvador Martínez, and Luis Puelles. 2008. "Early Mammillary Pouch Specification in the Course of Prechordal Ventralization of the Forebrain Tegmentum." Developmental Biology 320 (2): 366–77.

Garcia-Lopez, Raquel, Ana Pombero, and Salvador Martinez. 2009. "Fate Map of the Chick Embryo Neural Tube." Development, Growth & Differentiation 51 (3): 145–65.

Garcia-Lopez, Raquel, Claudia Vieira, Diego Echevarria, and Salvador Martinez. 2004. "Fate Map of the Diencephalon and the Zona Limitans at the 10-Somites Stage in Chick Embryos." Developmental Biology 268 (2): 514–30.

Geng, Xin, Christina Speirs, Oleg Lagutin, Adi Inbal, Wei Liu, Lilianna Solnica-Krezel,

Yongsu Jeong, Douglas J. Epstein, and Guillermo Oliver. 2008. "Haploinsufficiency of Six3 Fails to Activate Sonic Hedgehog Expression in the Ventral Forebrain and Causes Holoprosencephaly." Developmental Cell 15 (2): 236–47.

Georgia, Senta, Rosemary Soliz, Min Li, Pumin Zhang, and Anil Bhushan. 2006. "p57 and Hes1 Coordinate Cell Cycle Exit with Self-Renewal of Pancreatic Progenitors." Developmental Biology 298 (1): 22–31.

Gleiberman, A. S., N. G. Fedtsova, and M. G. Rosenfeld. 1999. "Tissue Interactions in the Induction of Anterior Pituitary: Role of the Ventral Diencephalon, Mesenchyme, and Notochord." Developmental Biology 213 (2): 340–53.

Golden, J. A., and C. L. Cepko. 1996. "Clones in the Chick Diencephalon Contain Multiple Cell Types and Siblings Are Widely Dispersed." Development 122 (1): 65–78.

Gripp, K. W., D. Wotton, M. C. Edwards, E. Roessler, L. Ades, P. Meinecke, A. Richieri-Costa, et al. 2000. "Mutations in TGIF Cause Holoprosencephaly and Link NODAL Signalling to Human Neural Axis Determination." Nature Genetics 25 (2): 205–8.

Hamburger, V., and H. L. Hamilton. 1951. "A Series of Normal Stages in the Development of the Chick Embryo." Journal of Morphology 88 (1): 49–92.

Herrick, C. Judson. 1910. "The Morphology of the Forebrain in Amphibia and Reptilia." Journal of Comparative Neurology and Psychology 20 (5). The Wistar Institute of Anatomy and Biology: 413–547.

Herzog, Wiebke, Carmen Sonntag, Sophia von der Hardt, Henry H. Roehl, Zoltan M. Varga, and Matthias Hammerschmidt. 2004. "Fgf3 Signaling from the Ventral Diencephalon Is Required for Early Specification and Subsequent Survival of the Zebrafish Adenohypophysis." Development 131 (15): 3681–92.

His, W. 1893. "Vorschläge Zur Eintheilung Des Gehirns. Arch. Anat. Entwickelungsges" 3: 172–79.

Ingham, Philip W. 2012. "Hedgehog Signaling." Cold Spring Harbor Perspectives in Biology 4 (6). doi:10.1101/cshperspect.a011221

Inoue, T., S. Nakamura, and N. Osumi. 2000. "Fate Mapping of the Mouse Prosencephalic Neural Plate." Developmental Biology 219 (2): 373–83.

Jacobson, Antone G., David M. Miyamoto, and S-H Mai. 1979. "Rathke's Pouch Morphogenesis in the Chick Embryo." The Journal of Experimental Zoology 207 (3). Wiley Subscription Services, Inc., A Wiley Company: 351–66.

Jacobson, Carl-Olof. 1959. "The Localization of the Presumptive Cerebral Regions in the Neural Plate of the Axolotl Larva." Development 7 (1). The Company of Biologists Ltd: 1–21.

Jeong, Yongsu, Kenia El-Jaick, Erich Roessler, Maximilian Muenke, and Douglas J. Epstein. 2006. "A Functional Screen for Sonic Hedgehog Regulatory Elements across a 1 Mb Interval Identifies Long-Range Ventral Forebrain Enhancers." Development 133 (4): 761–72.

Jeong, Yongsu, Federico Coluccio Leskow, Kenia El-Jaick, Erich Roessler, Maximilian Muenke, Anastasia Yocum, Christele Dubourg, et al. 2008. "Regulation of a Remote Shh Forebrain Enhancer by the Six3 Homeoprotein." Nature Genetics 40 (11): 1348–53.

Kawamura, K., and S. Kikuyama. 1998. "Morphogenesis of the Hypothalamus and Hypophysis: Their Association, Dissociation and Reassociation before and after 'Rathke.'" Archives of Histology and Cytology 61 (3): 189–98.

Kennedy, Breandán N., George W. Stearns, Vincent A. Smyth, Visvanathan Ramamurthy, Fredericius van Eeden, Irina Ankoudinova, David Raible, James B. Hurley, and Susan E. Brockerhoff. 2004. "Zebrafish rx3 and mab21l2 Are Required during Eye Morphogenesis." Developmental Biology 270 (2): 336–49.

Keynes, Roger, and Robb Krumlauf. 1994. "BOX GENES AND REGIONALIZATION OF THE NERVOUS SYSTEM." Annual Review of Neuroscience 17: 109–32.

Kiecker, Clemens, and Andrew Lumsden. 2005. "Compartments and Their Boundaries in Vertebrate Brain Development." Nature Reviews. Neuroscience 6 (7): 553–64.

Kimmel, C. B., R. M. Warga, and T. F. Schilling. 1990. "Origin and Organization of the Zebrafish Fate Map." Development 108 (4): 581–94.

Kimmell, Kristopher T., Mahlon Johnson, Rakhil Rubinova, and G. Edward Vates. 2014/6. "Cushing-Type Ectopic Pituitary Adenoma with Unusual Pathologic Features." Interdisciplinary Neurosurgery 1 (2): 31–33.

Kingsbury, B. F. 1920. "THE DEVELOPMENTAL ORIGIN OF THE NOTOCHORD." Science 51 (1312): 190–93.

Kobayashi, Daisuke, Makoto Kobayashi, Ken Matsumoto, Toshihiko Ogura, Masato Nakafuku, and Kenji Shimamura. 2002. "Early Subdivisions in the Neural Plate Define Distinct Competence for Inductive Signals." Development 129 (1): 83–93.

Krumlauf, R. 1993. "Hox Genes and Pattern Formation in the Branchial Region of the Vertebrate Head." Trends in Genetics: TIG 9 (4): 106–12.

Kuhlenbeck, H. 1973. "The Central Nervous System of Vertebrates. 3, Part II: Overall Morphological Pattern." Basel: Karger.

Lagutin, Oleg V., Changqi C. Zhu, Daisuke Kobayashi, Jacek Topczewski, Kenji Shimamura, Luis Puelles, Helen R. C. Russell, Peter J. McKinnon, Lilianna Solnica-Krezel, and Guillermo Oliver. 2003. "Six3 Repression of Wnt Signaling in the Anterior Neuroectoderm Is Essential for Vertebrate Forebrain Development."

Genes & Development 17 (3): 368–79.

Larsen, C. W., L. M. Zeltser, and A. Lumsden. 2001. "Boundary Formation and Compartition in the Avian Diencephalon." The Journal of Neuroscience: The Official Journal of the Society for Neuroscience 21 (13): 4699–4711.

Lavado, Alfonso, Oleg V. Lagutin, and Guillermo Oliver. 2008. "Six3 Inactivation Causes Progressive Caudalization and Aberrant Patterning of the Mammalian Diencephalon." Development 135 (3): 441–50.

Le Douarin, N. M. 1993. "Embryonic Neural Chimaeras in the Study of Brain Development." Trends in Neurosciences 16 (2): 64–72.

Liu, Fang, Hans-Martin Pogoda, Caroline Alayne Pearson, Kyoji Ohyama, Heiko Löhr, Matthias Hammerschmidt, and Marysia Placzek. 2013. "Direct and Indirect Roles of Fgf3 and Fgf10 in Innervation and Vascularisation of the Vertebrate Hypothalamic Neurohypophysis." Development 140 (5): 1111–22.

Lovicu, F. J., and J. W. McAvoy. 1999. "Spatial and Temporal Expression of p57(KIP2) during Murine Lens Development." Mechanisms of Development 86 (1-2): 165–69.

Lowe, L. A., S. Yamada, and M. R. Kuehn. 2001. "Genetic Dissection of Nodal Function in Patterning the Mouse Embryo." Development 128 (10): 1831–43.

Lyons, A. B., and C. R. Parish. 1994. "Determination of Lymphocyte Division by Flow Cytometry." Journal of Immunological Methods 171 (1): 131–37.

Machinis, Kalotina, and Serge Amselem. 2005. "Functional Relationship between LHX4 and POU1F1 in Light of the LHX4 Mutation Identified in Patients with Pituitary Defects." The Journal of Clinical Endocrinology and Metabolism 90 (9): 5456–62.

MacKay, Harry, and Alfonso Abizaid. 2014. "Embryonic Development of the Hypothalamic Feeding Circuitry: Transcriptional, Nutritional, and Hormonal Influences." Molecular Metabolism 3 (9): 813–22.

Manning, Liz, Kyoji Ohyama, Bernhard Saeger, Osamu Hatano, Stuart A. Wilson, Malcolm Logan, and Marysia Placzek. 2006. "Regional Morphogenesis in the Hypothalamus: A BMP-Tbx2 Pathway Coordinates Fate and Proliferation through Shh Downregulation." Developmental Cell 11 (6): 873–85.

Martí, E., R. Takada, D. A. Bumcrot, H. Sasaki, and A. P. McMahon. 1995. "Distribution of Sonic Hedgehog Peptides in the Developing Chick and Mouse Embryo." Development 121 (8): 2537–47.

Martin, J. R. 1992. "Pressor Response to Posterior Hypothalamic Administration of Carbachol Is Mediated by Muscarinic M3 Receptor." European Journal of Pharmacology 215 (1): 83–91.

Mathieu, Juliette, Anukampa Barth, Frederic M. Rosa, Stephen W. Wilson, and Nadine Peyriéras. 2002. "Distinct and Cooperative Roles for Nodal and Hedgehog Signals during Hypothalamic Development." Development 129 (13): 3055–65.

McCabe, Mark James, Kyriaki S. Alatzoglou, and Mehul T. Dattani. 2011. "Septo-Optic Dysplasia and Other Midline Defects: The Role of Transcription Factors: HESX1 and beyond." Best Practice & Research. Clinical Endocrinology & Metabolism 25 (1): 115–24.

Mercier, Sandra, Véronique David, Leslie Ratié, Isabelle Gicquel, Sylvie Odent, and Valérie Dupé. 2013. "NODAL and SHH Dose-Dependent Double Inhibition Promotes an HPE-like Phenotype in Chick Embryos." Disease Models & Mechanisms 6 (2): 537–43.

Merkle, Florian T., Asif Maroof, Takafumi Wataya, Yoshiki Sasai, Lorenz Studer, Kevin Eggan, and Alexander F. Schier. 2015. "Generation of Neuropeptidergic Hypothalamic Neurons from Human Pluripotent Stem Cells." Development 142 (4): 633–43.

Michaud, J. L. 2001. "The Developmental Program of the Hypothalamus and Its Disorders." Clinical Genetics 60 (4): 255–63.

Minor, Robin K., Joy W. Chang, and Rafael de Cabo. 2009. "Hungry for Life: How the Arcuate Nucleus and Neuropeptide Y May Play a Critical Role in Mediating the Benefits of Calorie Restriction." Molecular and Cellular Endocrinology 299 (1): 79–88.

Moore, Robert Y. 2007. "Suprachiasmatic Nucleus in Sleep–wake Regulation." Sleep Medicine 8, Supplement 3 (December): 27–33.

Muthu, Victor, Helen Eachus, Pam Ellis, Sarah Brown, and Marysia Placzek. 2016. "Rx3 and Shh Direct Anisotropic Growth and Specification in the Zebrafish Tuberal/anterior Hypothalamus." Development 143 (14): 2651–63.

Norlin, S., U. Nordström, and T. Edlund. 2000. "Fibroblast Growth Factor Signaling Is Required for the Proliferation and Patterning of Progenitor Cells in the Developing Anterior Pituitary." Mechanisms of Development 96 (2): 175–82.

Ohuchi, H., Y. Hori, M. Yamasaki, H. Harada, K. Sekine, S. Kato, and N. Itoh. 2000. "FGF10 Acts as a Major Ligand for FGF Receptor 2 IIIb in Mouse Multi-Organ Development." Biochemical and Biophysical Research Communications 277 (3): 643–49.

Ohyama, Kyoji, Raman Das, and Marysia Placzek. 2008. "Temporal Progression of Hypothalamic Patterning by a Dual Action of BMP." Development 135 (20): 3325–31.

Ohyama, Kyoji, Pamela Ellis, Shioko Kimura, and Marysia Placzek. 2005. "Directed Differentiation of Neural Cells to Hypothalamic Dopaminergic Neurons."

Development 132 (23): 5185–97.

Oliver, G., A. Mailhos, R. Wehr, N. G. Copeland, N. A. Jenkins, and P. Gruss. 1995. "Six3, a Murine Homologue of the Sine Oculis Gene, Demarcates the Most Anterior Border of the Developing Neural Plate and Is Expressed during Eye Development." Development 121 (12): 4045–55.

Paredes, Raúl G. 2003. "Medial Preoptic Area/anterior Hypothalamus and Sexual Motivation." Scandinavian Journal of Psychology 44 (3): 203–12.

Park, H. L., C. Bai, K. A. Platt, M. P. Matise, A. Beeghly, C. C. Hui, M. Nakashima, and A. L. Joyner. 2000. "Mouse Gli1 Mutants Are Viable but Have Defects in SHH Signaling in Combination with a Gli2 Mutation." Development 127 (8): 1593–1605.

Patkar, D., T. Patankar, A. Krishnan, S. Prasad, J. Shah, and J. Limdi. 1999. "MR Imaging in Children with Ectopic Pituitary Gland and Anterior Hypopituitarism." Journal of Postgraduate Medicine 45 (3): 81–83.

Patten, Iain, Paul Kulesa, Michael M. Shen, Scott Fraser, and Marysia Placzek. 2003. "Distinct Modes of Floor Plate Induction in the Chick Embryo." Development 130 (20): 4809–21.

Pearson, Caroline Alayne, Kyoji Ohyama, Liz Manning, Soheil Aghamohammadzadeh, Helen Sang, and Marysia Placzek. 2011. "FGF-Dependent Midline-Derived Progenitor Cells in Hypothalamic Infundibular Development." Development 138 (12). Oxford University Press for The Company of Biologists Limited: 2613–24.

Pearson, Caroline Alayne, and Marysia Placzek. 2013. "Development of the Medial Hypothalamus: Forming a Functional Hypothalamic-Neurohypophyseal Interface." In Current Topics in Developmental Biology, edited by Paul Thomas, Volume 106:49–88. Academic Press.

Pera, E. M., and M. Kessel. 1997. "Patterning of the Chick Forebrain Anlage by the Prechordal Plate." Development 124 (20): 4153–62.

Pevny, Larysa, and Marysia Placzek. 2005. "SOX Genes and Neural Progenitor Identity." Current Opinion in Neurobiology 15 (1): 7–13.

Pfaeffle, Roland W., Chad S. Hunter, Jesse J. Savage, Mario Duran-Prado, Rachel D. Mullen, Zachary P. Neeb, Urs Eiholzer, et al. 2008. "Three Novel Missense Mutations within the LHX4 Gene Are Associated with Variable Pituitary Hormone Deficiencies." The Journal of Clinical Endocrinology and Metabolism 93 (3): 1062–71.

Placzek, Marysia, and James Briscoe. 2005. "The Floor Plate: Multiple Cells, Multiple Signals." Nature Reviews. Neuroscience 6 (3): 230–40.

Pombero, Ana, and Salvador Martinez. 2009. "Telencephalic Morphogenesis during the

Process of Neurulation: An Experimental Study Using Quail-Chick Chimeras." The Journal of Comparative Neurology 512 (6): 784–97.

Pontecorvi, Marco, Colin R. Goding, William D. Richardson, and Nicoletta Kessaris. 2008. "Expression of Tbx2 and Tbx3 in the Developing Hypothalamic-Pituitary Axis." Gene Expression Patterns: GEP 8 (6): 411–17.

Puelles, L., and J. L. Rubenstein. 1993. "Expression Patterns of Homeobox and Other Putative Regulatory Genes in the Embryonic Mouse Forebrain Suggest a Neuromeric Organization." Trends in Neurosciences 16 (11): 472–79.

Puelles, Luis, Margaret Martinez-de-la-Torre, S. Bardet, and J. L. R. Rubenstein. 2012. "Chapter 8 - Hypothalamus." In The Mouse Nervous System, 221–312. San Diego: Academic Press.

Puelles, Luis, and John L. R. Rubenstein. 2003. "Forebrain Gene Expression Domains and the Evolving Prosomeric Model." Trends in Neurosciences 26 (9): 469–76. 2015.

Puelles, Luis, and John L. R. Rubenstein. 2015."A New Scenario of Hypothalamic Organization: Rationale of New Hypotheses Introduced in the Updated Prosomeric Model." Frontiers in Neuroanatomy 9 (March): 27.

Quaroni, A., J. Q. Tian, P. Seth, and C. Ap Rhys. 2000. "p27(Kip1) Is an Inducer of Intestinal Epithelial Cell Differentiation." American Journal of Physiology. Cell Physiology 279 (4): C1045–57.

Ratié, Leslie, Michelle Ware, Frédérique Barloy-Hubler, Hélène Romé, Isabelle Gicquel, Christèle Dubourg, Véronique David, and Valérie Dupé. 2013. "Novel Genes Upregulated When NOTCH Signalling Is Disrupted during Hypothalamic Development." Neural Development 8 (December): 25.

Reichert, Heinrich, and Bruno Bello. 2010. "Hox Genes and Brain Development in Drosophila." In Hox Genes, edited by Jean S. Deutsch, 145–53. Advances in Experimental Medicine and Biology 689. Springer New York.

Riccio, Orbicia, Marielle E. van Gijn, April C. Bezdek, Luca Pellegrinet, Johan H. van Es, Ursula Zimber-Strobl, Lothar J. Strobl, Tasuku Honjo, Hans Clevers, and Freddy Radtke. 2008. "Loss of Intestinal Crypt Progenitor Cells Owing to Inactivation of Both Notch1 and Notch2 Is Accompanied by Derepression of CDK Inhibitors p27Kip1 and p57Kip2." EMBO Reports 9 (4): 377–83.

Rizzoti, Karine. 2015. "Genetic Regulation of Murine Pituitary Development." Journal of Molecular Endocrinology 54 (2): R55–73.

Rizzoti, Karine, and Robin Lovell-Badge. 2005. "Early Development of the Pituitary Gland: Induction and Shaping of Rathke's Pouch." Reviews in Endocrine & Metabolic Disorders 6 (3): 161–72.

Rizzoti, Karine, and Robin Lovell-Badge. 2016. "Pivotal Role of Median Eminence Tanycytes for Hypothalamic Function and Neurogenesis." Molecular and Cellular Endocrinology, August. doi:10.1016/j.mce.2016.08.020.

Roessler, E., E. Belloni, K. Gaudenz, P. Jay, P. Berta, S. W. Scherer, L. C. Tsui, and M. Muenke. 1996. "Mutations in the Human Sonic Hedgehog Gene Cause Holoprosencephaly." Nature Genetics 14 (3): 357–60.

Roessler, Erich, Wuhong Pei, Maia V. Ouspenskaia, Jayaprakash D. Karkera, Jorge Ivan Veléz, Sharmilla Banerjee-Basu, Gretchen Gibney, et al. 2009. "Cumulative Ligand Activity of NODAL Mutations and Modifiers Are Linked to Human Heart Defects and Holoprosencephaly." Molecular Genetics and Metabolism 98 (1-2): 225–34.

Rohr, K. B., K. A. Barth, Z. M. Varga, and S. W. Wilson. 2001. "The Nodal Pathway Acts Upstream of Hedgehog Signaling to Specify Ventral Telencephalic Identity." Neuron 29 (2): 341–51.

Rubenstein, J. L., S. Martinez, K. Shimamura, and L. Puelles. 1994. "The Embryonic Vertebrate Forebrain: The Prosomeric Model." Science 266 (5185): 578–80.

Salic, Adrian, and Timothy J. Mitchison. 2008. "A Chemical Method for Fast and Sensitive Detection of DNA Synthesis in Vivo." Proceedings of the National Academy of Sciences of the United States of America 105 (7): 2415–20.

Sánchez-Arrones, Luisa, José L. Ferrán, Matías Hidalgo-Sanchez, and Luis Puelles. 2015. "Origin and Early Development of the Chicken Adenohypophysis." Frontiers in Neuroanatomy 9 (February): 7.

Sánchez-Arrones, Luisa, José Luis Ferrán, Lucía Rodríguez-Gallardo, and Luis Puelles. 2009. "Incipient Forebrain Boundaries Traced by Differential Gene Expression and Fate Mapping in the Chick Neural Plate." Developmental Biology 335 (1): 43–65.

Saper, Clifford B. 2006. "Staying Awake for Dinner: Hypothalamic Integration of Sleep, Feeding, and Circadian Rhythms." Progress in Brain Research 153: 243–52.

Saper, Clifford B., and Bradford B. Lowell. 2014. "The Hypothalamus." Current Biology: CB 24 (23): R1111–16.

Saravanamuthu, Senthil S., Chun Y. Gao, and Peggy S. Zelenka. 2009. "Notch Signaling Is Required for Lateral Induction of Jagged1 during FGF-Induced Lens Fiber Differentiation." Developmental Biology 332 (1): 166–76.

Sarkar, Abby, and Konrad Hochedlinger. 2013. "The Sox Family of Transcription Factors: Versatile Regulators of Stem and Progenitor Cell Fate." Cell Stem Cell 12 (1): 15–30.

Schindler, Stephanie, Stefan Geyer, Maria Strauß, Alfred Anwander, Ulrich Hegerl,

Robert Turner, and Peter Schönknecht. 2012. "Structural Studies of the Hypothalamus and Its Nuclei in Mood Disorders." Psychiatry Research 201 (1): 1–9.

Schoenwolf, G. C., H. Bortier, and L. Vakaet. 1989. "Fate Mapping the Avian Neural Plate with Quail/chick Chimeras: Origin of Prospective Median Wedge Cells." The Journal of Experimental Zoology 249 (3): 271–78.

Schoenwolf, G. C., and P. Sheard. 1990. "Fate Mapping the Avian Epiblast with Focal Injections of a Fluorescent-Histochemical Marker: Ectodermal Derivatives." The Journal of Experimental Zoology 255 (3): 323–39.

Sheng, H. Z., K. Moriyama, T. Yamashita, H. Li, S. S. Potter, K. A. Mahon, and H. Westphal. 1997. "Multistep Control of Pituitary Organogenesis." Science 278 (5344): 1809–12.

Sherr, C. J., and J. M. Roberts. 1999. "CDK Inhibitors: Positive and Negative Regulators of G1-Phase Progression." Genes & Development 13 (12): 1501–12.

Shimamura, K., and J. L. Rubenstein. 1997. "Inductive Interactions Direct Early Regionalization of the Mouse Forebrain." Development 124 (14): 2709–18.

Shimogori, Tomomi, Daniel A. Lee, Ana Miranda-Angulo, Yanqin Yang, Hong Wang, Lizhi Jiang, Aya C. Yoshida, et al. 2010. "A Genomic Atlas of Mouse Hypothalamic Development." Nature Neuroscience 13 (6): 767–75.

Sjödal, My, and Lena Gunhaga. 2008. "Expression Patterns of Shh, Ptc2, Raldh3, Pitx2, Isl1, Lim3 and Pax6 in the Developing Chick Hypophyseal Placode and Rathke's Pouch." Gene Expression Patterns: GEP 8 (7-8): 481–85.

Sobrier, Marie-Laure, Mohamad Maghnie, Marie-Pierre Vié-Luton, Andrea Secco, Natascia di Iorgi, Renata Lorini, and Serge Amselem. 2006. "Novel HESX1 Mutations Associated with a Life-Threatening Neonatal Phenotype, Pituitary Aplasia, but Normally Located Posterior Pituitary and No Optic Nerve Abnormalities." The Journal of Clinical Endocrinology and Metabolism 91 (11): 4528–36.

Staudt, Nicole, and Corinne Houart. 2007. "The Prethalamus Is Established during Gastrulation and Influences Diencephalic Regionalization." PLoS Biology 5 (4): e69.

Studer, M., A. Lumsden, L. Ariza-McNaughton, A. Bradley, and R. Krumlauf. 1996. "Altered Segmental Identity and Abnormal Migration of Motor Neurons in Mice Lacking Hoxb-1." Nature 384 (6610): 630–34.

Swaab, D. F., J. S. Purba, and M. A. Hofman. 1995. "Alterations in the Hypothalamic Paraventricular Nucleus and Its Oxytocin Neurons (putative Satiety Cells) in Prader-Willi Syndrome: A Study of Five Cases." The Journal of Clinical Endocrinology and Metabolism 80 (2): 573–79.

Swaab, Dick F. 2004. "Neuropeptides in Hypothalamic Neuronal Disorders." International Review of Cytology 240: 305–75.

Szabó, Nora-Emöke, Tianyu Zhao, Murat Cankaya, Thomas Theil, Xunlei Zhou, and Gonzalo Alvarez-Bolado. 2009. "Role of Neuroepithelial Sonic Hedgehog in Hypothalamic Patterning." The Journal of Neuroscience: The Official Journal of the Society for Neuroscience 29 (21): 6989–7002.

Takagi, Hiroyasu, Keiko Nagashima, Makiko Inoue, Ichiro Sakata, and Takafumi Sakai. 2008. "Detailed Analysis of Formation of Chicken Pituitary Primordium in Early Embryonic Development." Cell and Tissue Research 333 (3): 417–26.

Takuma, N., H. Z. Sheng, Y. Furuta, J. M. Ward, K. Sharma, B. L. Hogan, S. L. Pfaff, H. Westphal, S. Kimura, and K. A. Mahon. 1998. "Formation of Rathke's Pouch Requires Dual Induction from the Diencephalon." Development 125 (23): 4835–40.

Thisse, Bernard, Vincent Heyer, Aline Lux, Violaine Alunni, Agnès Degrave, Iban Seiliez, Johanne Kirchner, Jean-Paul Parkhill, and Christine Thisse. 2004. "Spatial and Temporal Expression of the Zebrafish Genome by Large-Scale In Situ Hybridization Screening." In Methods in Cell Biology, Volume 77:505–19. Academic Press.

Treier, M., A. S. Gleiberman, S. M. O'Connell, D. P. Szeto, J. A. McMahon, A. P. McMahon, and M. G. Rosenfeld. 1998. "Multistep Signaling Requirements for Pituitary Organogenesis in Vivo." Genes & Development 12 (11): 1691–1704.

Treier, M., S. O'Connell, A. Gleiberman, J. Price, D. P. Szeto, R. Burgess, P. T. Chuang, A. P. McMahon, and M. G. Rosenfeld. 2001. "Hedgehog Signaling Is Required for Pituitary Gland Development." Development 128 (3): 377–86.

Trowe, Mark-Oliver, Li Zhao, Anna-Carina Weiss, Vincent Christoffels, Douglas J. Epstein, and Andreas Kispert. 2013. "Inhibition of Sox2-Dependent Activation of Shh in the Ventral Diencephalon by Tbx3 Is Required for Formation of the Neurohypophysis." Development 140 (11): 2299–2309.

Tsai, Pei-San, Leah R. Brooks, Johanna R. Rochester, Scott I. Kavanaugh, and Wilson C. J. Chung. 2011. "Fibroblast Growth Factor Signaling in the Developing Neuroendocrine Hypothalamus." Frontiers in Neuroendocrinology 32 (1): 95–107.

Wang, Liheng, Kana Meece, Damian J. Williams, Kinyui Alice Lo, Matthew Zimmer, Garrett Heinrich, Jayne Martin Carli, et al. 2015. "Differentiation of Hypothalamic-like Neurons from Human Pluripotent Stem Cells" 125 (February). The American Society for Clinical Investigation: 796–808.

Ware, Michelle, and Frank R. Schubert. 2011. "Development of the Early Axon Scaffold in the Rostral Brain of the Chick Embryo." Journal of Anatomy 219 (2): 203–16.

Warr, Nicholas, Nicola Powles-Glover, Anna Chappell, Joan Robson, Dominic Norris, and Ruth M. Arkell. 2008. "Zic2-Associated Holoprosencephaly Is Caused by a Transient Defect in the Organizer Region during Gastrulation." Human Molecular Genetics 17 (19): 2986–96.

Webb, Emma A., and Mehul T. Dattani. 2010. "Septo-Optic Dysplasia." European Journal of Human Genetics: EJHG 18 (4): 393–97.

Wittkowski, Von W. 1980. "Glia der Neurohypophyse." In Neuroglia I, edited by Professor Dr A. Oksche, H. Leonhardt, K. Niessing, E. Scharrer, B. Scharrer, M. Weitzman, and W. Wittkowski, 667–756. Handbuch der mikroskopischen Anatomie des Menschen, 4 / 10. Springer Berlin Heidelberg.

Woods, Kathryn S., Maria Cundall, James Turton, Karine Rizotti, Ameeta Mehta, Rodger Palmer, Jacqueline Wong, et al. 2005. "Over- and Underdosage of SOX3 Is Associated with Infundibular Hypoplasia and Hypopituitarism." American Journal of Human Genetics 76 (5): 833–49.

Woo, K., and S. E. Fraser. 1995. "Order and Coherence in the Fate Map of the Zebrafish Nervous System." Development 121 (8): 2595–2609.

Yamaguchi, Terry P. 2001. "Heads or Tails: Wnts and Anterior–posterior Patterning." Current Biology: CB 11 (17): R713–24.

Zalc, Antoine, Shinichiro Hayashi, Frédéric Auradé, Dominique Bröhl, Ted Chang, Despoina Mademtzoglou, Philippos Mourikis, et al. 2014. "Antagonistic Regulation of p57kip2 by Hes/Hey Downstream of Notch Signaling and Muscle Regulatory Factors Regulates Skeletal Muscle Growth Arrest." Development 141 (14): 2780–90.

Zhang, P., C. Wong, R. A. DePinho, J. W. Harper, and S. J. Elledge. 1998. "Cooperation between the Cdk Inhibitors p27(KIP1) and p57(KIP2) in the Control of Tissue Growth and Development." Genes & Development 12 (20): 3162–67.

Zhang, P., C. Wong, D. Liu, M. Finegold, J. W. Harper, and S. J. Elledge. 1999. "p21(CIP1) and p57(KIP2) Control Muscle Differentiation at the Myogenin Step." Genes & Development 13 (2): 213–24.

Zhao, Li, Solsire E. Zevallos, Karine Rizzoti, Yongsu Jeong, Robin Lovell-Badge, and Douglas J. Epstein. 2012. "Disruption of SoxB1-Dependent Sonic Hedgehog Expression in the Hypothalamus Causes Septo-Optic Dysplasia." Developmental Cell 22 (3): 585–96.

Zhao, Tianyu, Xunlei Zhou, Nora Szabó, Michael Leitges, and Gonzalo Alvarez-Bolado. 2007. "Foxb1-Driven Cre Expression in Somites and the Neuroepithelium of Diencephalon, Brainstem, and Spinal Cord." Genesis 45 (12): 781–87.

Zhou, Zhi-Dong, Udhaya Kumari, Zhi-Cheng Xiao, and Eng-King Tan. 2010. "Notch as a Molecular Switch in Neural Stem Cells." IUBMB Life 62 (8): 618–23.